UPTAKE AND REGENERATION OF SILICIC ACID

BY MARINE PHYTOPLANKTON

RECOMMENDED:

Thomas C. Loyer

T. Ted Cooney

W. S. Ruth

D. Burrell

John J. Stevens
Chairman, Advisory Committee

APPROVED:

A. Mitchell
Director

May 30, 1975
Date

C. Lan
Vice President for Research

30 May 1975
Date

UPTAKE AND REGENERATION OF SILICIC ACID BY MARINE PHYTOPLANKTON

A

DISSERTATION

Presented to the Faculty of the

University of Alaska in Partial Fulfillment

of the Requirements

for the Degree of

DOCTOR OF PHILOSOPHY

By

David Michael Nelson, A.B.

Fairbanks, Alaska

August, 1975

ABSTRACT

A set of tracer techniques using the stable isotope ^{30}Si to measure rates of silicic acid uptake and silica dissolution in diatom cultures and natural marine phytoplankton populations is described.

Silicic acid uptake by the marine diatom *Thalassiosira pseudonana* in batch culture is describable by the Michaelis-Menten equation for enzyme kinetics, and no threshold concentration for uptake is evident. A clone of *T. pseudonana* isolated from a high nutrient environment demonstrated a higher maximum uptake rate than a clone of the same species from the Sargasso Sea. Light dependence of uptake in *T. pseudonana* grown under optimal light conditions prior to the experiment is weak or nonexistent. Exponentially growing populations of *T. pseudonana* lose silica by dissolution at rates ranging from 6 to 15% of the maximum uptake rate.

Silicic acid uptake by natural phytoplankton populations in the Baja California and northwest Africa upwelling regions extends to approximately twice the depth to which carbon and nitrogen uptake were observed and is seldom, if ever, substrate limited. Light dependence of uptake in natural populations is highly variable.

Silica dissolution increases with depth off northwest Africa, and is sufficient in the upper 50 m in the Cap Blanc region to supply all silicic acid consumed by the phytoplankton.

Hypotheses concerning the role of herbivores in silicic acid regeneration, the effect of light on silicic acid uptake by natural phytoplankton populations and the use of ^{30}Si uptake as an estimate of primary production are proposed.

ACKNOWLEDGEMENTS

One of my greatest pleasures in submitting this dissertation is the opportunity it provides to thank John J. Goering for the many things he's done for me. His support, his encouragement, his example during the past six years have enriched my education profoundly, and have made the work reported here possible. I can't imagine working for a finer person, and am very grateful to have had the chance.

I also wish to thank William S. Reeburgh for his continual interest in my work, and for numerous discussions which have broadened my outlook on oceanography.

A substantial amount of the sample preparation and isotopic analysis reported here was performed by David W. Boisseau, who also provided valuable suggestions for improving the procedures employed.

Practically all experiments reported in this dissertation were performed away from the University of Alaska, and I am grateful to many people for their hospitality and the research opportunities extended to me. Access to both the ideas and the culture collection of Robert R. L. Guillard of the Woods Hold Oceanographic Institution made the kinetic experiments reported in Chapter III possible, and the collaboration of Susan S. Kilham of the University of Michigan on these experiments, and of Farooq Azam of the Scripps Institution of Oceanography on earlier kinetic experiments, aided greatly in making the culture work successful. I was also fortunate to participate in cruises to the Baja California and northwest Africa upwelling regions sponsored by the IDOE Coastal Upwelling Ecosystems Analysis (CUEA) program, and am thankful both to the

CUEA organization for this opportunity and to a number of CUEA workers for access to their unpublished data, which were of great assistance to me in interpreting the silicon data.

I wish to thank Frances Sweet for her skill and patience in drafting the seemingly endless revisions of the figures, and catching a number of my errors in the process.

Sharon L. Nelson has asked not to be acknowledged for typing my dissertation, but I am grateful to her for so many things that a couple hundred hours behind a typewriter seem insignificant.

TABLE OF CONTENTS

LIST OF FIGURES

LIST OF TABLES

CHAPTER I

INTRODUCTION

Primary production, the conversion of inorganic matter into living plant material has two absolute requirements: matter and energy. The only source of energy which plants can utilize is sunlight, and the absorption of sunlight by seawater limits biologically utilizable energy to the upper few tens of meters of the ocean. It is in this "euphotic zone" that all primary production of organic matter in the ocean takes place. Inorganic forms of most biologically important elements, such as carbon, hydrogen and oxygen are present in abundant supply in the euphotic zone and to date only three elements are known whose inorganic concentrations are substantially decreased by photosynthetic activity. These elements are nitrogen, phosphorus, and silicon.

Nitrogen and phosphorus, as fundamental constituents of proteins and nucleic acids, respectively, are essential to all life. Silicon, which is used in the formation of structural hard parts of diatoms, silicoflagellates, radiolarians and sponges, probably is not. Nevertheless, the overriding importance of diatoms as primary producers in the ocean raises silicon to the level of a major plant nutrient and there is strong evidence that primary production in the ocean is at times limited by the availability of silicon (Armstrong, 1965: Dugdale and Goering, 1970). Comparison of recent studies of the kinetics of silicon limited growth of diatoms (Guillard, Kilham and Jackson, 1973; Paasche, 1973 a and b; Harrison, 1974) with the distribution of silicic

acid in the surface waters of the ocean (Sverdrup, Johnson and Fleming, 1941; Armstrong, 1965) indicates that very large regions of the ocean may contain insufficient silicon to support substantial diatom growth. Knowledge of the silicon requirements of diatoms in nature, and of the sources and rates of supply of silicic acid to the euphotic zone are therefore essential to an understanding of marine production processes.

Role of Silicon in Phytoplankton Ecology

Physiology of silicification

At the pH of seawater (8.1 to 8.2) dissolved inorganic silicon exists as monomeric orthosilicic acid, H_4SiO_4, which is about 5% dissociated to $H_3SiO_4^-$ (Stumm and Morgan, 1970). Silicic acid is taken up by diatoms and deposited as hydrated amorphous silica, $SiO_2 \cdot nH_2O$, in the form of a test or shell external to the cell membrane of the organism. Little is known about the biochemical pathways involved in silicic acid uptake and silica deposition, but the following physiological points have been established for some diatom species:

A. Silicification, the overall process which includes silicic acid uptake, all intracellular biochemical transformations of silicon and deposition of the silica shell, is an energy requiring pathway closely linked to aerobic respiration (Lewin, 1955). The respiratory inhibitors cyanide, fluoride, azide, arsenite, iodoacetate and fluoroacetate all inhibit silicic acid uptake without killing the cells. 2-4 dinitrophenol, an inhibitor of ATP production, inhibits silicic acid uptake while causing the respiration rate to double.

B. Silica is deposited intracellularly within a vesicle bounded by a membrane, the silicalemma (Lewin, Reimann, Busby and Volcani, 1966). The newly deposited frustule is transported, tightly bound within the silicalemma, to the site of final deposition in the newly forming cell wall. The original cell membrane (plasmalemma) is broken down and a new plasmalemma is formed interior to the new cell wall. The silica in the cell wall is covered by an organic coating which serves to inhibit silica dissolution (Lewin, 1961). This coating could be derived from the silicalemma, the original plasmalemma or synthesized *de novo* (Darley, 1970).

C. Under conditions of silicon starvation the cell undergoes normal nuclear and cytoplasmic division, but no new cell wall is deposited and the separation of two daughter cells does not take place (Lewin, 1962). Upon introduction of silicic acid to the medium there is a period of rapid uptake, accompanied by the cessation of lipid synthesis and a decrease in cellular carbon and carbohydrate content, indicating that the energetic capabilities of the cell are being diverted from other processes and utilized for silicification (Coombs, Darley, Holm-Hansen and Volcani, 1967). After this rapid uptake period, the biprotoplastic cells divide simultaneously, and continue to go through the stages of mitotic cell division synchronously for several generations.

Recently a silicic acid requirement has been demonstrated for DNA polymerase production in the diatom *Cylindrotheca fusiformis*

(Sullivan and Volcani, 1973 a and b). It is not known at present how phyletically general this requirement is.

Kinetics of silicic acid uptake and silicon limited growth

The specific uptake rate of a nutrient, V (Sheppard, 1962), may be defined by the following equation:

$$V = \frac{1}{S_1} \frac{dS_1}{dt} \tag{1}$$

where S_1 is the cellular concentration, in moles · liter^{-1} of the element under consideration. Similarly the specific growth rate, μ (Monod, 1942), may be defined by

$$\mu = \frac{1}{x} \frac{dx}{dt} \tag{2}$$

where x is the number of cells in a given volume of medium. In a population whose cell mass and elemental composition are not changing with time V and μ are equal. If $V > \mu$ for a given element in a given population, then the amount of that element per cell, which has been termed the cell quota, Q (Droop, 1968), is increasing with time, while if $V < \mu$, then Q is decreasing with time.

It has been shown for several nutrients (Dugdale, 1967; Droop, 1968; Eppley, Rogers and McCarthy, 1969; MacIsaac and Dugdale, 1969; Paasche, 1973 b; Goering, Nelson and Carter, 1973) that the specific uptake rate is a function of the external substrate concentration, S_2, and that the function may be described by a rectangular hyperbola of the form defined by the Michaelis-Menten equation for enzyme kinetics

$$V = V_{max} \frac{S_2}{K_T + S_2} \tag{3}$$

where V_{max} is the maximum specific uptake rate, and K_T the substrate concentration at which $V = \frac{V_{max}}{2}$.

Caperon and Meyer (1972 b) have suggested that equation (3) should be refined, at least in the case of nitrate uptake to allow for the existence of a threshold substrate concentration, S_0, below which no uptake takes place. By this new equation

$$V = V_{max} \frac{S_2 - S_0}{K_T' + (S_2 - S_0)} \qquad (4)$$

where K_T' is the value of $(S_2 - S_0)$ at which $V = \frac{V_{max}}{2}$.* The data of Paasche (1973 b) indicate that such a threshold concentration may exist for silicic acid uptake, although he recognized that determining low uptake rates of silicic acid uptake from changes in external substrate concentration is difficult due to the unknown rate of dissolution of cellular silica.

An equation of the Michaelis-Menten form has been used to describe the nutrient limited growth of bacteria (Monod, 1942) and extended to algae (Droop, 1968; Eppley and Thomas, 1969; Fuhs, 1969; Guillard, Kilham and Jackson, 1973; Paasche, 1973 a)

$$\mu = \mu_{max} \frac{S_2}{K_S + S_2} \qquad (5)$$

where μ_{max} is the maximum specific growth rate of the population and

---

* Guillard, Kilham and Jackson (1973) pointed out that nutrient kinetic data can be fit equally well by any equation, such as the Teissier equation or the Langmuir absorption isotherm which generates a rectangular hyperbola. The Michaelis-Menten equation, whose derivation is biochemical may be a confusing choice for describing nutrient uptake kinetics since nutrient uptake is undoubtedly carried out via biochemical enzymatic pathways. However, since a substantial body of literature has developed which uses Michaelis-Menten kinetics to describe nutrient uptake by algae, equations (3) and (4) will be used for the same purpose in this dissertation with the explicit understanding that they are strictly curve-fitting devices, and no knowledge of the biochemical mechanism of silicic acid uptake is implied.

K_S the substrate concentration at which $\mu = \frac{\mu_{max}}{2}$. Caperon and Meyer (1972 b) found that equation (5) did not fit their experimental data on nitrogen limited growth of four algal species and suggested a substantially different mechanism for nutrient limitation of algal growth

$$\mu = \mu_{max} \frac{Q-Q_0}{K_Q + (Q-Q_0)} \qquad (6)$$

where Q is the cell quota, Q_0 the cell quota at or below which no growth takes place, and K_Q the value of $(Q-Q_0)$ at which $\mu = \frac{\mu_{max}}{2}$. Equation (6) implies an intracellular pool of the limiting nutrient, which has been taken up by the cell but not yet transformed into a final cellular product. This pool is therefore available for use in cell growth. At Q_0 the pool is empty, and no growth takes place. But as $(Q-Q_0)$, which is a measure of the size of the intracellular pool, increases the growth rate increases in a manner describable by Monod-type growth kinetics. Caperon and Meyer thus postulate that μ is a function of the intracellular, rather than the extracellular nutrient concentration and that this function is hyperbolic.

It is not clear that either equation (5) or (6) describes the silicon limited growth of diatoms. Guillard, Kilham and Jackson (1973) found equation (5) to provide a good fit to their data on silicon limited growth of *Thalassiosira pseudonana*, while Paasche (1973 a), using a clone of *T. pseudonana* provided by Guillard, did not. Paasche's data are fit well by equation (6) if it is assumed that $Q_0 \tilde{=} 0.6$pg Si $\cdot$ cell^{-1}. Davis (1973) and Harrison (1974) found that

neither equation (5) nor (6) fitted their data on silicon limited growth of *Skeletonema costatum*. A plot of μ versus Q (Harrison, 1974) indicated a Q_0 which equaled, perhaps coincidentally, *ca.* 0.6pg Si · $cell^{-1}$, but the relationship between μ and Q appeared to be linear rather than hyperbolic.

Davis (1973) and Harrison (1974) developed a model of silicic acid uptake and silicon limited growth in *Skeletonema costatum* whereby uptake and growth at relatively low silicic acid concentration are controlled by the availability of the limiting nutrient to the cell-medium interface in a manner describable by equations (3) and (5), respectively, but at higher substrate concentrations both uptake and growth are limited by the internal mechanism of the cells' silicification process. According to this model, plots of V or μ versus S_2 are best represented by truncated hyperbolas in which the maximum rates of uptake or growth are less than the potential V_{max} of the uptake system, which is operating at the cell-medium interface in accordance with equation (3). Davis (1973) and Harrison (1974) thus claim that the experimentally obtained value of V_{max} or μ_{max} is a variable rather than a constant.

There is some experimental evidence of variability in V_{max}. Measured values of V_{max} for ammonium and nitrate (MacIsaac and Dugdale, 1972) have shown varying degrees of light dependence. Nitrate V_{max} is decreased by increasing ammonium concentration in *Dunaliela terteolecta* and *Skeletonema costatum* (Conway, 1973), and there is indirect evidence (Dugdale and Goering, 1970) that nitrate V_{max} may be dependent upon

silicic acid concentration in a diatom-dominated natural phytoplankton population off Peru. Evidence for the variability of μ_{max} is abundant when one considers that growth kinetic experiments are performed with all growth factors optimized except the one under investigation. Thus a μ measured under the limitation of any one nutrient is, conceptually, a μ_{max} for any other nutrient. The possibility of multiple nutrient limitation of algal growth has been considered theoretically by Droop (1973, 1974) and is clearly a subject which requires experimental attention in the future.

Dissolution of Biogenic Silica

Silica dissolves in water via the reaction:

$$SiO_2 + 2H_2O \rightleftarrows H_4SiO_4$$

The solubility of silica is dependent upon the temperature, pressure, and pH of the solution, and the free energy of the solid phase (Stumm and Morgan, 1970). Biogenic silica, that produced by diatoms and other siliceous organisms, is X-ray amorphous, indicating a lack of internal crystalline structure. This high degree of molecular disorder results in high free energy and high solubility relative to crystalline silicate minerals (Wollast, 1974). The effects of pressure (Jones and Pytkowicz, 1973) and pH (Stumm and Morgan, 1970) are slight over the range of these variables found in surface seawater, leaving temperature as the only factor which has a substantial effect upon the solubility of silica in the near-surface waters of the ocean. The equilibrium

solubility of amorphous silica in seawater at pH 8.1 and 1 atm pressure ranges from 1.23 X 10^{-3}M at 5°C (Siever, 1962) to 1.84 X 10^{-3}M at 25°C (Stöber, 1967).

Comparison of these solubilities with the range of silicic acid concentrations found in the ocean (Sverdrup, Johnson and Fleming, 1941; Armstrong, 1965) shows that seawater is everywhere undersaturated with respect to biogenic silica, and that surface seawater may be three or four orders of magnitude undersaturated. Biogenic silica should thus undergo spontaneous inorganic dissolution in seawater.

The importance of silica dissolution as a source of silicic acid to the euphotic zone depends upon the rate of the dissolution reaction, and on this point there is substantial disagreement. Cooper (1933) indicated that regeneration of silicic acid may proceed at a rate roughly ten times that of nitrate or phosphate in the English Channel, while Dugdale (1972) felt that the rate of silicic acid regeneration was negligible compared with those of other nutrients in the Peru upwelling system. Lewin (1961) found that the dissolution rate of diatom silica under laboratory conditions was highly variable and that three different ranges of dissolution rate could be observed which depended upon the condition of the particulate silica. In her experiments living diatoms were not observed to undergo dissolution, diatoms killed by any of several methods dissolved at a low rate, and diatoms treated with nitric acid to remove the organic coating which encases the silica in the cell wall dissolved at a rate five to eight times higher than that of killed, but untreated, cells. Additionally she found that aluminum, beryllium,

iron, gallium, gadolinium, and yttrium could combine in some way with killed diatom cells and decrease the dissolution rate. A common feature of these six metals is that they form highly insoluble hydroxides, and it is reasonable to assume that they bind strongly to the hydroxyl groups which are present at the surface of hydrated amorphous silica. A major conclusion to be drawn from Lewin's experiments is that the dissolution rate of diatom silica is highly dependent upon the amount of actual, exposed silica/water interface present in the system.

Kinetics of dissolution of silica in seawater

The dissolution of silica may be expressed as a specific dissolution rate, V_{dis}, which is directly comparable with the specific uptake rate, V defined in equation (1):

$$V_{dis} = -\frac{1}{S_1}\frac{dS_1}{dt} \qquad (7)$$

V_{dis} has dimensions of time^{-1} and is the number of moles of silica dissolved per mole of silica present in the system per unit time. It is the difference between V and V_{dis} which determines the silicon balance for a given population.* Some laboratory values of V_{dis} for biogenic

---

* A characteristic of V and V_{dis} which is not obvious from equations (1) and (7) is that they are dependent upon different parameters [See equations (3) and (10).] and thus independent of each other. Rigorously:

$$V = \frac{1}{S_1}\left(\frac{\partial S_1}{\partial t}\right)_{V_{dis}=0}, \quad V_{dis} = -\frac{1}{S_1}\left(\frac{\partial S_1}{\partial t}\right)_{V=0}; \quad \frac{1}{S_1}\frac{dS_1}{dt} = V - V_{dis}.$$

It is therefore possible, when V is sufficiently high, to have a positive V_{dis} even at high positive values of dS_1/dt. It is this independent effect of uptake and dissolution upon dS_1/dt that makes measurement of either on the basis of concentration change alone difficult (e.g., Lewin, 1961; Paasche, 1973 b).

silica, obtained by using equation (7) to recalculate the data of various authors, are presented in Table 1.

The dissolution of quartz in water has been shown to be a simple first order reaction which is described by the following rate equation (van Lier, De Bruyn and Overbeek, 1960):

$$\frac{dS_2}{dt} = \frac{\Omega}{v} k_2 (S_{2(eq)} - S_2) \tag{8}$$

where Ω is the surface area of the solid, v the volume of the solution, S_2 the external silicic acid concentration, $S_{2(eq)}$ the silicic acid concentration of a solution in equilibrium with the solid phase, and k_2 an apparent first order rate constant whose value is dependent upon temperature and pH.

Hurd (1972) has demonstrated that equation (8) also applies to the dissolution of amorphous biogenic silica, the only difference being that K_2 and $S_{2(eq)}$ are each approximately an order of magnitude higher for biogenic silica than for quartz. Equation (8) may be converted into an expression for V_{dis} if one assumes that dissolution of particulate silica is the source of all silicic acid added to the solution. That is:

$$\frac{dS_2}{dt} = -\frac{dS_1}{dt} \tag{9}$$

This assumption is implicit in the kinetic studies of both quartz and amorphous silica dissolution (van Lier, De Bruyn and Overbeek, 1960; Hurd, 1972). Then, combining equations (7), (8), and (9):

$$V_{dis} = \frac{\Omega}{v\, S_1} k_2 (S_{2(eq)} + S_2) \tag{10}$$

TABLE 1

Specific dissolution rates of diatom silica obtained by applying equation (10) to experimental data of various authors

Species	Temperature (C)	V_{dis} (day^{-1})	Investigator	Remarks
Skeletonema costatum	10	0.03	Kamatani (1969)	Cells killed by darkening
" "	20	0.05	"	" " " "
" "	30	0.09	"	" " " "
Chaetoceros gracilis	30	0.09	"	" " " "
" *decipiens*	30	0.01	"	" " " "
Navicula pelliculosa	10	0.08	Lewin (1961)	Cells cleaned w/HNO_3
" "	15	0.13	"	" " "
" "	19	0.27	"	" " "
" "	35	0.43	"	" " "
" "	19	0.03	"	Cells killed but not cleaned
Natural population	19	0.02	"	" " " " "
" "	19	0.10	"	Cells cleaned w/HNO_3
" "	6	0.02	"	Cells killed but not cleaned
" "	6	0.10	"	Cells cleaned w/HNO_3
Unidentified centric	11	0.02	Grill & Richards (1964)	Cells killed by darkening
Natural population	variable	0.02	Antia *et al.* (1963)	" " " "

The term $\frac{\Omega}{v\ S_1}$ has dimensions of area $\cdot$ mass^{-1}, and is the specific surface area of the solid phase. It can be seen from equation (10) that at a given temperature, pH, and silicic acid concentration (that is, at a given value of $[k_2(S_{2(eq)} - S_2)]$) V_{dis} is a linear function of the specific surface area of the solid phase.

Some measurements of the specific surface area of biogenic silica have been reported (Weiler and Mills, 1965; Wollast and Garrells, 1971; Hurd, 1973) and it appears that most of the biogenic silica produced in the ocean may have a specific surface area of between 50 and 150 $m^2 \cdot g^{-1}$. Figure 1 is a plot of V_{dis} versus $\frac{\Omega}{v\ S_1}$ at 3 C and 25 C, which is obtained from equation (10) using literature values for k_2 (Hurd, 1972) and $S_{2(eq)}$ (Siever, 1962; Stöber, 1967) for biogenic silica. The shaded area represents the range which includes most reported values of $\frac{\Omega}{v\ S_1}$ (Weiler and Mills, 1965; Wollast and Garrells, 1971, Hurd, 1973) and corresponding values of V_{dis} predicted by equation (10). Figure 1 is generated from data on acid cleaned biogenic silica and as such represents the range of the upper limits on V_{dis}. For example, acid cleaned biogenic silica with a specific surface area of 50 $m^2 \cdot g^{-1}$ would have a predicted V_{dis} of 0.02 hr^{-1} at 25 C on the basis of Figure 1. Factors such as the presence of an organic coating or of metal ions bound to the silica surface would presumably cause V_{dis} to be less than 0.02 hr^{-1}.

It is tempting to hypothesize, although difficult to ascertain experimentally, that the presence of an organic coating or metals bound to the silica surface depresses V_{dis} by decreasing the effective specific

FIGURE 1

Relationship between the specific dissolution rate, V_{dis} and specific surface area, $\frac{\Omega}{v \cdot S_1}$, of biogenic silica at pH 8.1 and 1 atm pressure predicted from equation (10), based upon literature values of the dissolution rate constant and equilibrium solubility of biogenic silica. Shaded area represents the approximate range of $\frac{\Omega}{v \cdot S_1}$ and temperature, and corresponding predicted range of V_{dis} in the ocean.

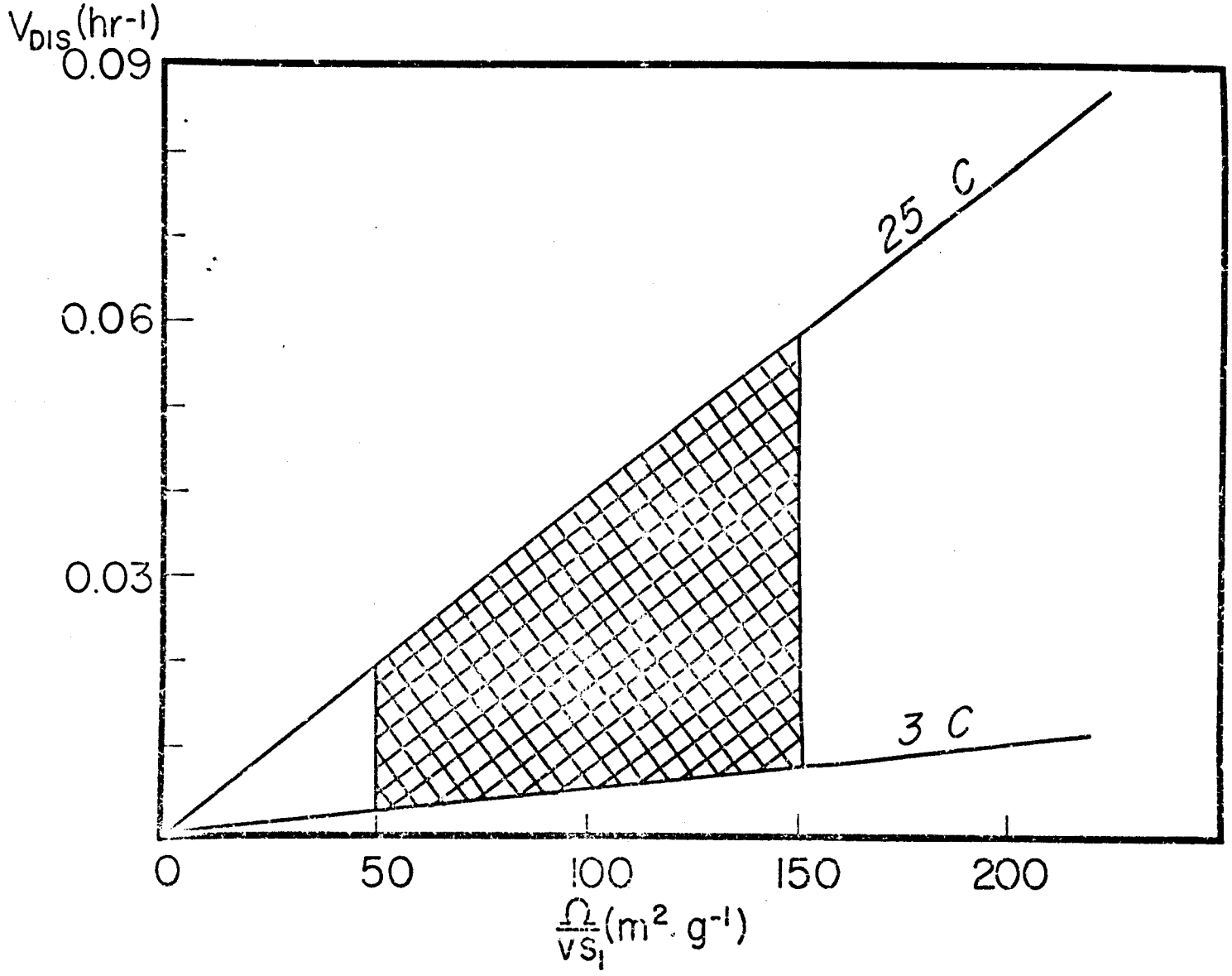
V_{DIS} (hr-1)
0.09
0.06
0.03
25 C
3 C
0
50
100
150
200
$\frac{\Omega}{VS_i}$ ($m^2 . g^{-1}$)

surface area, $\frac{\Omega'}{v\ S_1}$ which may be visualized as the amount of actual silica/water interface per unit mass of particulate silica and that V_{dis} of any biogenic silica, regardless of the presence or absence of such inhibitors could be predicted by a modification of equation (10) if $\frac{\Omega'}{v\ S_1}$ could be measured:

$$V_{dis} = \frac{\Omega'}{v\ S_1} k_2\ (S_{2(eq)} - S_2) \qquad (11)$$

Conversely, if V_{dis} could be measured directly, then $\frac{\Omega'}{v\ S_1}$ could be computed using equation (11). Indeed, if V_{dis} were observed to vary in a system where temperature, pH and S_2 were relatively constant it would be difficult to explain variability of V_{dis} in any manner other than on the basis of variation in $\frac{\Omega'}{v\ S_1}$.

Vertical distribution of silica dissolution rates in the ocean

Between 95 and 99% of the silica produced by organisms in the ocean dissolves before it reaches the bottom (Calvert, 1968; Lisitzin, 1972). Thus in the column of water which lies beneath a statistically average square meter of ocean surface the total amounts of silicic acid uptake and silica dissolution are about equal. Silica is produced by diatoms and silicoflagellates, whose distribution is limited to near-surface waters because of their requirement for light, by radiolarians, which are found throughout the water column, and by sponges, which are benthic. The resulting potentially complicated vertical profile of biogenic silica production is simplified greatly in most mass balances of silicon in the ocean (e.g., Harriss, 1966; Heath, 1973) by the assumption that diatoms are the dominant silica secreting organisms and

that production of biogenic silica is insignificant below the euphotic zone. There is considerable confusion, however, as to where the silica produced in the euphotic zone is dissolving.

Typical depth distributions of silicic acid differ from those of nitrate or phosphate in that there is no silicic acid maximum at intermediate depth. Instead silicic acid concentration increases from near the surface to the bottom (Sverdrup, Johnson and Fleming, 1941). This has been interpreted in the past to mean that silica produced near the surface dissolves at a fairly uniform rate as it sinks to the bottom (Armstrong, 1965), with the resulting corrolary that the rate of silica dissolution in near-surface waters is low compared to the rate of uptake (Dugdale, 1972). In fact, however, the profile of silicic acid in the deep water may result largely from the combined effects of inorganic reactions involving mineral silicate phases (Mackenzie, Garrells, Bricker and Bickley, 1967), diffusion of silicic acid from the sediment (Fanning and Pilson, 1974), and deep water circulation (Berger, 1970). Park (1967) reported that most of the silicic acid in the deep water off Oregon and all of the change in silicic acid concentration with depth below *ca.* 200 m must result from processes other than the dissolution of locally produced biogenic silica.

Wollast (1974) has combined empirical data on dissolution rate constants of biogenic silica with a theoretical treatment of the dependence of sinking rate on particle radius to estimate the ultimate depths to which diatom skeletons of various sizes should penetrate in the ocean. Based on these calculations, along with certain assumptions

about the statistical distribution of diatom skeletal radius and specific surface area, he estimated that 45% of the silica produced by diatoms is dissolved in the upper 1,000 m. Hurd (1972) pointed out that the variables which affect the dissolution rate of silica are all distributed vertically in the ocean in a way which makes surface water more corrosive to silica than deep water. Based upon the vertical profiles of temperature and silicic acid concentration in the equatorial Pacific, he estimated that the dissolution rate of silica in surface water should be sixteen times that found in deep water.

In the two studies just cited two independent estimates, one (Wollast, 1974) considering only the properties of the particulate matter and the other (Hurd, 1972) considering only the properties of the water each predicted that the highest rates of silica dissolution should occur in the near-surface region of the ocean. In nature these two effects may be cumulative and may provide a mechanism to explain the vertical distributions of diatom debris observed by Kozlova (1964) which indicated that at least 98% of the silica produced in the Antarctic dissolved at depths less than 1,000 m and more than 80% may have dissolved at depths less than 100 m.

A greater number of direct field observations of the vertical distribution of diatom remains would be useful in establishing the vertical site of silica dissolution in the ocean.

Methods of Measuring Rates of Silicic Acid Uptake and Silica Dissolution

Observations of silicic acid depletion during the progress of a diatom bloom are abundant (e.g., Cooper, 1952; Armstrong, 1965; Dugdale and Goering, 1970) and useful in documenting the likelihood of silicon limitation in the ocean. They are not, however, uptake rate measurements due to the number of chemical and hydrographic parameters left unknown.

The early studies of silicon uptake (Lewin, 1954, 1955, 1957; Jorgensen, 1957) were performed on individual diatom species in batch culture. This was an advance which allowed measured rates of silicic acid depletion to be interpreted directly as uptake rates of given species under given experimental conditions. However, results of batch culture experiments are more difficult to interpret than was once thought, due to the possibility of important transient states in both the experimental conditions and the population (Caperon, 1968; Williams, 1971; Conway, 1973; Harrison, 1974).

The influence of transient states may be eliminated by studying nutrient uptake or nutrient limited growth kinetics of a population in a chemostat (Herbert, Elsworth and Telling, 1956). A chemostat is a continuous culture apparatus in which a population is maintained at steady state, and chemostats have been employed to study silicic acid uptake and silicon limited growth in diatoms with considerable success (Paasche, 1973 a and b; Davis, 1973; Harrison, 1974). However, chemostat techniques are not applicable to natural phytoplankton populations, and chemostat data may even be of questionable value in interpreting

field data due to the scarcity of steady state conditions in nature (Jannasch, 1974).

Dissolution rates of biogenic silica have been measured in batch culture (Jorgensen, 1955; Lewin, 1961; Kamatani, 1969), in strictly inorganic experiments (Stöber, 1967; Hurd, 1972) and in the field (Berger, 1968).

With the exception of the field study of Berger (1968), in which dissolution of radiolarion skeletons was measured as a decrease in weight of particulate material during an *in situ* incubation, all silicic acid uptake and silica dissolution rates reported in the studies cited above were measured as the difference between an initial (pre-incubation or inflow) and a final (post-incubation or outflow) silicic acid concentration. The rate of change in silicic acid concentration is the net difference between the rates of uptake and dissolution and is subject to unambiguous interpretation only in those studies in which one of the rates may be set equal to zero (e.g., Stöber, 1967; Hurd, 1972).

In the next chapter a tracer method is described which uses the stable isotope ^{30}Si to measure rates of silicic acid uptake and silica dissolution in diatom cultures and natural phytoplankton populations. A silicon tracer method has the following advantages over methods which employ silicic acid concentration change as a measure of the uptake or dissolution rate:

A. sufficient sensitivity to allow measurement of uptake and dissolution rates during short term incubations at the

population densities found in nature.

B. the ability to distinguish between uptake and dissolution and to measure the rates of these two processes separately within a given system.

Objectives of the Research Reported in this Dissertation

Knowledge of the role of silicon in marine production is primitive when compared with knowledge of the dynamics of carbon, nitrogen and phosphorus. The first studies of the kinetics of silicic acid uptake and silicon limited growth in diatoms (Davis, 1973; Guillard, Kilham and Jackson, 1973; Paasche, 1973 a and b; Harrison, 1974) and of silicic acid uptake rates in the field (Goering, Nelson and Carter, 1973) have appeared only recently in spite of the fact that the potential limiting role of silicon has long been recognized (e.g., Thompson and Robinson, 1932; Dugdale, 1972). A major reason for the slow development of knowledge of the marine silicon cycle has been the lack of an appropriate analytical tool for determining rates of chemical transformations of silicon in the environment.

A comprehensive picture of the dynamics of silicon in the surface waters of the ocean does not exist and has not emerged from the research reported here, but progress in that direction has been made by the development of the following, which form the substance of this dissertation:

A. a ^{30}Si tracer technique for the determination of rates of biological uptake of silicic acid and dissolution of biogenic

silica, which is applicable to the study of diatom populations in pure culture and natural phytoplankton populations in the ocean.

B. a body of preliminary data on rates of silicic acid uptake and silica dissolution in laboratory and natural populations.

C. a set of testable hypotheses concerning the role of silicon in the regulation of primary production.

Much of the material which follows is based upon small numbers of experiments. Some is speculative. The development of ^{30}Si tracer techniques is the only aspect of this research which is in any sense completed. Nevertheless, I believe that even this preliminary research provides strong indications of the highly dynamic behavior of silicon in the euphotic zone, and of the importance of regenerative proccesses in the surface region of the ocean.

CHAPTER II

SILICON-30 TRACER METHODOLOGY

During the past twenty years the isotopic tracer has replaced the microscope as the most important single tool in the hands of the biological oceanographer. The use of the radioisotope ^{14}C (Steeman-Nielsen, 1952) and the stable isotope ^{15}N (Neese, Dugdale, Dugdale and Goering, 1962) as tracers in aquatic systems has led to a dramatically greater understanding of the role of these two elements in phytoplankton ecology and their transformations within the environment.

The power of the tracer method results from its specificity, which allows the investigator to go into a complex biochemical, physiological or ecological system and determine the rate of a single process. In this chapter a tracer method for measuring rates of chemical transformations of silicon in the ocean is described. The procedures employed are explained in general terms and in fairly rigorous detail with the purpose of providing a reference for the design of further experiments. Specific experiments reported in this dissertation will be described in the following chapters.

Silicon has three stable isotopes, ^{28}Si, ^{29}Si, and ^{30}Si and two radioisotopes, ^{31}Si and ^{32}Si.* Conceptually, any one of these five isotopes can be used as a tracer. ^{32}Si, a β-emitter with a half-life of *ca.* 700 years (Lindner, 1953) would be the ideal choice because it

* ^{26}Si ($t_{1/2}$ = 1.7 sec) and ^{27}Si ($t_{1/2}$ = 4.9 sec) have no potential as tracers due to their short half-lives.

would provide the sensitivity of a radioisotope and also allow any laboratory with equipment for ^{14}C counting to perform silicon uptake experiments. Unfortunately, ^{32}Si is difficult to produce (Zoller, 1966) and not available commercially. ^{31}Si, a β-emitter with a half life of 2.65 hours (Sullivan, 1957) has been used successfully in uptake experiments with diatom cultures (Azam, Hemmingsen and Volcani, 1974). However, its short half life makes even culture experiments difficult and completely precludes its use in the field.

^{28}Si, ^{29}Si, and ^{30}Si are all stable and available commercially in high purity. However, since they do not emit radiation they are not as easily detectable as are radioisotopes. As is the case with ^{15}N, the final measurement of the amount of substrate taken up in an experiment employing a stable isotope of silicon must be a mass spectrometric analysis of the isotopic composition of the sample after an incubation period.

The relative abundances of the three stable isotopes of silicon (Sullivan, 1957) are given in Table 2.

TABLE 2

Relative natural abundances of the stable isotopes of silicon

Silicon isotope	Relative natural abundance (atom %)
^{28}Si	92.18
^{29}Si	4.71
^{30}Si	3.12

The tracer method presented here uses the heaviest and rarest of these isotopes, ^{30}Si, to measure the rate of incorporation of dissolved silicic acid into particulate matter, and the rate of dissolution of particulate silica.

Silicic Acid Uptake

The uptake rate of silicic acid can be measured by a modification of the method of Goering, Nelson and Carter (1973). The procedure consists of four steps: preparation of isotopically labeled silicic acid solutions, an incubation experiment, isotopic analysis of the particulate silicon at the end of the incubation period, and calculation of uptake rates from isotopic composition data.

Preparation of isotopically labeled silicic acid solutions

The ^{30}Si tracer procedure requires two different solutions of isotopically labeled silicic acid: a ^{30}Si-enriched solution for use as a tracer in the incubation, and a ^{29}Si-enriched solution for use as a carrier in the subsequent sample preparation and mass spectrometry. $^{29}SiO_2$ and $^{30}SiO_2$ are both available in greater than 90% isotopic purity from the Isotope Sales Division of the Oak Ridge National Laboratory. The SiO_2 is weighed into a clean, dry platinum crucible and a four-fold excess, by weight, of anhydrous Na_2CO_3 added. The reagents are mixed thoroughly, and the crucible placed over a propane/compressed air blast burner at the highest possible heat for a period

of five minutes. At temperatures above 1,100 C the following fusion reaction occurs:

$$Na_2CO_{3(\ell)} + SiO_{2(s)} \rightarrow Na_2SiO_{3(\ell)} + CO_{2(g)}$$

The reaction has gone to completion when there is no more solid phase present and a clear melt is obtained. Once the fusion is completed the crucible is removed from the burner and allowed to cool. The pellet which crystallizes out, a mixture of Na_2SiO_3 and Na_2CO_3 is dissolved in sufficient distilled water to provide a 20.0 μg atom Si · ml^{-1} ^{30}Si tracer solution or a 10.0 μg atom Si · ml^{-1} ^{29}Si carrier solution. These solutions are stable indefinitely if stored in polyethylene bottles, but should not be frozen due to the possibility of the formation of long-lived polymers of silicic acid (Strickland and Parsons, 1968).

Incubation of a sample

It is the incubation step which allows the ^{30}Si tracer method to be employed within the framework of a specific experimental design. A sample is inoculated with ^{30}Si-labeled silicic acid and allowed to incubate for a period of time and under experimental conditions of the investigator's choosing. At the end of the incubation period the particulate matter is collected on a 0.8 μm polycarbonate membrane filter and retained for ^{30}Si analysis.

There are few restrictions on the choice of a sample and of the incubation conditions to be employed in an experiment. The sample must be at least a two-phase system consisting of an aqueous solution and a

solid phase, and the experimental conditions must be chosen such that the amount of particulate silicon does not increase greatly during the incubation period (Sheppard, 1962). In addition, the following experimental parameters must be known:

v_s; the volume of the sample (ℓ)

v_ℓ; the volume of labeled H_4SiO_4 solution added (ℓ)

Δt; the duration of the incubation (hr)

$S_{2(a)}$; the ambient silicic acid concentration of the solution before the addition of labeled silicic acid (μg atoms Si · ℓ^{-1})

$S_{2(\ell)}$; the silicic acid concentration of the added labeled solution (μg atoms Si · ℓ^{-1})

$S_{1(i)}$; the initial concentration of particulate silicon (μg atoms Si · ℓ^{-1})

$^{30}A_\ell$; the atom % ^{30}Si of the labeled silicic acid

$^{30}A_n$; the atom % ^{30}Si of natural silicon (= 3.12)

Knowledge of these experimental parameters allows $^{30}A_i$, the initial

atom % ^{30}Si of the total (ambient plus labeled) silicic acid pool to be computed:

$$^{30}A_i = \frac{^{30}A_n \cdot S_{2(a)} + \frac{v_\ell}{v_s} \cdot ^{30}A_\ell \cdot S_{2(\ell)}}{S_{2(a)} + \frac{v_\ell}{v_s} \cdot S_{2(\ell)}} \qquad (12)$$

$^{30}A_i$, along with S_1 and Δt is used in conjunction with the isotopic content of the final particulate silicon to compute the uptake rate.

Isotopic analysis of particulate silicon

sample preparation

Particulate silicon collected at the end of the incubation period is analyzed for isotopic composition by conversion to barium fluosilicate, $BaSiF_6$, followed by solid sample mass spectrometry. To avoid contamination with natural silicon all reactions must be carried out in clean, covered, non-glass containers. The procedure is as follows:

1. Each filter is placed in a platinum crucible, dampened with a few drops of distilled water, covered and ashed by placing the crucible in a muffle furnace at room temperature and heating to 900 C. Muffle furnace space and the number of platinum crucibles available determine the number of samples that can be ashed at one time.

2. The crucibles are removed from the muffle furnace and allowed to cool to room temperature.

3. Six drops of 49% HF are added to the ash in each crucible and the samples covered and allowed to react for one hour. During this time a quantitative conversion of SiO_2 to H_2SiF_6 occurs.

4. 1.00 ml of 10.0 μg atoms Si · ml^{-1} H_4SiO_4 solution (> 90 atom % ^{29}Si) is added as a carrier. The H_4SiO_4 is converted to H_2SiF_6 instantaneously. This step has two purposes:

A. It ensures that the sample contains sufficient silicon to produce a strong mass spectrometer signal.

B. It allows the post-incubation particulate silicon concentration $S_{1(f)}$ to be computed by isotope dilution.

5. The solution is swirled around the bottom of the crucible to ensure thorough mixing, and then poured into a 15 ml disposable polystyrene centrifuge tube. Quantitative transfer of the solution is not essential.

6. The solution in the centrifuge tube should be clear, but if an insoluble residue remains the sample is centrifuged at 1,500 · g for five minutes, the supernatant transferred to another 15 ml disposable polystyrene centrifuge tube, and the residue and first centrifuge tube discarded.

7. Four drops of 5% $BaCl_2 \cdot 2H_2O$ solution are added to each sample and the solution stored for one hour, during which $BaSiF_6$ precipitates. If no precipitate forms one drop of 10% NaOH is added and the $BaSiF_6$ is given another hour to precipitate.

8. The samples are centrifuged at 1,500 · g for five minutes, the supernatant discarded and the precipitate resuspended in 0.5 ml of distilled water.

9. The samples are again centrifuged at 1,500 · g for five minutes, the supernatant discarded and the precipitate resuspended in

0.5 ml of absolute methanol. This step is repeated.

10. The samples are placed in a vacuum oven at 75-80 C and 0.4-0.5 atm and allowed to dry overnight, after which they are ready for mass spectrometry.

It has been our experience that samples can be prepared in batches. The size of a batch is limited by the number of platinum crucibles available, and one person can prepare two or three batches in a normal working day.

mass spectrometry

Silicon isotopic analyses on all samples reported in this dissertation were performed on a Finnigan Corporation Model 3100 D quadrupole mass spectrometer. It is likely that $BaSiF_6$ can be analyzed for silicon isotopes on any mass spectrometer with a solid sample capability, and the analysis has been performed successfully on at least one other instrument (Goering, Nelson and Carter, 1973). For analysis on the Finnigan mass spectrometer, each sample is loaded into a small Pyrex sample crucible and placed in the tip of the instrument's solid sample probe. The probe is inserted into the analyzer tube of the instrument and heated slowly by a resistance heating element within the probe assembly while the temperature of the probe is monitored continuously. Water retained by the sample is evolved over the temperature range of 150-300 C. When the probe temperature reaches 350 C the mass spectrometer is tuned to scan through the m/e (mass to charge ratio) range of 84 through 87. The 84 peak is monitored to make certain that no significant background is present, and 85, 86, and 87 correspond to

$^{28}SiF_3^+$, $^{29}SiF_3^+$, and $^{30}SiF_3^+$, respectively. At 350 C $BaSiF_6$ begins to decompose thermally and silicon tetrafluouride, SiF_4, is produced by the reaction:

$$BaSiF_{6(s)} \xrightarrow{350\text{-}500\ C} BaF_{2(s)} + SiF_{4(g)}$$

The SiF_4 is fragmented and ionized by electron bombardment within the ion source of the mass spectrometer. Perceptible peaks are produced corresponding to SiF_4^+, SiF_3^+, SiF_2^+, SiF^+, and Si^+ ions but SiF_3^+ is the main fragment produced. The signal at *m/e* 85, 86, and 87 becomes perceptible at a probe temperature of 350 C and increases steadily with temperature to a maximum at just over 400 C. The maximum signal remains for three to five minutes during which several (10-15) scans through the *m/e* range 84 through 87 are recorded. The heating element in the solid probe is then turned off, and when the probe has cooled to 250 C, it is removed from the instrument and the next sample loaded. It has been our experience that 25 to 30 samples can be analyzed by this procedure in a normal working day.

A schematic of the overall sample preparation and analysis procedure is given in Figure 2.

Uptake rate calculation

The mass spectrometric data consist of three peaks, whose heights--I_{85}, I_{86}, and I_{87}--correspond to the intensities of the ion currents at *m/e* 85, 86, and 87, respectively. Since these peaks are produced by the SiF_3^+ ion and fluorine has only one stable nuclide, the

FIGURE 2

Sample preparation scheme for the isotopic analysis of particulate silicon and dissolved silicic acid.

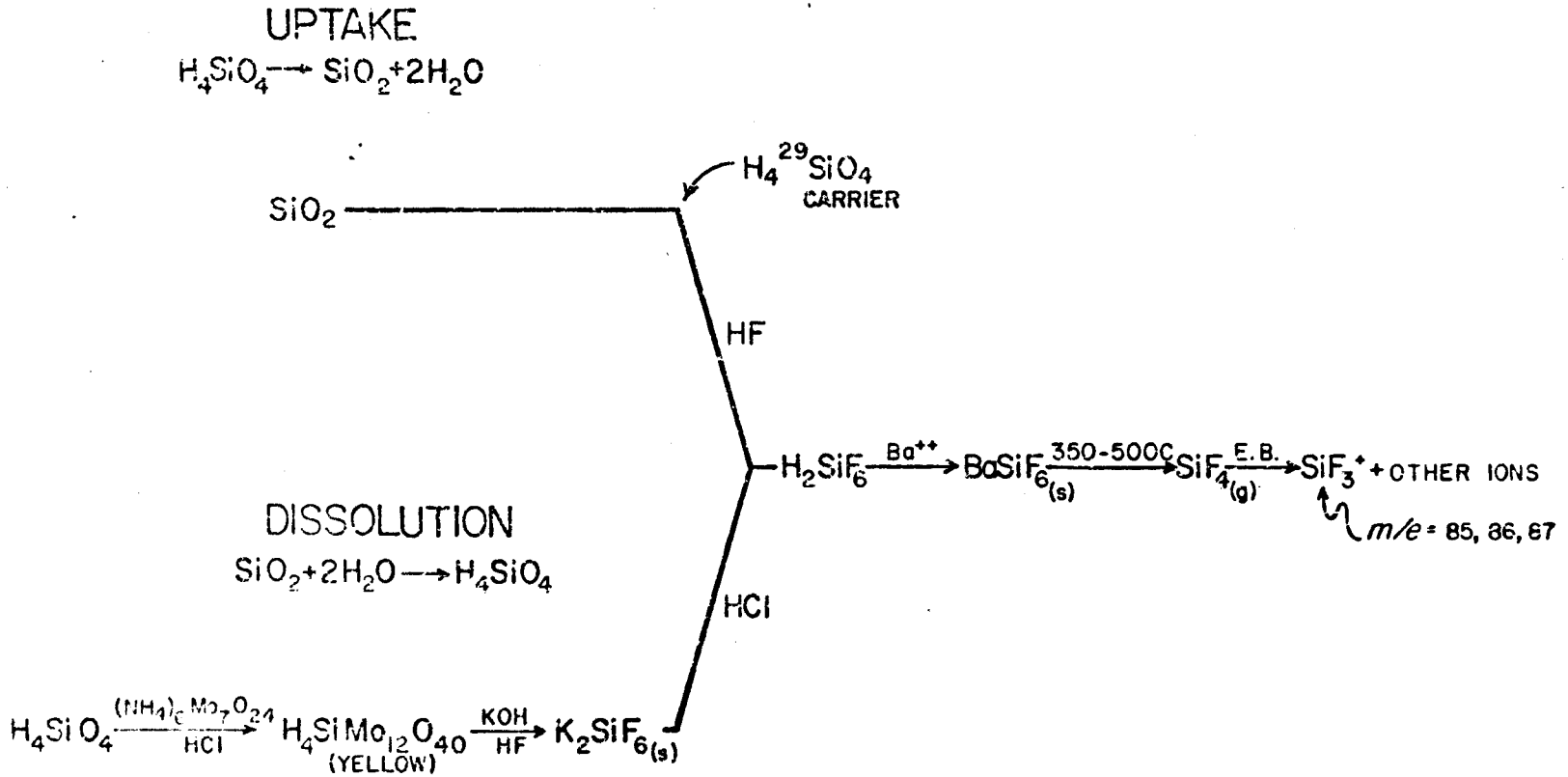
UPTAKE
$H_4SiO_4 \longrightarrow SiO_2 + 2H_2O$
SiO_2
$H_4{}^{29}SiO_4$
CARRIER
HF
$H_2SiF_6 \xrightarrow{Ba^{++}} BaSiF_{6(s)} \xrightarrow{350\text{-}500C} SiF_{4(g)} \xrightarrow{E.B.} SiF_3^+ + OTHER\ IONS$
m/e = 85, 86, 87
DISSOLUTION
$SiO_2 + 2H_2O \longrightarrow H_4SiO_4$
HCl
$H_4SiO_4 \xrightarrow[HCl]{(NH_4)_6Mo_7O_{24}} H_4SiMo_{12}O_{40}$ (YELLOW) $\xrightarrow[HF]{KOH} K_2SiF_{6(s)}$

relative values of I_{85}, I_{86}, and I_{87} directly reflect the relative abundances of ^{28}Si, ^{29}Si, and ^{30}Si in the sample.

The sample consists of silicon from two sources: the particulate silicon recovered at the end of the incubation, whose concentration and isotopic composition are unknown, and the ^{29}Si carrier added during the sample preparation, whose concentration and isotopic composition are known. The isotopic composition of the carrier silicon used in experiments reported here is given in Table 3.

TABLE 3

Isotopic composition of carrier silicon used in sample preparation

Silicon isotope	Relative abundance (atom %)
^{28}Si	4.36
^{29}Si	95.28
^{30}Si	0.36

To clarify the following discussion the actual numerical values from Tables 2 and 3, rather than six additional subscripted variables, will be used to represent the isotopic composition of natural and carrier silicon.

The total amount of silicon (incubated sample, plus carrier) in

the sample $S_{1(t)}$ can be computed from mass spectrometric data by isotope dilution. Since

$$\frac{S_{1(t)}}{[^{29}Si]} = \frac{I_{85} + I_{86} + I_{87}}{I_{86}} \tag{13}$$

and approximating that the 10.0 μg atoms Si added as carrier silicic acid is the source of all ^{29}Si:

$$[^{29}Si] = 10 \times 0.9528 = 9.528 \text{ μg atoms Si} \tag{14}$$

Combining equations (13) and (14):

$$S_{1(t)} = 9.528 \left(\frac{I_{85} + I_{86} + I_{87}}{I_{86}} \right) \tag{15}$$

The amount of particulate silicon collected at the end of the experiment $S_{1(f)}$ is then easily calculated:

$$S_{1(f)} = \frac{S_{1(t)} - 10.0}{v_s} \tag{16}$$

The approximation made in equation (14) ignores the amount of ^{29}Si in the particulate silicon collected from the incubation. This results in an underestimate of $[^{29}Si]$ and a subsequent underestimate in $S_{1(f)}$ which ranges from zero to 2% over the typical oceanic range of particulate silicon values (0-5 μg atoms Si $\cdot$ ℓ^{-1}).

To calculate the uptake rate of silicon the isotopic composition of the final particulate silicon (free of carrier) must be known. I_{85}', I_{86}', and I_{87}', which represent the mass spectrometer peak heights which would have been obtained if no carrier silicon had been added, can be computed from the isotopic compositions of natural and

carrier silicon (Tables 2 and 3) as follows:

$$I_{85}' = I_{85} - \frac{4.36}{95.28} I_{86} \tag{17}$$

$$I_{86}' = \frac{4.71}{92.18} I_{85}' \tag{18}$$

$$I_{87}' = I_{87} - \frac{0.36}{95.28} I_{86} \tag{19}$$

The atom % ^{30}Si in the final particulate material, $^{30}A_f$, can then be computed:

$$^{30}A_f = \frac{100\ I_{87}'}{I_{85}' + I_{86}' + I_{87}'} \tag{20}$$

The specific uptake rate of silicon, V, is obtained from an equation of the form suggested by Sheppard (1962):

$$V = \frac{^{30}A_f - {}^{30}A_n}{\Delta t\ (^{30}A_i - {}^{30}A_n)} \tag{21}$$

V has dimensions of $time^{-1}$ and is the number of moles of silicic acid taken up per mole of particulate silicon per unit time. If the mass and elemental composition of phytoplankton cells remained constant with time, V for silicon would equal V for any other element and also μ, the specific growth rate of the population.

The absolute uptake rate of silicon, ρ, may now be computed:

$$\rho = V \cdot S_1 \tag{22}$$

Conceptually the average S_1 over the incubation period ($\frac{S_{1(i)} + S_{1(f)}}{2}$) should be used in computing ρ, but since the change in S_1 during a

properly designed experiment is small and $S_{1(f)}$ is already available from equation (16), it may be used.

Errors in uptake rate measurement

Equations (12) and (21) indicate that the value of V is dependent upon the following measured parameters: $S_{2(a)}$, $S_{2(\ell)}$, v_ℓ, v_s, Δt, and $^{30}A_f$. Since $S_{2(\ell)}$, v_ℓ, v_s, and Δt are experimental parameters set by the investigator, they can be known to within ±1%. Measurement of $S_{2(a)}$ by the automated colorimetric acid-molybdate method of Hager, Gordon and Park (1968) is also accurate to within ±1%, resulting in a maximum cumulative error in V from all sources other than mass spectrometry of ±5%. The accuracy of the mass spectrometric determinantion of $^{30}A_f$ is a function of the individual instrument employed in the analysis. Mass spectrometric analysis of isotopically enriched standards on the Finnigan quadrupole instrument used in these studies indicates that the measured value of $^{30}A_f$ is accurate to within 0.1 atom % in samples which contain at least 0.8 µg atoms Si prior to the addition of carrier. Equation (10) shows that a 0.1 atom % error in $^{30}A_f$ results in a < 5% error in V when $^{30}A_f - {}^{30}A_n > 2.0$ atom %. Therefore experimental conditions should be chosen to provide the maximum particulate silicon concentration and ^{30}Si enrichment consistent with the purpose of the experiment, and the total accumulated error in V is less than ±10% in experiments where:

A. $Si_{(f)} \cdot v_s > 0.8$ µg atoms Si.

B. $^{30}A_f - {}^{30}A_n > 2.0$ atom %.

Condition (A) corresponds to a minimum diatom population of 10^6 to 10^8 cells depending upon the cellular silicon content, and condition (B) is generally exceeded by an exponentially growing diatom population in a two-hour incubation.

In experiments with natural phytoplankton populations, where V is intended to represent the uptake rate of the population at a given location in the ocean, two additional sources of error exist: random errors resulting from sampling the population and systematic errors from the failure to duplicate *in situ* conditions in the experiment. Neither of these sourses of error has received rigorous statistical scrutiny from investigators studying marine nutrient cycles but sampling errors have been assumed to be negligible when compared with analytical errors. As a check on this assumption ten replicate samples of a diatom-dominated mixed algal population were collected from a depth of 3 m in Resurrection Bay near Seward, Alaska, and incubated with ^{30}Si-labeled silicic acid for six daylight hours. The results of the ten individual measurements, along with the mean, standard deviation and 95% confidence interval are given in Table 4.

TABLE 4

Results of ten replicate measurements of silicic acid uptake by a natural phytoplankton population in Resurrection Bay near Seward, Alaska.

Sample	$^{30}A_f$ (atom %)	$^{30}A_f - {}^{30}A_n$ (atom %)	V (hr^{-1})	S_1 (μg atoms $Si \cdot \ell^{-1}$)	ρ (μg atoms $Si \cdot \ell^{-1} \cdot hr^{-1}$)
1	4.67	1.55	0.0051	3.09	0.0158
2	4.72	1.60	0.0053	3.08	0.0163
3	4.75	1.63	0.0054	2.76	0.0149
4	4.60	1.48	0.0049	2.68	0.0131
5	4.64	1.52	0.0050	2.91	0.0146
6*	4.94	1.82	0.0052	2.98	0.0155
7*	4.85	1.73	0.0049	2.81	0.0138
8*	4.86	1.74	0.0049	3.15	0.0155
9*	5.02	1.90	0.0054	2.80	0.0151
10*	4.98	1.86	0.0053	2.72	0.0144
Mean			0.00514	2.898	0.01490
Standard Deviation (σ)			0.00020	0.169	0.00097
95% Confidence Limit (2σ)			0.00039	0.337	0.00194

* Samples 6-10 were incubated for seven hours because it took nearly one hour to filter samples, 1-5, and only five filter holders were available.

All of the variability in V in this single replication experiment may be accounted for on the basis of the ±10% analytical error discussed above. An assumption of a negligible effect of sampling errors on V is therefore supported experimentally.

The sources and magnitudes of possible systematic errors in nutrient uptake rate measurements in natural populations are largely unknown, and will not be included in error estimates on V reported here.

Silica Dissolution

The rate of silica dissolution in systems where silicic acid uptake may be occurring simultaneously can be measured by a reverse labeling technique which employs ^{28}Si, the most abundant isotope of silicon, as a tracer. In this procedure ^{30}Si-labeled silicic acid is added to a sample of whole natural seawater and the isotopic composition of the total silicic acid pool (ambient, plus added label) measured before and after an incubation. Dissolution of natural silica, containing silicon which is 92.18 atom % ^{28}Si, is measured as a increase in the ^{28}Si content of the dissolved silicic acid during the incubation period. Since dissolution is measured as a change in the isotopic composition rather than the total concentration of silicic acid the measurement is unaffected by biological uptake, which may alter the silicic acid concentration but is not isotopically selective.

This procedure is conceptually identical to the silicic acid uptake measurement method described earlier. In uptake measurements the rate

of conversion of ^{30}Si from dissolved to particulate matter is determined, while in dissolution rate measurements one determines the rate of conversion of ^{28}Si from the particulate to the dissolved form. The only differences between the two methods are those in the chemistry of sample preparation which result from the fact that in uptake rate measurements the isotopic composition of particulate silicon is measured, while in dissolution rate measurements the isotopic composition of dissolved silicic acid is determined. Measurement of the isotopic composition of dissolved silicic acid is accomplished by the conversion of silicic acid to silicomolybdic acid, $H_4SiMo_{12}O_{40}$, which is extracted into n-butanol to remove it from seawater. The silicomolybdic acid is later re-extracted into aqueous solution and converted into barium fluosilicate which is analyzed for silicon isotopes by solid sample mass spectrometry. The parallel nature of the uptake and dissolution rate procedures is illustrated in Figure 3.

Incubation of a sample

The same latitude in the choice of a sample and of incubation conditions is allowed in dissolution rate measurements as in uptake rate measurements. The one additional condition imposed on dissolution rate measurements is that while the initial atom % ^{30}Si of the particulate material in an uptake experiment is known to be the natural abundance of ^{30}Si, the initial atom % ^{28}Si of the dissolved silicic acid in a dissolution rate measurement is altered by the addition of $H_4{}^{30}SiO_4$, and must be measured. A seawater sample, after inoculation with ^{30}Si-labeled silicic acid is split in half. The silicic acid is

FIGURE 3

Summary of measured parameters and calculations employed in determining rates of silicic acid uptake and silica dissolution using ^{30}Si tracer techniques. Uptake and dissolution rate measurements are conceptually identical.

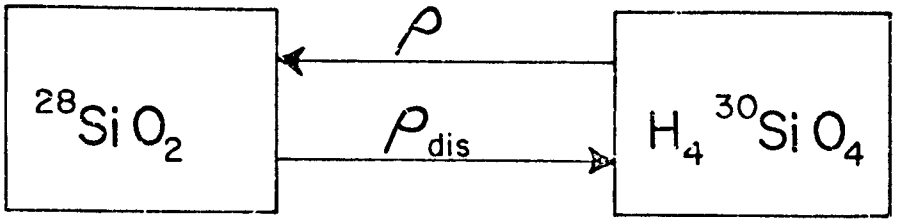

S_1	= CONCENTRATION OF PARTICULATE SILICON	S_2	= CONCENTRATION OF DISSOLVED SILICIC ACID
$^{30}A_n$	= INITIAL ATOM % ^{30}Si OF PARTICULATE SILICON	$^{28}A_i$	= INITIAL ATOM % ^{28}Si OF DISSOLVED SILICIC ACID
$^{30}A_i$	= INITIAL ATOM % ^{30}Si OF DISSOLVED SILICIC ACID	$^{28}A_n$	= INITIAL ATOM % ^{28}Si OF PARTICULATE SILICON
$^{30}A_f$	= FINAL ATOM % ^{30}Si OF PARTICULATE SILICON	$^{28}A_f$	= FINAL ATOM % ^{28}Si OF DISSOLVED SILICIC ACID
Δt	= INCUBATION TIME	Δt	= INCUBATION TIME
ρ	= ABSOLUTE UPTAKE RATE OF SILICIC ACID (CONC·TIME^{-1})	ρ_{dis}	= ABSOLUTE DISSOLUTION RATE OF SILICA (CONC·TIME^{-1})
V	= SPECIFIC UPTAKE RATE OF SILICIC ACID (TIME^{-1})	V_{dis}	= SPECIFIC DISSOLUTION RATE OF SILICA (TIME^{-1})

$$\rho = S_1\left(\frac{^{30}A_f - {}^{30}A_n}{\Delta t\,(^{30}A_i - {}^{30}A_n)}\right) \qquad \rho_{dis} = S_2\left(\frac{^{28}A_f - {}^{28}A_i}{\Delta t\,(^{28}A_n - {}^{28}A_i)}\right)$$

$$V = \frac{\rho}{S_1} \qquad V_{dis} = \frac{\rho_{dis}}{S_1}$$

extracted from one half of the sample immediately and from the other half after the incubation period. The incubation procedure is:

1. A sample is collected which is a little more than twice the volume of the sample to be incubated, and inoculated with ^{30}Si-enriched H_4SiO_4.

2. The sample is shaken vigorously to mix the labeled and natural H_4SiO_4, and a clean, non-glass incubation vessel rinsed with a small amount of inoculated sample.

3. The incubation vessel is filled with inoculated sample and set aside to incubate under conditions chosen by the investigator.

4. The remaining inoculated sample is filtered immediately through a 0.8 μm polycarbonate membrane filter into a clean polypropylene filter flask. The filter is retained for particulate silicon analysis.

5. 75 ml of 2:1 mixture of 0.03 M $(NH_4)_6\ Mo_7O_{24}$ and 1.0 N HCl is added to the filtrate. The solution is allowed to react for twenty minutes, during which a yellow color develops due to the formation of $H_4SiMo_{12}O_{40}$. The $(NH_4)_6\ Mo_7O_{24}$-HCl mixture must be made up fresh the day the experiment is performed.

6. The solution is transferred to a clean polypropylene separatory funnel. 100 ml of 6.0 N HCl is added, followed by 200 ml of reagent grade n-butanol. The sample is shaken vigorously and then allowed to separate for five to ten minutes. At this point the yellow $H_4SiMo_{12}O_{40}$ has migrated from the aqueous to the butanol phase. This is a modification of the solvent extraction procedure of Schink (1965) and is

employed as an initial step in concentrating and separating silicon from seawater.

7. The aqueous phase is discarded and the butanol phase stored in a clean polyethylene bottle until analyzed for silicon isotopes.

8. At the end of the incubation period steps (4) through (7) are repeated on the incubated sample.

Isotopic analysis of dissolved silicon

Silicon is re-extracted from n-butanol into aqueous solution and analyzed isotopically by conversion to barium fluosilicate followed by solid sample mass spectrometry. The procedure is:

1. The butanol extract is transferred to a 250 ml polypropylene separatory funnel and any aqueous phase discarded. During storage the butanol extracts may have turned from yellow to green or blue. This is due to the reduction of $H_4SiMo_{12}O_{40}$ to a high molecular weight complex, and does not adversely affect the sample.

2. 2.0 ml of 45% KOH solution is added. The sample is shaken vigorously and allowed to separate for five to ten minutes. The resulting butanol phase is clear, and the aqueous phase (*ca.* 10 ml due to the decreased miscibility of water and n-butanol of high pH) clear to dark blue depending on the amount of reduced silicomolybdate complex formed during sample storage. The aqueous phase is collected in a 20 ml platinum crucible, and the butanol phase discarded.

3. The crucible is covered and the sample heated gently on a hot plate for 30-45 minutes or until all blue color has disappeared and there is no strong odor of butanol.

4. Concentrated HCl is added dropwise until a bright yellow color ($H_4SiMo_{12}O_{40}$) appears.

5. 45% KOH is added dropwise (usually one or two drops) until the yellow color disappears. The purpose of steps (4) and (5) is to ensure that silicon is present as H_4SiO_4 in neutral aqueous solution.

6. The crucible is removed from the hot plate, four drops of 49% HF added and the sample allowed to cool to room temperature. In this step H_4SiO_4 is converted quantitatively to H_2SiF_6.

7. The sample is transferred to a 15 ml disposable polystyrene centrifuge tube, and ten drops of 45% KOH added. In this step H_2SiF_6 is dissociated and K_2SiF_6, a white precipitate, forms. This is the final step in the separation of silicon from the other dissolved species in seawater, as the potassium salts of all other anions in solution, chiefly Cl^-, F^-, $So_4^=$, and $Mo_4^=$ are highly soluble and only K_2SiF_6 precipitates. One hour is allowed for complete precipitation.

8. The sample is centrifuged at 1,500 · g for five minutes. The supernatant is discarded and the precipitate resuspended in 0.5 ml of distilled water.

9. One drop of concentrated HCl is added, and the precipitate is dissolved.

10. Four drops of 1.0 M $BaCl_2$ are added and another white precipitate, $BaSiF_6$, forms. One hour is allowed for complete precipitation.

11. The $BaSiF_6$ is washed with water and absolute methanol, dried and analyzed for silicon isotopic composition in exactly the same manner as the $BaSiF_6$ produced from particulate silicon samples.

As with particulate silicon filters to be analyzed for ^{30}Si uptake, the butanol extracts can be run in batches. The size of a batch is limited by the number of platinum crucibles available, and two to three batches can be prepared in a normal day. A schematic of the overall sample preparation and analysis procedure for both uptake and dissolution rate experiments is given in Figure 2.

Dissolution rate calculation

As in uptake rate measurements, the mass spectrometric data consist of three peaks at m/e = 85, 86, and 87, whose relative heights, I_{85}, I_{86}, and I_{87} represent the relative abundances of the three stable isotopes of silicon in the sample. However, in this case, no carrier silicon is added in the sample preparation because the dissolved silicic acid samples always contain enough silicon to produce a strong mass spectrometer signal. I_{85}, I_{86}, and I_{87}, therefore, directly reflect the relative abundances of $H_4{}^{28}SiO_4$, $H_4{}^{29}SiO_4$, and $H_4{}^{30}SiO_4$ in the sample at the time it was filtered.

It is possible to calculate $S_{2(t)}$, the total silicic acid concentration (ambient, plus label) of the seawater sample prior to incubation, by isotope dilution using the mass spectrum of the sample filtered immediately after inoculation. Since

$$\frac{S_{2(t)}}{[H_4{}^{30}SiO_4]} = \frac{I_{85} + I_{86} + I_{87}}{I_{87}} \tag{23}$$

and since

$$[H_4{}^{30}SiO_4] = \frac{{}^{30}A_1 \cdot v_1}{100v_s} \cdot S_{2(\ell)} \tag{24}$$

where $^{30}A_{\ell}$ is the atom % ^{30}Si of the labeled silicic acid, v_{ℓ} the volume of labeled silicic acid solution added, v_s the total sample volume at the time of inoculation and $S_{2(\ell)}$ the silicic acid concentration of the added labeled solution.

Combining equations (23) and (24):

$$S_{2(t)} = S_{2(\ell)} \left(\frac{^{30}A_{\ell} \cdot v_{\ell} \cdot (I_{85} + I_{86} + I_{87})}{100 \cdot v_s \cdot I_{87}} \right) \qquad (25)$$

The atom % ^{28}Si of the silicic acid at the beginning and at the end of the incubation, $^{28}A_i$ and $^{28}A_f$, respectively, are calculated from the mass spectra of the silicon isolated from pre-incubation and post-incubation seawater samples using the following relationships:

$$^{28}A_i = \left(\frac{100\ I_{85}}{I_{85} + I_{86} + I_{87}} \right)_i \qquad (26)$$

$$^{28}A_f = \left(\frac{100\ I_{85}}{I_{85} + I_{86} + I_{87}} \right)_f \qquad (27)$$

at this point ρ_{dis}, the absolute dissolution rate of silica can be calculated from the difference between $^{28}A_i$ and $^{28}A_f$ using an equation of the form suggested by Sheppard (1962):

$$\rho_{dis} = S_{2(t)} \left(\frac{^{28}A_f - {}^{28}A_i}{\Delta t(^{28}A_n - {}^{28}A_i)} \right) \qquad (28)$$

where $^{28}A_n$ is the atom % ^{28}Si of natural silicon (= 92.18). ρ_{dis} can

be divided by S_1, the particulate silicon concentration to give V_{dis} the specific dissolution rate of particulate silicon:

$$V_{dis} = \frac{\rho_{dis}}{S_1} \tag{29}$$

V_{dis} has dimensions of time^{-1} and can be compared directly with V, the specific uptake rate of silicon to determine the balance between gains and losses of particulate silicon in a natural seawater sample.

Errors in dissolution rate measurement

Equations (25) and (28) show that the value obtained for ρ_{dis} is dependent upon the following measured parameters: $S_{2(\ell)}$, v_ℓ, v_s, Δt, $^{28}A_i$, and $^{28}A_f$. $S_{2(\ell)}$ is not determined by colorimetric analysis, but computed at the time the labeled solution is prepared and is dependent upon the weight of ^{30}Si-enriched silica added to the crucible and the volume of the final solution after fusion with sodium carbonate. Therefore with normal care $S_{2(\ell)}$, v_ℓ, v_s, and Δt are all known to within ±1%. The precision of $^{28}A_i$ and $^{28}A_f$ depends upon the characteristics of the individual mass spectrometer used in the analysis. Repetitive analysis of isotopic standards on the Finnigan Corporation quadrupole instrument used in these studies indicates that the internal precision of an isotopic abundance measurement is ±0.1 atom % at the 95% confidence level. Errors of 0.1 atom % in $^{28}A_i$ or $^{28}A_f$ can have a pronounced effect on the precision of ρ_{dis}, which is proportional to $(^{28}A_f - {}^{28}A_i)$, especially when the difference is small. Table 5 indicates the percent error which is introduced into estimates of ρ_{dis} based on data from station 122 of *ATLANTIS II* cruise 082 off the

Northwest coast of Africa if a maximum error of 0.2 atom % is assumed for the quantity ($^{28}A_f - {}^{28}A_i$) and substituted into equation (28) to compute α_{dis}, the maximum error in ρ_{dis} arising from mass spectrometric error.

TABLE 5

Estimates of ρ_{dis} and errors in ρ_{dis} from station AII-082-122 May, 1974

Depth (m)	ρ_{dis} (μg atoms $Si \cdot \ell^{-1} \cdot hr^{-1}$)	α_{dis} (μg atoms $Si \cdot \ell^{-1} \cdot hr^{-1}$)	% error $\left(\frac{100\alpha_{dis}}{\rho_{dis}}\right)$
0	0.0060	0.0030	50.0
2	0.0017	0.0030	176.0
4	0.0199	0.0030	15.1
12	0.0163	0.0031	19.0
23	0.0265	0.0031	11.7
42	0.0843	0.0034	4.1

It can be seen from Table 5 that errors in ρ_{dis} introduced by errors in mass spectrometry vary inversely with the value of ρ_{dis}, and are always large compared with errors from other sources. Therefore, α_{dis} can be considered a maximum estimate of the overall error in the measurement of ρ_{dis}.

Equation (29) shows that the value of V_{dis} is dependent upon ρ_{dis} and S_1, the particulate silicon concentration. S_1 has been determined by the sodium carbonate fusion technique of Busby and Lewin (1967),

which is subject to errors of ±10%, and also by the isotope dilution procedure outlined earlier in this chapter. It has been tentatively concluded that the isotope dilution technique is subject to substantially less than 10% error, but until this is proven more conclusively the error in S_1 will be considered to be ±10% and the error reported in V_{dis} will be $\pm\left(\frac{100\alpha_{dis}}{\rho_{dis}}\right)$ or ±10%, whichever is greater.

CHAPTER III

KINETICS OF SILICIC ACID UPTAKE AND RATES OF SILICA DISSOLUTION IN THE MARINE DIATOM *THALASSIOSIRA PSEUDONANA*

A number of studies of the kinetics of silicic acid uptake (Davis, 1973; Goering, Nelson and Carter, 1973; Paasche, 1973 b; Harrison, 1974) and silicon limited growth (Guillard, Kilham and Jackson, 1973; Paasche, 1973 a; Harrison, 1974) of diatoms have been conducted, with results which are remarkably consistent with one another, considering the differences in organisms studied and experimental procedures employed. Maximum specific uptake rates of silicon and maximum growth rates both tend to fall within a range of 0.02 to 0.12 hr^{-1}. Uptake kinetic studies have all generated data which can be fit by rectangular hyperbolas and indicate that the uptake rate is strongly dependent upon the external substrate concentration in the range of 0 to 5 μg atoms Si · ℓ^{-1}. Growth kinetic studies have produced contradictory data on the precise nature of the limitation imposed on the growth rate of diatoms at low silicic acid concentrations (i.e., whether equation (5) or (6) or neither describes silicon limited growth kinetics). However, all show growth rates to be substantially less than maximum at silicic acid concentrations of 0 to 2 μg atoms Si · ℓ^{-1}.

Guillard, Kilham and Jackson (1973) have studied the silicon limited growth kinetics of *Thalassiosira pseudonana* in batch culture. Two physiologically distinct races of *T. pseudonana* have been isolated (Guillard and Ryther, 1962), one (clone 3H) from a coastal estuary and

the other (clone 13-1) from the Sargasso Sea. Guillard, Kilham and Jackson (1973) suggested that physiological differences between clones 3H and 13-1 represent genetic adaptations to high and low nutrient environments, respectively. They suggested that the two strains of *T. pseudonana* may conform to the hypothesis of Kilham (1971) which predicts that diatoms adapted to high silicon environments should have high values of μ_{max} and K_S when compared with diatoms adapted to low silicon environments. By this hypothesis diatoms with the highest V_{max} values should grow at a faster rate than other diatoms when silicic acid is abundant, while those with low K_S values should have a competitive growth advantage under conditions of silicon limitation. They interpreted their growth rate data to confirm such an hypothesis, with the estuarine clone demonstrating a higher growth rate than the Sargasso Sea clone at silicic acid concentrations higher than *ca.* 1 μg atom Si · ℓ^{-1}, and the reverse being true at silicic acid concentrations less than *ca.* 1 μg atom Si · ℓ^{-1}. Paasche (1973 a) studied the kinetics of silicon limited growth of clone 3H in a chemostat and obtained kinetic constants which are very similar to those of Guillard, Kilham and Jackson if calculated according to equation (5). He found, however, that his data were fitted poorly by equation (5) at low growth rates and that an hyperbola of the form described by equation (6) provided a better description of his data. Divergences of silicon limited growth rate data from equation (5) in a chemostat at low growth rates have also been reported for *Skeletonema costatum* (Harrison, 1974).

Paasche (1973 b) determined the kinetic parameters of silicic acid

uptake in five diatom species, including *T. pseudonana* (clone 3H) in batch culture. His data are best fit by equation (4) with a value of S_0 which ranges from 0.32 to 1.33 μg atoms Si · ℓ^{-1}. Because of the possible masking of low uptake rates by dissolution of cellular silica, he recognized that S_0 may be an artifact in experiments where the uptake rate is determined from a change in external substrate concentration. However, he attempted to correct for dissolution by measuring dS_2/dt in a medium containing cells killed by freezing. He found that V_{dis} was high, on the order of 10 to 20% of V_{max}, but that a positive value of S_0 persisted even after his data were corrected for dissolution. He interpreted S_0 to be the concentration of a chemical form of silicon which is reactive in a colorimetric acid-molybdate analysis but not available to the cell.

This chapter is a report of a study of the silicic acid uptake kinetics of *T. pseudonana* clones 3H and 13-1 using ^{30}Si tracer techniques in batch culture and of first attempts to measure silica dissolution rates in healthy, growing diatom populations.

Procedures

All experiments were carried out in the laboratory of R. R. L. Guillard at Woods Hole Oceanographic Institution using his unialgal cultures of *T. pseudonana* clones 3H and 13-1. Experiments were performed on cells which were in two presumably different physiological states: silicon replete, cells harvested directly from high silicic acid medium (f/2 (Guillard and Ryther, 1962)), and silicon depleted, cells allowed

to grow in silicon free f/2 medium for two or three days before being harvested for the experiment. Inocula were prepared by filtering the stock cultures at 170-260 g $\cdot$ cm^{-2} vacuum until a cell density of *ca.* 10^8 cells $\cdot$ ml^{-1} was obtained, as determined by cell counts in a hemocytometer. This provided a particulate silicon concentration of 2 to 4 µg atoms Si $\cdot$ ml^{-1} in the inoculum. Inocula of silicon depleted cells were added to the experimental vessels immediately after concentration, while inocula of silicon replete cells were maintained in the light for about two hours, during which the silicic acid concentration of the inoculum was reduced to < 1 µg atom Si $\cdot$ ℓ^{-1}.

Low silicon seawater was prepared by allowing diatoms to remove silicon from Sargasso Sea surface water stored in polyethylene bottles and subsequently removing the cells by filtration through 0.8 µm polycarbonate membrane filters. Two batches of low silicon water were obtained; one was measured by the colorimetric acid-molybdate method of Strickland and Parsons (1968) to have a silicic acid concentration of 0.8 µg atom Si $\cdot$ ℓ^{-1} and the other 0.3 µg atom Si $\cdot$ ℓ^{-1}. The 0.3 µg atom Si $\cdot$ ℓ^{-1} water was used in experiments where labeled silicic acid was added at concentrations of 7.0 µg atoms Si $\cdot$ ℓ^{-1} or less, while the 0.8 µg atom Si $\cdot$ ℓ^{-1} water was used in experiments conducted at higher silicic acid concentrations. ^{30}Si isotope dilution analyses performed as part of the dissolution rate measurements indicated that the silicic acid concentration of the "0.8 µg atom Si $\cdot$ ℓ^{-1}" water was actually 0.2 to 0.3 µg atom Si $\cdot$ ℓ^{-1} and that the "0.3 µg atom Si $\cdot$ ℓ^{-1}" water contained no detectable silicic acid.

In each uptake kinetic experiment the following series of experimental flasks was prepared:

TABLE 6

Series of silicic acid concentrations, inoculum volumes and medium volumes employed in silicic acid uptake kinetic experiments on *Thalassiosira pseudonana*, clones 3H and 13-1, using ^{30}Si tracer techniques.

S_2 (from added label) (μg atoms $Si \cdot \ell^{-1}$)	Inoculum Volume(ml)	Medium Volume(l)	Flask Material	Parameter measured
0.25	1.0	2.0	Pyrex	V
0.50	1.0	2.0	Pyrex	V
1.50	1.0	1.0	Pyrex	V
2.50	1.0	1.0	Pyrex	V
3.50	1.0	1.0	Pyrex	V
7.00	1.0	1.0	Pyrex	V
10.00	2.0	2.0	Polycarbonate	V & V_{dis}
15.00	2.0	2.0	Polycarbonate	V & V_{dis}

The medium in each of the two polycarbonate flasks was split in half immediately. One half was retained for incubation and the other filtered through a 0.8 μm membrane filter. The filter was retained for particulate silicon analysis and the filtrate analyzed for $^{28}A_i$ as described in Chapter II. The eight flasks were then covered with Pyrex petri dishes and incubated for four hours at 20 C and 3,500 lux. To keep the incubation time constant flasks were inoculated and started incubating in groups of two or three at 30-minute intervals. This procedure allowed each sample to be filtered immediately after removal from the

incubation chamber. To minimize depletion of silicic acid in the medium during the incubation, samples incubated at silicic acid concentrations of 0.25 and 0.50 µg atom Si · ℓ^{-1} contained half the cell density (10^8 cells · $2\ell^{-1}$ vs. 10^8 cells · ℓ^{-1}) of the other samples. It was estimated, based upon the data of Paasche (1973 b), that under the conditions described in Table 6 less than 10% of the silicic acid in each flask would be consumed in a four-hour incubation.

At the end of the four-hour incubation each sample was filtered through a 0.8 µm membrane filter and the filter retained for analysis of ^{30}Si uptake. The filtrate from the six Pyrex flasks was discarded and that from the two polycarbonate flasks analyzed for $^{28}A_f$ as described in Chapter II. All filters and butanol extracts were returned to the University of Alaska for silicon isotopic analysis.

Two experiments were performed to determine the light dependence of silicic acid uptake in silicon depleted populations of clone 3H. 1.0 ml of inoculum was added to each of sixteen 250 ml Pyrex Erlenmeyer flasks containing 200 ml of low silicon seawater. Sufficient ^{30}Si labeled silicic acid was added to achieve a concentration of 2.5 µg atoms Si · ℓ^{-1} in eight flasks and 25.0 µg atoms Si · ℓ^{-1} in the other eight. These experiments were designed to determine the light dependence of instantaneous rates of silicic acid uptake under silicon unlimited and silicon limited conditions, respectively. Each series of eight flasks was incubated for four hours at the following series of light intensities: 0, 75, 350, 650, 1,300, 2,700, 4,300, and 10,300 lux. Incubations were initiated in groups of four at 30-minute intervals to allow immediate

filtration of each sample at the end of the incubation. The filters were retained for analysis of ^{30}Si uptake and the filtrates discarded.

In all uptake rate experiments the specific uptake rate, V, was calculated according to equation (21) and in dissolution rate experiments the specific dissolution rate, V_{dis}, was computed using equation (29). In all kinetic experiments V was plotted versus S_2, and in those plots where it was determined visually that the dependence of V upon S_2 was describable by a rectangular hyperbola the kinetic parameters V_{max} and K_T were determined by a least squares fit of a straight line to a plot of $S_2 \cdot V^{-1}$ versus S_2, which is based upon a linearized form of equation (3):

$$\frac{S_2}{V} = \frac{K_T + S_2}{V_{max}} \qquad (30)$$

where the value of S_2 at the X-intercept is $-K_T$ and the value of $S_2 \cdot V^{-1}$ at the Y-intercept is $K_T \cdot V_{max}^{-1}$ (Goering, Nelson and Carter, 1973).

Results

Concentration dependence of uptake rate

Plots of V versus S_2 for silicon replete and depleted 3H, and silicon replete and depleted 13-1 are given in Figure 4. All four plots are approximately hyperbolic, although if the dependence of V upon S_2 in silicon replete 3H is hyperbolic, V_{max} does not occur within the concentration range used in these experiments. Plots of $S_2 \cdot V^{-1}$ versus S_2 were constructed for these four kinetic experiments (Figures 5a, b, c, and d).

FIGURE 4

Plot of the specific uptake rate of silicic acid, V, versus silicic acid concentration, S_2, for clones 3H and 13-1 of *Thalassiosira pseudonana*.

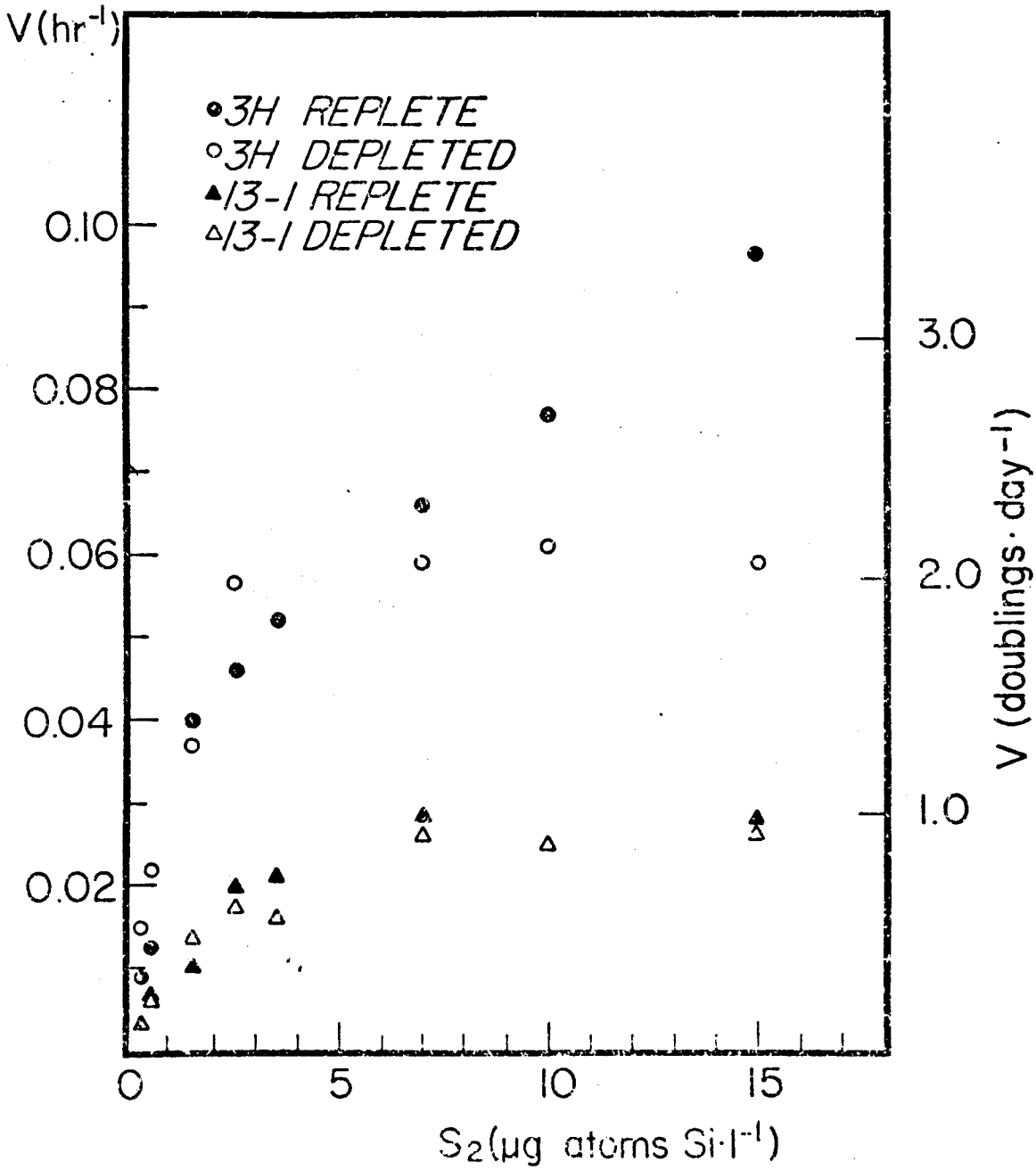
V(hr⁻¹)
3H REPLETE
3H DEPLETED
13-1 REPLETE
13-1 DEPLETED
0.10
0.08
0.06
0.04
0.02
3.0
2.0
1.0
V (doublings · day⁻¹)
0
5
10
15
S₂(µg atoms Si·l⁻¹)

FIGURE 5

Linearized plot of data from Figure 4 to determine the kinetic parameters V_{max} and K_T.

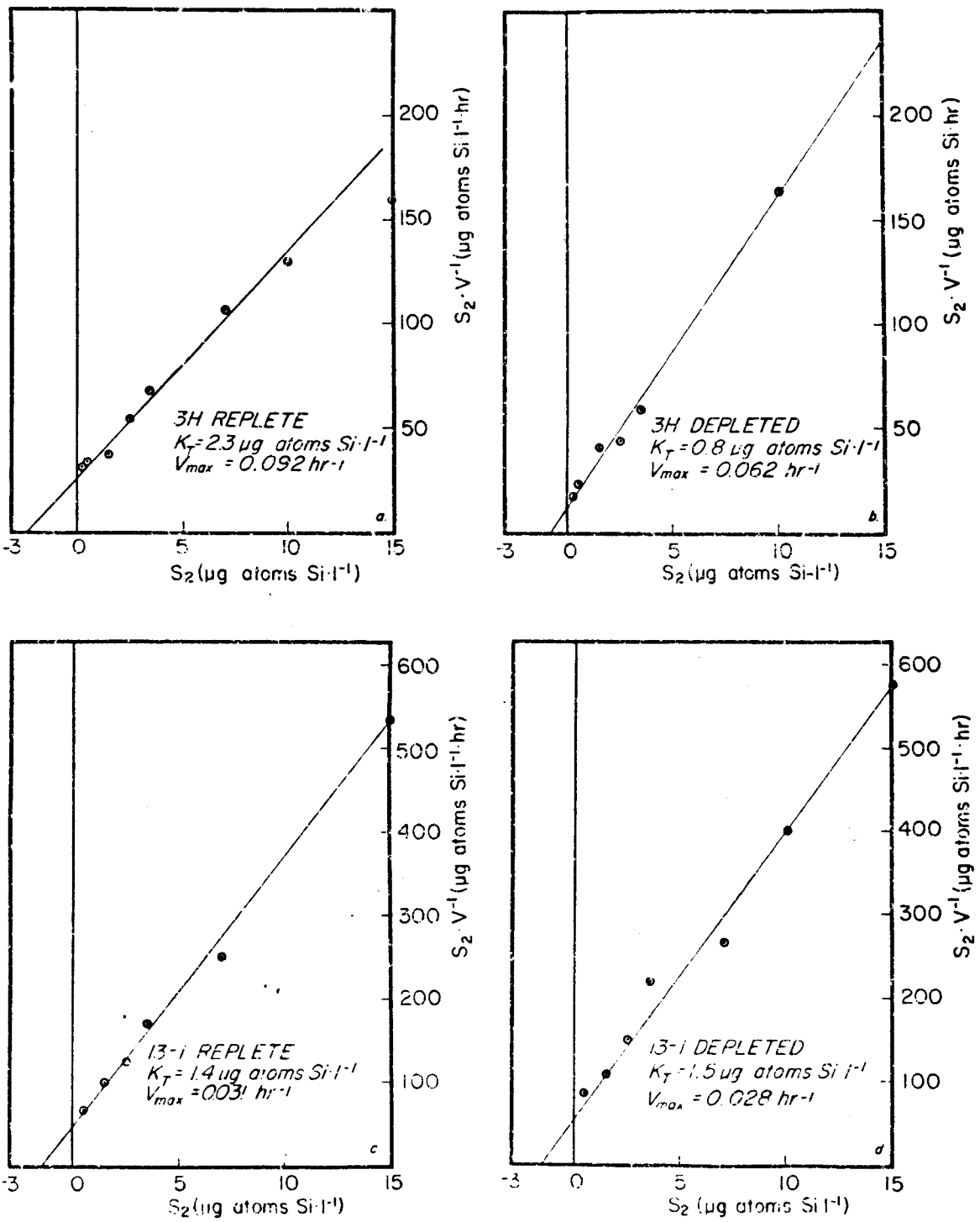
3H REPLETE
K_T = 2.3 µg atoms Si·l⁻¹
V_{max} = 0.092 hr⁻¹
a.
3H DEPLETED
K_T = 0.8 µg atoms Si·l⁻¹
V_{max} = 0.062 hr⁻¹
b.
13-1 REPLETE
K_T = 1.4 µg atoms Si·l⁻¹
V_{max} = 0.031 hr⁻¹
c
13-1 DEPLETED
K_T = 1.5 µg atoms Si l⁻¹
V_{max} = 0.028 hr⁻¹
d
S_2 (µg atoms Si·l⁻¹)
$S_2 \cdot V^{-1}$ (µg atoms Si·l⁻¹·hr)
-3
0
5
10
15
50
100
150
200
300
400
500
600

The parameters V_{max} and K_T were computed using equation (30) and are presented in Table 7.

TABLE 7

Kinetic parameters of silicic acid uptake in *Thalassiosira pseudonana*, clones 3H and 13-1

Experiment	$V_{max}(hr^{-1})$	$K_T(\mu g \text{ atoms } Si \cdot \ell^{-1})$
3H Replete*	0.092	2.3
3H Depleted	0.062	0.8
13-1 Replete	0.031	1.4
13-1 Depleted	0.028	1.5

Figure 5a shows a considerable divergence of the data on silicon replete 3H from the hyperbolic model defined by equations (3) and (30), but Figures 5b, c, and d confirm that this model is a good description of the results of the other three uptake kinetic experiments. Figure 4 indicates that a threshold silicic acid concentration, S_0, is not required to describe the results of these uptake kinetic experiments.

Light dependence of uptake rate

Plots of V versus light intensity for silicon depleted 3H under silicon unlimited (25.0 μg atoms Si · ℓ^{-1}) and silicon limited (2.5 μg atoms Si · ℓ^{-1}) conditions are presented in Figure 6. These data clearly do not conform to a rectangular hyperbola, so the kinetic parameters V_{max} and K_{LT} (MacIsaac and Dugdale, 1972; Davis, 1973; Goering, Nelson and Carter, 1973) are not applicable. Instead the uptake rate of

* V versus S_2 curve is not hyperbolic so parameters V_{max} and K_T have little meaning.

FIGURE 6

Plot of the specific uptake rate of silicic acid, V, versus light intensity for clone 3H of *Thalassiosira pseudonana* when substrate concentration is limiting (2.5 µg atoms Si · ℓ^{-1}) and non-limiting (25.0 µg atoms Si · ℓ^{-1}) to uptake.

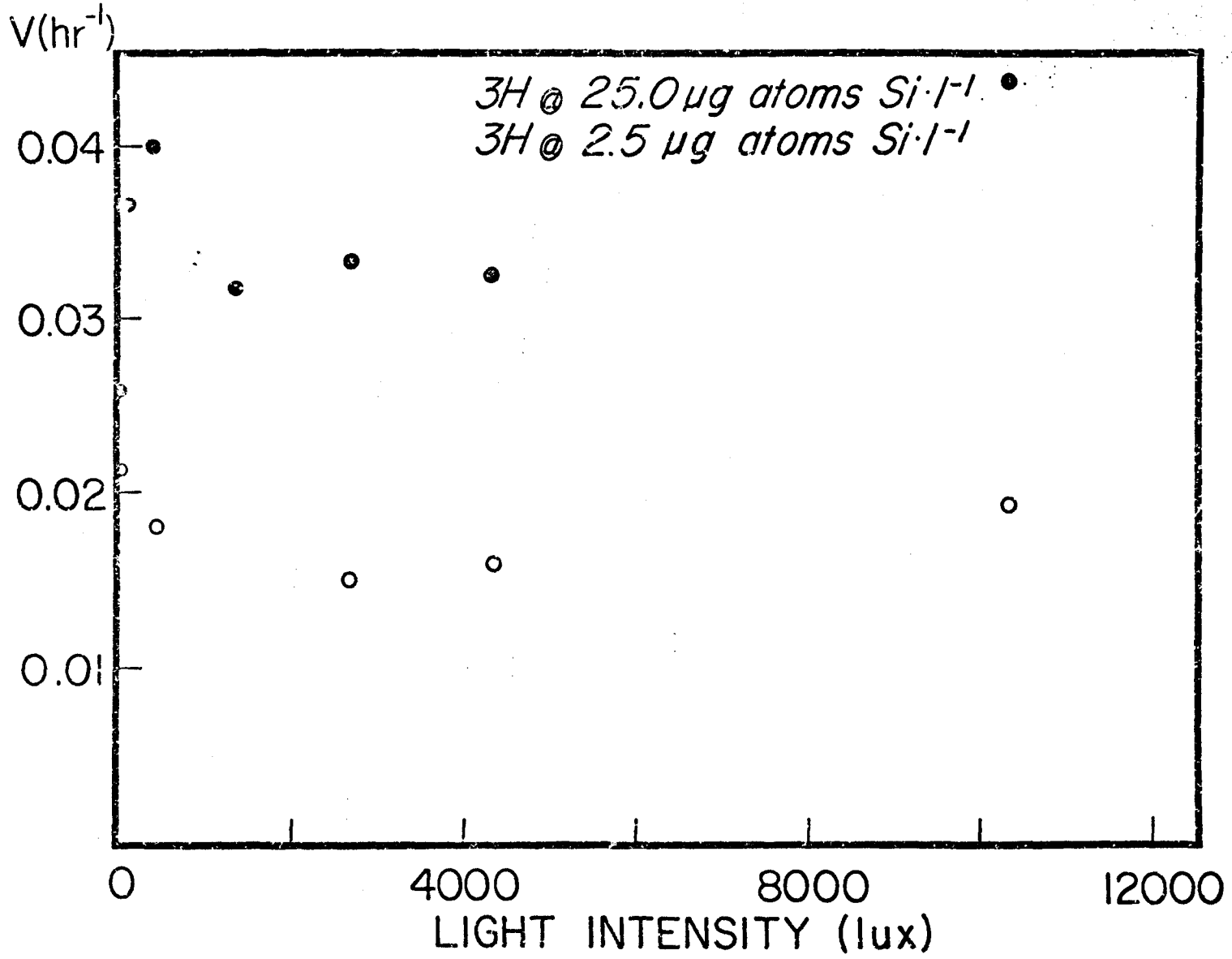
V(hr⁻¹)
0.04
0.03
0.02
0.01
3H @ 25.0 µg atoms Si·l⁻¹
3H @ 2.5 µg atoms Si·l⁻¹
0
4000
8000
12000
LIGHT INTENSITY (lux)

silicic acid is independent of light intensity at low silicic acid concentration, and only weakly light dependent under conditions of saturating substrate concentration.

Silica dissolution

Results of dissolution rate experiments on clones 3H and 13-1 of *Thalassiosira pseudonana* are presented in Table 8. Error estimates are explained in Chapter II and are large due to the relatively short (four-hour) incubation time employed.

TABLE 8

Specific dissolution rates of exponentially growing populations of *Thalassiosira pseudonana* clones 3H and 13-1, measured by the ^{30}Si tracer method.

Dissolution Rate Experiment	$V_{dis}(hr^{-1})$
3H Replete	0.0075 ± 0.0040
3H Depleted	0.0085 ± 0.0040
13-1 Replete	0.0020 ± 0.0040
13-1 Depleted	0.0043 ± 0.0040

However, even with the large uncertainties imposed by the short incubation time it is evident that there is dissolution of silica from diatom populations which are growing exponentially. These populations were taking up silicic acid at a rate sufficient to mask the dissolution rate in experiments which measure dissolution by determining dS_2/dt.

Discussion

Threshold concentration for silicic acid uptake

Figures 4 and 5 indicate that the rate of silicic acid uptake in *T. pseudonana* is dependent upon the external substrate concentration in the range of 0.25 to 15.0 μg atoms Si · ℓ^{-1}, and that this dependence may be described by equation (3). The data of Paasche (1973 b) which indicated a threshold silicic acid concentration of *ca.* 0.67 μg atom Si · ℓ^{-1}, below which no uptake takes place in *T. pseudonana* are not confirmed by these experiments. Paasche recognized that S_0 can be an experimental artifact in studies which measure uptake from dS_2/dt if the raw data are not corrected for dissolution of cellular silica or if the dissolution rate is underestimated. Comparison of Tables 7 and 8 indicates that V_{dis} ranged from 6.5 to 15% of V_{max} in these tracer experiments which is in good general agreement with Paasche's estimate of 10 to 20%. If anything, the measured values of V_{dis} are somewhat lower than Paasche's estimates, making it unlikely that his observation of a threshold concentration is a simple artifact arising from failure to correct his data adequately for silica dissolution. However, Paasche's interpretation of S_0 as the concentration of some molybdate-reactive but biologically unavailable form of silicon is difficult to reconcile with the present understanding of the inorganic aqueous chemistry of silicon (Stumm and Morgan, 1970). Both Paasche's (1973 b) observations of the existence of a threshold substrate concentration for silicic acid uptake and the observations reported here of the absence of such a threshold are based upon small numbers of experiments, so the question must be considered unresolved.

Silicic acid uptake kinetics and silicon limited growth kinetics in clones 3H and 13-1

The silicic acid uptake kinetic studies reported here (Figure 4) provide support for one of the two conclusions drawn by Guillard, Kilham and Jackson (1973) concerning adaptation of clones 3H and 13-1 to high and low silicon environments, respectively. V_{max} for the estuarine clone 3H clearly exceeds that of the Sargasso Sea clone 13-1, and by approximately the same amount (*ca.* 1 doubling · day^{-1}) that μ_{max} for clone 3H was found to exceed μ_{max} for clone 13-1.* Thus in a high silicon environment which initially contains a mixture of the two strains of *T. pseudonana* the ratio of 3H to 13-1, expressed either in number of cells or in silicon content of the population should roughly double each day, resulting eventually in a population dominated by 3H regardless of its initial composition.

Although the difference between V_{max} for 3H and V_{max} for 13-1 is almost identical to the difference in μ_{max} reported for these same two clones, comparison of the two sets of data shows that for both 3H and 13-1:

$$V_{max} \simeq \mu_{max} - 1 \text{ doubling} \cdot \text{day}^{-1} \qquad (31)$$

That is, at saturating silicic acid concentrations and maximal growth rates the cell quota, Q, for silicon is decreasing by half each day in both populations. A similar difference between V_{max} and μ_{max} for clone 3H is reported by Paasche (1973 a and b). During vegetative cell

* The growth rate experiments of Guillard, Kilham and Jackson (1973) were performed on silicon depleted populations, so their μ_{max} should be compared with V_{max} reported here for silicon depleted 3H and 13-1.

division of diatoms the average cell size, and therefore the cell quota for any element, decreases with time and would result in a difference between V_{max} and μ_{max} in the direction of that described by equation (31). The data of Davis (1973) and Harrison (1974) on uptake and growth kinetics of *Skeletonema costatum* in chemostats do not conform to equation (31), which is to be expected since a chemostat is designed to eliminate changes in the population, including changes in cell mass and cell quota, with time. It is likely that equation (31) reflects a transient state of the population in batch culture, namely $\frac{dQ}{dt} \neq 0$, which would not have been apparent in either the growth kinetic study or the uptake kinetic study taken alone.

The observation of Guillard, Kilham and Jackson (1973) that clone 13-1 has a significantly lower K_S for silicon limited growth than clone 3H is not reflected by any similar difference between the K_T values for silicic acid uptake in the two strains. While clone 3H clearly demonstrates higher rates of both silicon uptake and growth at high silicic acid concentrations, clone 13-1 fails to demonstrate any greater efficiency than clone 3H to take up silicon at silicic acid concentrations down to 0.25 μg atom Si · ℓ^{-1}. The hyperbolas fitted to the μ versus S_2 data of Guillard, Kilham and Jackson (1973) indicate that clone 13-1 should grow at a higher rate than 3H at silicic acid concentrations less than *ca.* 1 μg atom Si · ℓ^{-1}. However, their raw data demonstrate a higher growth rate for 3H than for 13-1 at all silicic acid concentrations, although growth rates of the two clones were very nearly equal at S_2 values of 0.32, 1.06, and 1.50 μg atoms Si · ℓ^{-1}. If the concepts of

silicon limited growth kinetics in *Skeletonema costatum* developed by Davis (1973) and Harrison (1974) are correct and applicable to *Thalassiosira pseudonana*, then the data of Guillard, Kilham and Jackson (1973) may be fit more appropriately by truncated, rather than intersecting hyperbolas. The non-existence of a crossover point between μ versus S_2 curves for clones 3H and 13-1 is strongly supported by results of uptake kinetic experiments reported here (Figure 4), in which curves of V versus S_2 for the two clones clearly do not intersect.

One troubling point if the above interpretations of experimental data are correct is the apparent absence in either the growth rate or uptake rate data of any evidence of adaptation in the Sargasso Sea clone, 13-1, to enhance its fitness in a low silicon environment. Neither set of experiments provides proof of such an adaptation if taken alone, but comparison of the two sets of kinetic data indicates that an adaptation of this type may exist. Superimposing curves of $V \cdot V_{max}^{-1}$ over curves of $\mu \cdot \mu_{max}^{-1}$, both versus S_2 (Figures 7a and b) indicates that silicic acid concentrations less than *ca.* 5 µg atoms Si $\cdot \ell^{-1}$ may be much more severely limiting to silicic acid uptake than to growth ($V \cdot V_{max}^{-1} < \mu \cdot \mu_{max}^{-1}$) in clone 13-1. Nearly the opposite is true of clone 3H where in the region between *ca.* 2 µg atoms Si $\cdot \ell^{-1}$ and 6 µg atoms Si $\cdot \ell^{-1}$ silicic acid uptake may be less inhibited than cell growth ($V \cdot V_{max}^{-1} > \mu \cdot \mu_{max}^{-1}$). A greater number of experiments is necessary to establish whether Figures 7a and b represent a consistent difference between the two races of *T. pseudonana*, but if they do then clone 13-1 has the ability, which clone 3H lacks, to adjust its cellular

FIGURE 7

Plots of $\mu \cdot \mu_{max}^{-1}$, calculated from data of Guillard, Kilham and Jackson (1973) and $V \cdot V_{max}^{-1}$ from experiments reported here for clones 3H and 13-1 of *Thalassiosira pseudonana*.

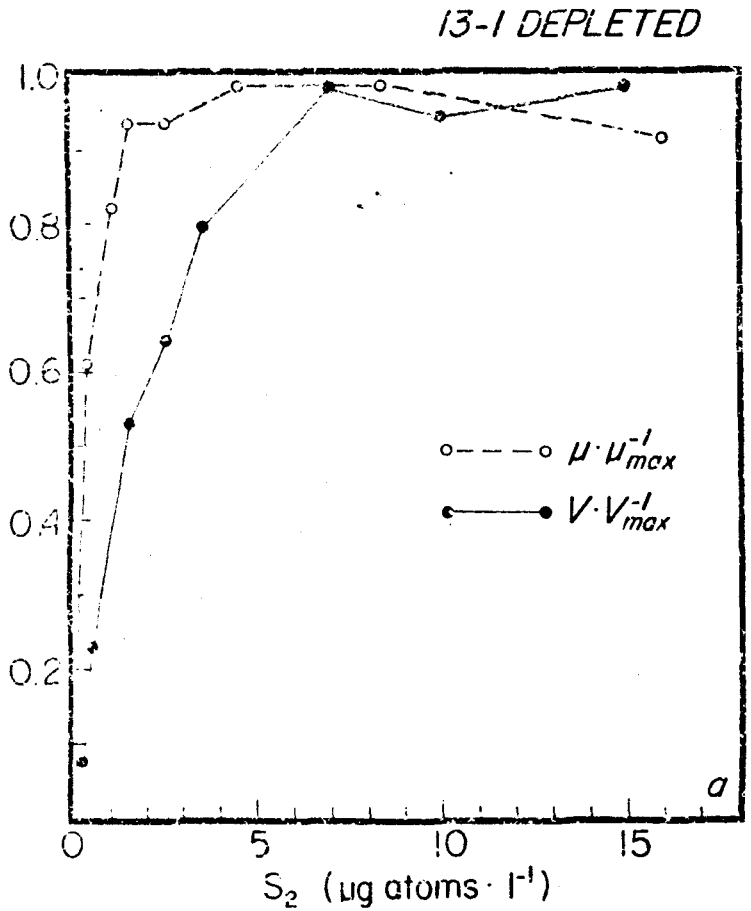
13-1 DEPLETED
1.0
0.8
0.6
0.4
0.2
0
5
10
15
S_2 (µg atoms · l^{-1})
$\mu \cdot \mu_{max}^{-1}$
$V \cdot V_{max}^{-1}$
a

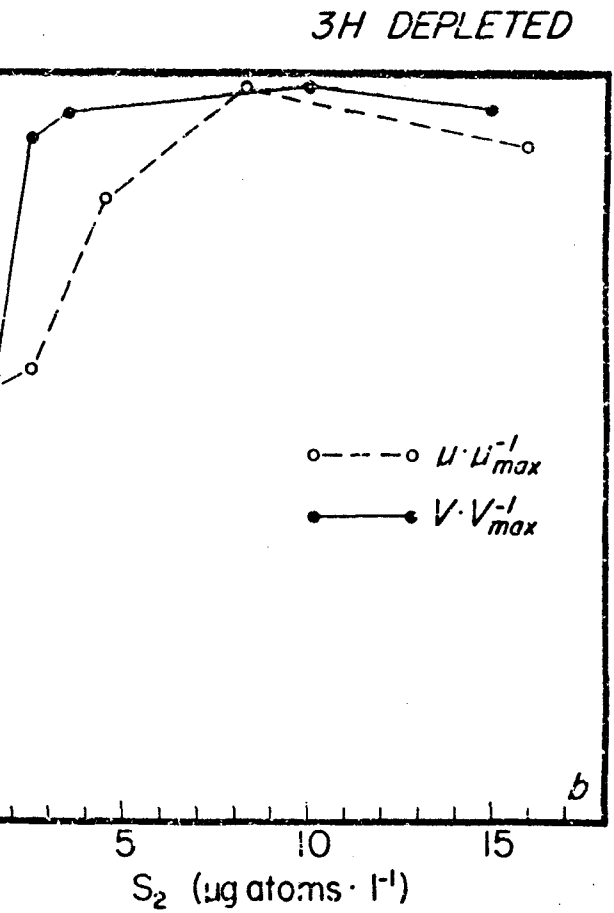
3H DEPLETED
$\mu \cdot \mu_{max}^{-1}$
$V \cdot V_{max}^{-1}$
b
5
10
15
S_2 (µg atoms · l^{-1})

silicon requirement downward to maintain a near-maximum growth rate in a low silicon environment. This interpretation is different from merely saying that $K_S < K_T$ in clone 13-1 because it results from a direct comparison of experimental data and is thus independent of any artifacts produced by curve-fitting such as the inapplicability of a half saturation constant to a truncated hyperbola.*

Light dependence of silicic acid uptake

Results of experiments to determine the light dependence of silicic acid uptake in clone 3H of *T. pseudonana* indicate that the specific uptake rate is independent of light intensity at a silicic acid concentration of 2.5 µg atoms Si · ℓ^{-1}, and only weakly light dependent at 25.0 µg atoms Si · ℓ^{-1} (Figure 6). These results are in sharp contrast with the data of Davis (1973) on *Skeletonema costatum*, which indicated a hyperbolic response of uptake rate to light intensity. Davis' data were obtained in five to seven day perturbation experiments in continuous culture, while those reported here result from four-hour tracer experiments in batch culture. Thus Davis was determining something very close to the steady state response of silicic acid uptake to light intensity, while experiments reported here measured the effect of light intensity on something which approximates instantaneous uptake rates. The absence of light dependence in four-hour incubations, and the presence of strong light dependence in five to seven day incubations suggest that a stress

---

* V_{max} and μ_{max} are the specific rates of uptake and growth when the substrate under consideration is non-limiting, and are thus independent of the kinetic equation chosen to describe the response of the population to substrate limitation.

develops with time in a diatom population maintained at sub-optimal light intensities, and affects the cells' ability to take up silicic acid. There is a reasonable mechanism for the development of such a stress.

Lewin (1955) reported that assimilation of silicon by diatoms is closely linked to aerobic respiration and ATP production. This implies that the cell is expending photosynthetically fixed energy to take up silicic acid. Thus a population transferred from optimal to sub-optimal light conditions should continue to take up silicic acid at a high rate initially, but as the cells' energetic reserves become depleted with time the uptake rate should become dependent upon the rate of fixation of new energy. If this reasoning is accurate then the degree of light independence of instantaneous silicic acid uptake in a diatom population is a measure of the population's general energetic condition.

If a light stress which develops with time in algal populations affects nutrient uptake rates, then the time scale for development of this stress is an important factor in understanding nutrient uptake in natural populations, where cells are subjected to light conditions which change both diurnally and due to circulation of water between the surface and depths where little light penetrates. Laboratory studies to document the existence of a time dependent light stress and to determine the time scale for its development would aid greatly in the interpretation of field data.

Silica dissolution in exponentially growing diatom populations

Results of preliminary tracer experiments to determine the rate of silica dissolution in exponentially growing populations of *T. pseudonana*

clones 3H and 13-1 appear to contradict the claim of Lewin (1961) that populations of healthy, growing diatoms do not undergo dissolution. Instead the dissolution rates are similar to those observed by Paasche (1973 b) in populations of *T. pseudonana* which had been killed by freezing, a process in which the organic coating produced by the cell to retard dissolution remains intact. Due to the experimental procedures Lewin employed, it may be assumed that dissolution rates were masked by silicic acid uptake in experiments performed on populations of living cells. The similarity between dissolution rates determined in our experiments on living *T. pseudonana* and in those of Paasche (1973 b) on dead *T. pseudonana* suggests it is unlikely that living cells of this species have any mechanism beyond the production of an organic coating to prevent silica dissolution.

The effect of the organic coating may be inferred from a comparison of the measured values of V_{dis} in *T. pseudonana* (Table 8) and the predicted values of V_{dis} of biogenic silica (Figure 1). If it is assumed that *T. pseudonana* has a specific surface area of *ca.* 100 $m^2 \cdot g^{-1}$, then its predicted specific dissolution rate at 20 C would be *ca.* 0.035 hr^{-1}. The measured rates range from *ca.* 5 to 25% of this figure, indicating that *ca.* 75 to 95% of the predicted dissolution is being prevented by some factor. These figures are in general agreement with the data of Lewin (1961) which demonstrate a five to eight fold increase in the dissolution rate of cells cleaned with nitric acid to remove the organic coating.

CHAPTER IV

DYNAMICS OF SILICON IN TWO COASTAL UPWELLING ECOSYSTEMS

Although the average intensity of solar radiation impinging on the surface of the ocean is about equal to that on land (Sverdrup, Johnson and Fleming, 1941) the average rate of primary production per square meter of ocean surface is less than a third of the average terrestrial production rate (Odum, 1959). This energetic inefficiency of marine primary production results from the fact that plants cannot grow in a medium deficient in even one necessary inorganic substrate and most of the surface water of the ocean is severely depleted in three: nitrate, phosphate and silicic acid. All three of these nutrients are abundant at depths of a few hundred meters everywhere in the ocean, and the sole reason for the relative barrenness of most of the world ocean is the lack of a mechanism for injecting this nutrient-rich water into the surface layer, where there is sufficient light to drive photosynthesis.

In the few places where such a mechanism exists the biological results are spectacular. A rich diatom bloom, with the attendant dense populations of herbivorous and carnivorous marine life is a permanent feature of oceanic upwelling regions in the Antarctic and, to a lesser extent, the Central Equatorial Pacific (Sverdrup, Johnson and Fleming, 1941). Coastal upwelling regions located off the west coasts of major land masses comprise approximately 0.1% of the ocean's surface area and account for nearly 50% of the world's fish catch (Ryther, 1969). Peru, with no worldwide fishing fleet to rival those of the Soviet Union,

Japan or the United States, nevertheless leads all nations in tonnage caught (Delury, 1973) because of the rich upwelling region which lies off the Peruvian coast.

The highly productive ecosystems associated with coastal upwelling regions have recently received a substantial amount of scientific attention through the International Decade of Ocean Exploration's Coastal Upwelling Ecosystems Analysis (CUEA) program. This chapter is a report of studies of the dynamics of silicon in upwelling regions conducted in conjunction with CUEA cruises to Baja California in 1973 (MESCAL II) and northwest Africa in 1974 (JOINT I).*

Nutrient Dynamics and Primary Production in Upwelling Regions

Tropical and sub-tropical regions of the Earth experience intensified equatorward winds in the spring of the year (Wooster and Reid, 1963). Because of the deflecting force of the Earth's rotation, the resulting wind stress on the sea surface results in net transport of near-surface water 90° to the right of the wind direction in the Northern Hemisphere and 90° to the left of the wind direction in the Southern Hemisphere (i.e., from east to west under equatorward winds in both hemispheres) (Ekman, 1905; Neumann and Pierson, 1966). Near the west coasts of land masses this transport causes a net offshore flow of surface water which is compensated for by a net onshore flow at depth and

---

* These cruises were extensive data-gathering efforts and no attempt to present or analyze all cruise data will be made here. Data reports from MESCAL II (Whitledge and Bishop, 1974) and a preliminary analysis of the Baja California ecosystem (Walsh, Kelley, Whitledge, Huntsman and Pillsbury, 1975) appear elsewhere. Results of a number of studies from JOINT I will appear in a forthcoming volume of *Deep Sea Research*.

upwelling in the coastal region. The deep water transported to the surface is high in dissolved inorganic nutrients, and the combination of high nutrient concentrations with the availability of solar energy provides an environment favorable to algal growth and consequently to the maintenance of herbivorous and higher trophic levels. Several variants of this generalized model occur in the ocean, and ecosystems structured to exploit specific patterns of primary production generated by different wind and circulation regimes appear to result (Walsh, 1973). In each case the critical link is the temporal and spatial distribution of primary production caused by the easing or elimination of nutrient limitation at the site of upwelling and subsequent re-establishment of nutrient limitation as the upwelled water is transported away from its source or when a change in the wind regime causes upwelling to cease.

The following is a brief description of the upwelling systems off the coasts of Baja California and northwest Africa, where silicon dynamics studies reported in this chapter were carried out. The reader is referred to the literature cited therein for more detailed analyses of these two ecosystems.

Baja California

The coastal region off Baja California has been observed to undergo a transition from a stratified oceanic system to an upwelling system with the onset of strong northerly winds in March (Walsh, Kelley, Whitledge, MacIsaac and Huntsman, 1974). The phytoplankton of the preupwelling system is dominated by the red tide dinoflagellate *Gonyaulax polyedra*, which is replaced by a diatom-dominated algal community with

Coscinodiscus sp. the most numerically abundant form after the onset of upwelling. During April and May the wind stress and resultant upwelling appear to be intermittent phenomena, and the phytoplankton oscillates between a diatom- and a dinoglagellate-dominated community as the system oscillates between an upwelling and a stratified hydrographic regime (Walsh, Kelley, Whitledge, Huntsman and Pillsbury, 1975). The red crab *Pleuroncodes planipes* is the predominant herbivore during diatom-dominated upwelling periods, but appears to feed on zooplankton during stratified, dinoglagellate-dominated periods (Longhurst, Lorenzen and Thomas, 1967).

During periods of upwelling the mean vertical velocity is *ca.* 1.0×10^{-2} cm $\cdot$ sec^{-1} and mean nutrient concentrations of the upwelling water at 40-50 m depth are approximately 20 µg atoms $\cdot$ ℓ^{-1} nitrate nitrogen, 20 µg atoms $\cdot$ ℓ^{-1} silicic acid silicon and 1.8 µg atoms $\cdot$ ℓ^{-1} phosphate phosphorus, resulting in a mean phytoplankton production of 7.1 g C $\cdot$ m^{-2} $\cdot$ day^{-1} based upon nitrogen input (Walsh, 1973). Offshore from the region of strongest upwelling and during non-upwelling periods the total combined nitrogen concentration ($[NO_3^-] + [NO_2^-] + [NH_4^+]$) is frequently depleted to less than 1 µg atom N $\cdot$ ℓ^{-1}, while the phosphate concentration is rarely less than 0.75 µg atom P $\cdot$ ℓ^{-1} and the silicic acid concentration seldom less than 3 µg atoms Si $\cdot$ ℓ^{-1} (Whitledge and Bishop, 1974). This implies that primary production off Baja California is nitrogen limited in the absence of upwelled nutrients.

Northwest Africa

Upwelling off the northwest African coast begins to the south of Dakar in December, and moves northward with time, being strongest in the

Cap Blanc region during April, May and June (Cushing, 1971). Northerly winds are strong and fairly constant during this period, resulting in a broad region of offshore Ekman transport and a wind-mixed surface layer which frequently extends to the bottom (60-100 m) over the continental shelf (Mittelstaedt and Kolterman, 1973; Codispoti, unpublished). In contrast to the Baja California upwelling region, wind reversals and cessations of upwelling are not frequent off Cap Blanc in the spring and oscillations between a diatom- and a dinoflagellate-dominated phytoplankton are not known to occur; diatoms dominate the photoplankton off Cap Blanc throughout the spring (Walsh, 1973). Zooplankton appear to be the most important grazers although one of the major components of the pelagic nekton biomass, the clupeid *Sardinella aurita*, is a facultative herbivore and may graze when phytoplankton is abundant (Blackburn, 1975).

The upwelling velocity, as well as the nitrate and phosphate concentrations of the upwelling water are approximately the same off northwest Africa as off Baja California, but the mean phytoplankton production off Cap Blanc is only 2.3 to 3.1 g C $\cdot$ m^{-2} $\cdot$ day^{-1} as opposed to 7.1 g C $\cdot$ m^{-2} $\cdot$ day^{-1} off Baja California (Walsh, 1973). The mean silicic acid concentration of the upwelling water is somewhat lower off northwest Africa (14 µg atoms Si $\cdot$ ℓ^{-1}) than off Baja California (20 µg atoms Si $\cdot$ ℓ^{-1}) and there is generally less silicic acid than nitrate in northwest Africa surface water (MacIsaac, Harmon and Friederich, unpublished). However, surface silicic acid concentrations are seldom less than 1.5 µg atoms Si $\cdot$ ℓ^{-1}, which should not severely limit diatom growth (Guillard, Kilham and Jackson, 1973; Paasche,

1973 a). The cause of anomalously low primary production in the northwest Africa upwelling system is not clear, but nutrient limitation appears not to be responsible.

Procedures

Baja California

Silicic acid uptake rates were determined at 31 stations during R/V *Thomas G. Thompson* cruise 078 (MESCAL II) off Baja California from late March through early May of 1973, using the ^{30}Si method described in Chapter II. Station locations are given in Figure 8. The 13 stations taken at the point labeled "TS" in Figure 8 comprise a time series spanning the period from March 28 to May 2, and stations 17-25 were taken at six-hour intervals while the ship followed a surface current drogue from March 31 through April 2. At each station seawater was collected in 30 ℓ Niskin bottles from depths to which 100, 50, 25, 10 and 1% of surface light penetrated as calculated from Secchi disc readings, and at stations 18 and 22 seawater was also collected from depths corresponding to 0.1 and 0.01% of surface light intensity. A 2.3 ℓ sample from each depth was drawn into a Plexiglas incubation bottle, inoculated with 1.0 ml of ^{30}Si-labeled silicic acid solution (20.0 μg atoms Si · ml^{-1}; 49.5 to 95.6 atom % ^{30}Si), shaken vigorously and sealed. Incubation bottles for samples from 50, 25, 10 and 1% light depths were fitted with neutral density metal screens (Perforated Products, Inc. #145, 50/10 Pslot, 125P and 125W, respectively) which simulated *in situ* light intensities. Water from the surface (100%

FIGURE 8

Locations of stations where silicic acid uptake rates were measured on MESCAL II. A time series of 13 stations (3, 9, 27, 30, 35, 38, 40, 49, 53, 59, 67, 78 and 82) was occupied at the location labeled "TS".

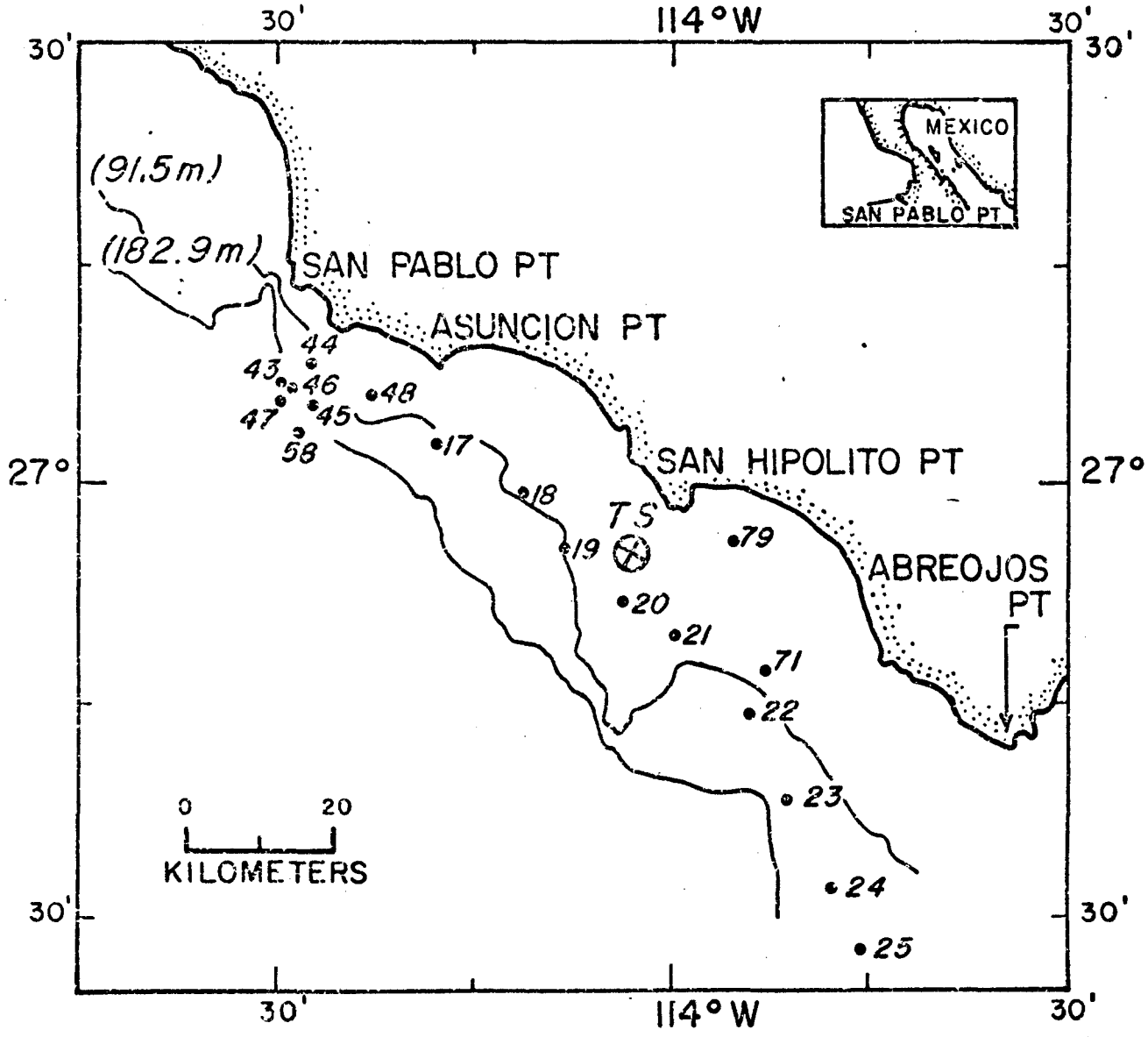
30'
114°W
30'
30'
30'
(91.5m)
(182.9m)
SAN PABLO PT
ASUNCION PT
SAN HIPOLITO PT
ABREOJOS PT
MEXICO
SAN PABLO PT
44
43
46
48
47
45
58
17
18
19
TS
79
20
21
71
22
23
24
25
27°
27°
0
20
KILOMETERS
30'
30'
30'
114°W
30'

light) was incubated in a clear Plexiglas bottle with no screen and water from the 0.1 and 0.01% light depths was incubated in opaque Plexiglas bottles. To monitor the light dependence of silicic acid uptake by near-surface phytoplankton an additional sample from the 50% light depth was incubated in an opaque Plexiglas bottle. Samples were incubated on deck under natural light for six hours* in Plexiglas incubation chests which were maintained at sea-surface temperature by a continuous flow of surface seawater. At the end of the incubation period the Plexiglas bottles were removed from the chests and each sample filtered through a 0.8 μm polycarbonate membrane filter. The filters were dried at *ca.* 60 C and stored in sealed plastic petri dishes until analyzed for silicic acid uptake as described in Chapter II. Silicic acid uptake studies were conducted in conjunction with other primary production and nutrient uptake rate measurements and with collection of supporting hydrographic and chemical data. Measurements at these stations included vertical profiles of primary production using ^{14}C (Huntsman, Jones and Barber, unpublished), nitrate and ammonium uptake using ^{15}N (Conway, Harmon and Dugdale, unpublished), particulate nitrogen and chlorophyll (Conway, Harmon and Dugdale, unpublished) temperature and salinity (Whitledge and Bishop, 1974) and dissolved nitrate, nitrite, ammonium, phosphate and silicic acid (Whitledge and Friederich, unpublished).

In addition to the vertical profiles, experiments were performed

---

* Samples collected at six-hour intervals during the drogue study were incubated for four hours.

to determine the silicic acid uptake kinetics of natural phytoplankton populations at stations 25 and 67. These stations were selected for kinetic experiments because the silicic acid concentration of the near-surface water was less then 5.0 µg atoms Si · ℓ^{-1}, and kinetic experiments cannot be performed successfully at higher ambient concentrations (Goering, Nelson and Carter, 1973). Seawater was collected in a 30 ℓ Niskin bottle from the 50% light depth and a series of six samples drawn into 2.3 ℓ Plexiglas incubations all fitted with identical neutral density 50% light screens. ^{30}Si-labeled silicic acid (95.6 atom % ^{30}Si) was added to the incubation bottles at a series of concentrations resulting in additions of 0.085, 0.435, 0.875, 1.75, 6.5, and 13.0 µg atoms Si · ℓ^{-1}. Samples were sealed, incubated, filtered, stored and analyzed in the same manner as samples from vertical profiles.

At stations 35 and 71 six 2.3 ℓ seawater samples were collected from the 50% light depth, inoculated with 1.0 ml of ^{30}Si-labeled silicic acid (20.0 µg atoms Si · ℓ^{-1}; 95.6 atom % ^{30}Si) and incubated at 100, 50, 25, 10, 1 and 0% of the surface light intensity for six daylight hours. The purpose of these experiments was to provide a more detailed analysis of the effect of light on silicic acid uptake by near-surface phytoplankton. At station 9 this experiment was performed on populations collected from all five light depths and at station 82 on populations from the 50% and 10% light depths in an effort to assess whether effect of light was different in populations growing at high and low light intensities.

Northwest Africa

Silicic acid uptake rates were determined at 36 stations during R/V *Atlantis II* cruise 082 (JOINT I) off the northwest coast of Africa from early March through late May of 1974. Station locations are given in Figure 9. At 24 stations* a profile of the silicic acid uptake rate versus depth was obtained. Seawater was collected in 30 ℓ Niskin bottles from depths to which 100, 50, 30, 15, 5, 1 and 0.1% of surface light penetrated, as determined by a submersible quantum meter, and at several stations** an additional sample was collected from a depth corresponding to 0.01% of surface light. A 1.2 ℓ sample from each depth was drawn into a Plexiglas incubation bottle, inoculated with ^{30}Si-labeled silicic acid solution (10.0 μg atoms Si · ml^{-1}; 83.9 atom % ^{30}Si), shaken vigorously and sealed. Incubation bottles for samples from the 50, 30, 15, 5 and 1% light depths were fitted with neutral density metal screens (Perforated Products, Inc., #145, 50/10 Pslot, 25P, 40T and 125W, respectively) which simulated *in situ* light intensities. Water from the surface (100% light) was incubated in a clear Plexiglas bottle with no screen and that from the 0.1 and 0.01% light depths in opaque Plexiglas bottles. As on MESCAL II, an additional sample from the 50% light depth was incubated in an opaque Plexiglas bottle to monitor the light dependence of silicic acid uptake by near-surface phytoplankton and at stations 70 and 78 samples from all seven light depths were incubated in opaque Plexiglas bottles.

---

* The first 24 stations listed in Appendix B.

** Stations 30, 52, 89, 97, 99, 127, 164 and 175.

FIGURE 9

Locations of stations where silicic acid uptake rates were measured on JOINT I.

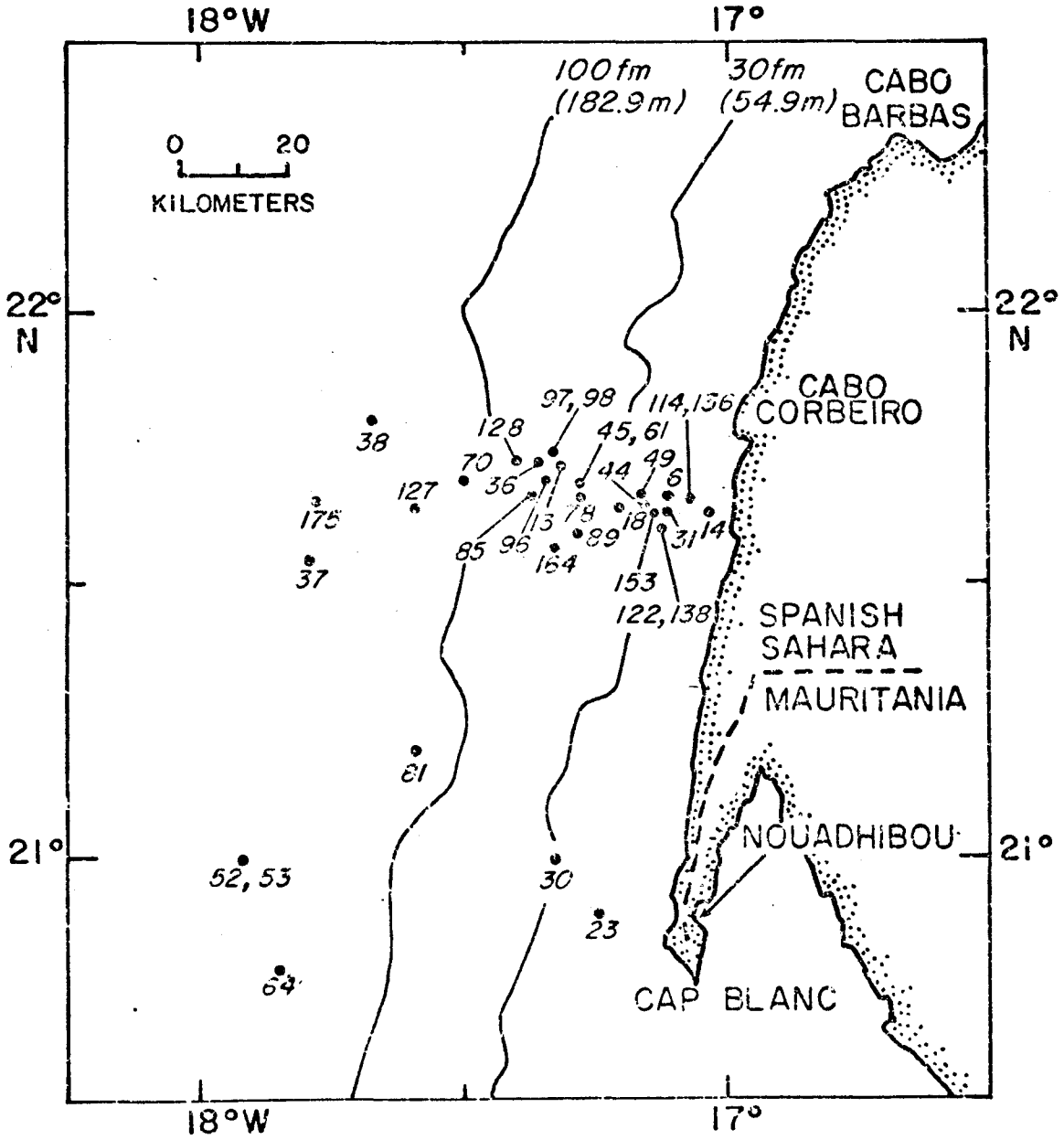
18°W
17°
100fm
(182.9m)
30fm
(54.9m)
CABO
BARBAS
0
20
KILOMETERS
22°
N
CABO
CORBEIRO
97, 98
114, 136
128
45, 61
38
70
49
44
6
36
127
175
78
18
13
14
89
31
85
96
164
37
153
122, 138
SPANISH
SAHARA
MAURITANIA
81
NOUADHIBOU
21°
52, 53
30
23
64
CAP BLANC
18°W
17°

Incubation conditions and filtration, sample storage and analysis procedures were identical to those employed on MESCAL II, as were the types and sources of supporting data collected.

In addition to the 24 vertical profiles, experiments were performed to determine the silicic acid uptake kinetics of phytoplankton collected from the 50% light depth at stations 31, 37 and 38, which were selected for their low ambient silicic acid concentrations. Samples were 1.2 ℓ in volume, and were inoculated with 1.0 ml of ^{30}Si-labeled silicic acid solution (83.9 atom % ^{30}Si) at concentrations resulting in additions of 0.20, 0.40, 1.10, 2.20, 4.50, 9.0 and 13.5 μg atoms Si · ℓ^{-1}. At station 119, where the ambient surface silicic acid concentration was 5.58 μg atoms Si · ℓ^{-1}, labeled silicic acid (10.0 μg atoms Si · ℓ^{-1}; 83.9 atom % ^{30}Si) was added in amounts resulting in additions of 8.3, 16.7, 25.0, 33.3, 41.7 and 83.3 μg atoms Si · ℓ^{-1}. This high concentration kinetic experiment was performed to determine whether uptake by the naturally occurring assemblage of living and dead diatoms and suspended inorganic particles was independent of silicic concentration in a range of concentrations known to be saturating for uptake in pure diatom cultures. In all kinetic experiments, incubation and subsequent procedures were identical to those employed at vertical profile stations.

At stations 6, 31, 38, 62, 69 and 135, seven 1.2 ℓ seawater samples were collected from the 50% light depth, inoculated with 1.0 ml of ^{30}Si-labeled silicic acid solution (10.0 μg atoms Si · ml^{-1}; 83.9 atom % ^{30}Si) and incubated at 100, 50, 30, 15, 5, 1 and 0% of the surface light

intensity for six daylight hours to obtain a more detailed analysis of the light dependence of silicic acid uptake by near-surface phytoplankton. At stations 62 and 69 this experiment was also performed on populations from the 0.1% light depth.

During five periods when the ship was operating close to shore and suspended Sahara sand was visible in the air, airborne particulate matter was collected by drawing air with a vacuum pump through a 30 μm nylon net for periods of one to three days. The collected particlate matter was resuspended in 2.4 ℓ of membrane-filtered low nutrient seawater to which 6.0 ml of ^{30}Si-labeled silicic acid (10.0 μg atoms Si · ml^{-1}; 83.9 atom % ^{30}Si) had been added. The suspensions were incubated for periods ranging from 6 to 71 hours at *ca.* 20 C while being stirred constantly by a magnetic stirrer. These experiments were conducted to determine whether suspended sand, which was visible in the water at several near-shore stations and presumably present at most or all stations, absorbed labeled silicic acid resulting in an overestimate of the biological uptake rate.

Silica dissolution rates were measured at five stations which formed a transect extending offshore along the 21°40'N parallel for a distance of *ca.* 60 km, extending from *ca.* 10 km from the coast to *ca.* 7 km beyond the edge of the continental shelf. Additionally two stations were occupied 75-80 km south of the main transect, one *ca.* 10 km offshore and the other *ca.* 15 km beyond the shelf break. Locations of stations where dissolution rates were measured are given in Figure 10.

At each station seawater was collected in 30 ℓ Niskin bottles from

FIGURE 10

Locations of stations where silica dissolution rates were measured on JOINT I.

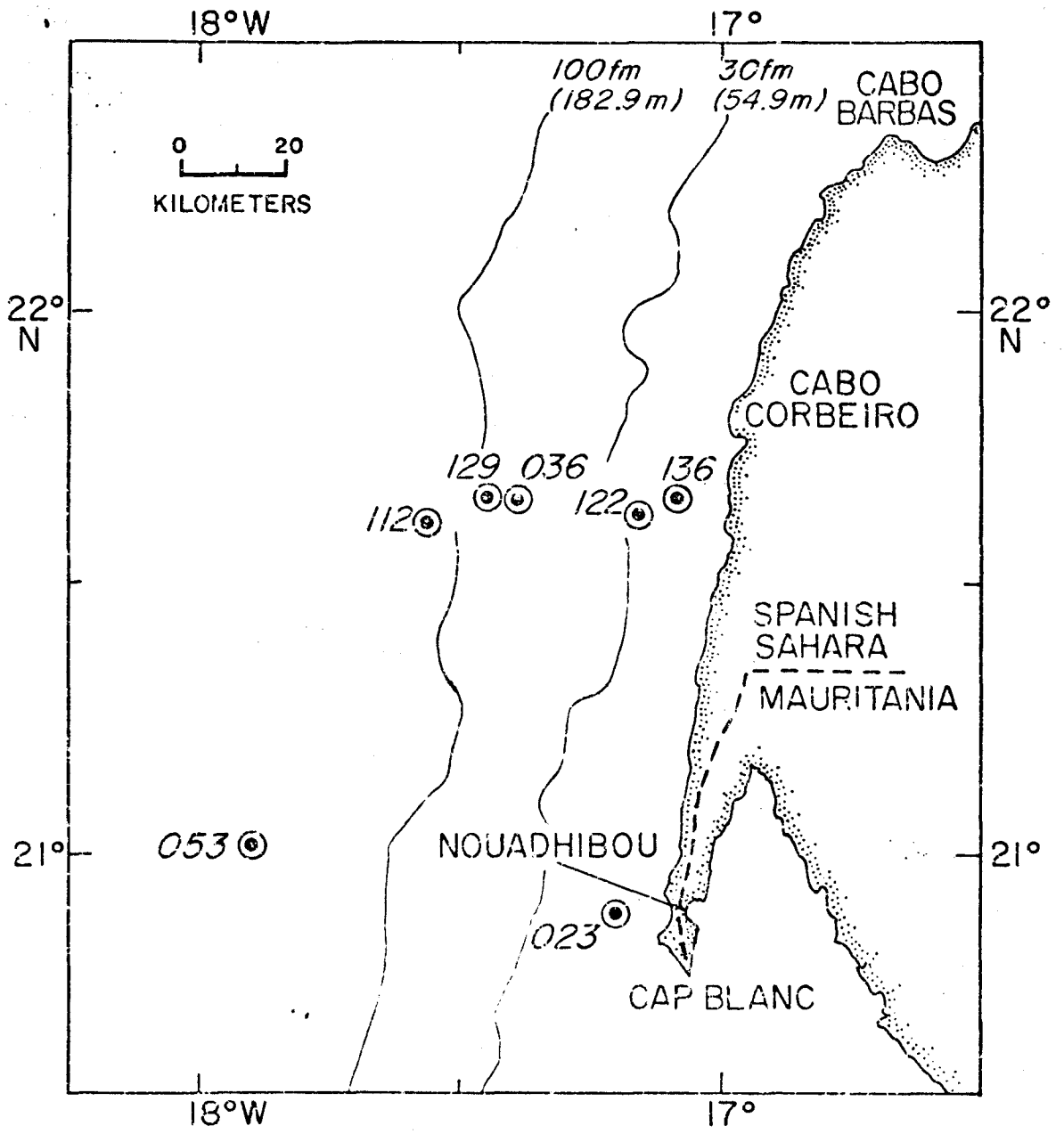
18°W
17°
100fm
(182.9m)
30fm
(54.9m)
CABO
BARBAS
0
20
KILOMETERS
22°
N
22°
N
CABO
CORBEIRO
129
036
136
122
112
SPANISH
SAHARA
MAURITANIA
21°
053
NOUADHIBOU
21°
023
CAP BLANC
18°W
17°

the 100, 50, 30, 15, 5, 1 and 0.1% light depths. A 2.4 ℓ sample from each depth was drawn into a 4 ℓ polyethylene bottle, inoculated with 2.0 ml of ^{30}Si-labeled silicic acid solution (20.0 μg atoms Si · ml^{-1}; 83.9 atom % ^{30}Si) and shaken vigorously. A 1.2 ℓ Plexiglas incubation bottle was rinsed twice with 50-100 ml of inoculated sample and then filled and sealed. Incubation bottles were fitted with the same neutral density metal screens used in uptake experiments, and samples were incubated on deck under natural light for 24 hours in the same incubation chests used in uptake experiments. The inoculated sample remaining after each incubation bottle was filled was filtered immediately through a 0.8 μm polycarbonate membrane filter; the filter was retained for particulate silicon analysis and the filtrate analyzed to determine $^{28}A_i$ as described in Chapter II. After 24 hours the Plexiglas bottles were removed from the incubation chests and each sample filtered through a 0.8 μm polycarbonate membrane filter. The filter was analyzed for silicic acid uptake and the filtrate analyzed to determine $^{28}A_f$. Absolute and specific silica dissolution rates, ρ_{dis} and V_{dis}, were determined using equations (20) and (21).

Baja California Results

Results of all silicic acid uptake rate measurements performed on MESCAL II are given in Appendix A. The following features of the silicon cycle off Baja California are apparent based on these data.

Vertical profile of silicic acid uptake

The specific uptake rate of silicic acid was more uniform with

depth than were specific uptake rates of nitrate, ammonium or carbon during upwelling periods on MESCAL II. Specific uptake rates of the four substrates* from all stations where samples were collected and incubated in daylight hours during the first ten days of MESCAL II** were averaged, and the mean values are plotted versus depth in Figure 11. This time period represents the longest observed single period of constant upwelling conditions, free of wind reversals, and has been described as a period of "quasi steady-state" upwelling conditions (Walsh, Kelley, Whitledge, Huntsman and Pillsbury, 1975). Time-averaged data, rather than individual station curves, are presented to show the general vertical distribution of nutrient uptake prevailing during this period, and also because at several stations uptake data for either carbon, nitrate or ammonium are unavailable and at some others vertical profiles for these substrates are incomplete. Points are plotted at the time-averaged depths of 100, 50, 25, 10 and 1% light penetration.

Figure 11 shows that almost all uptake of carbon and nitrogen, but not silicon, was limited to the region of 1% or greater light penetration (a common operational definition of the euphotic zone) during this period. Profiles at stations 18 and 22, taken during the same time period, indicate that silicic acid uptake was greatly reduced, but

---

* Specific uptake rates of nitrate and ammonium (Conway, Harmon and Dugdale, unpublished) were available directly. Carbon data of Huntsman, Jones and Barber (unpublished) were recalculated by dividing the reported ^{14}C assimilation rate ($\mu g\ C \cdot \ell^{-1} \cdot hr^{-1}$) by the particulate carbon concentration ($\mu g\ C \cdot \ell^{-1}$) to obtain the specific uptake rate of carbon (hr^{-1}).

** Stations 3, 9, 17, 20, 21, 24, 27 and 30.

FIGURE 11

Time-averaged vertical profiles of specific uptake rates of silicic acid ($V_{H_4SiO_4}$), ammonium ($V_{NH_4}+$), nitrate ($V_{NO_3}-$) and carbon (V_C) from the period of quasi steady-state upwelling during MESCAL II. Depths are also time-averaged of 100, 50, 25, 10 and 1% surface light penetration.

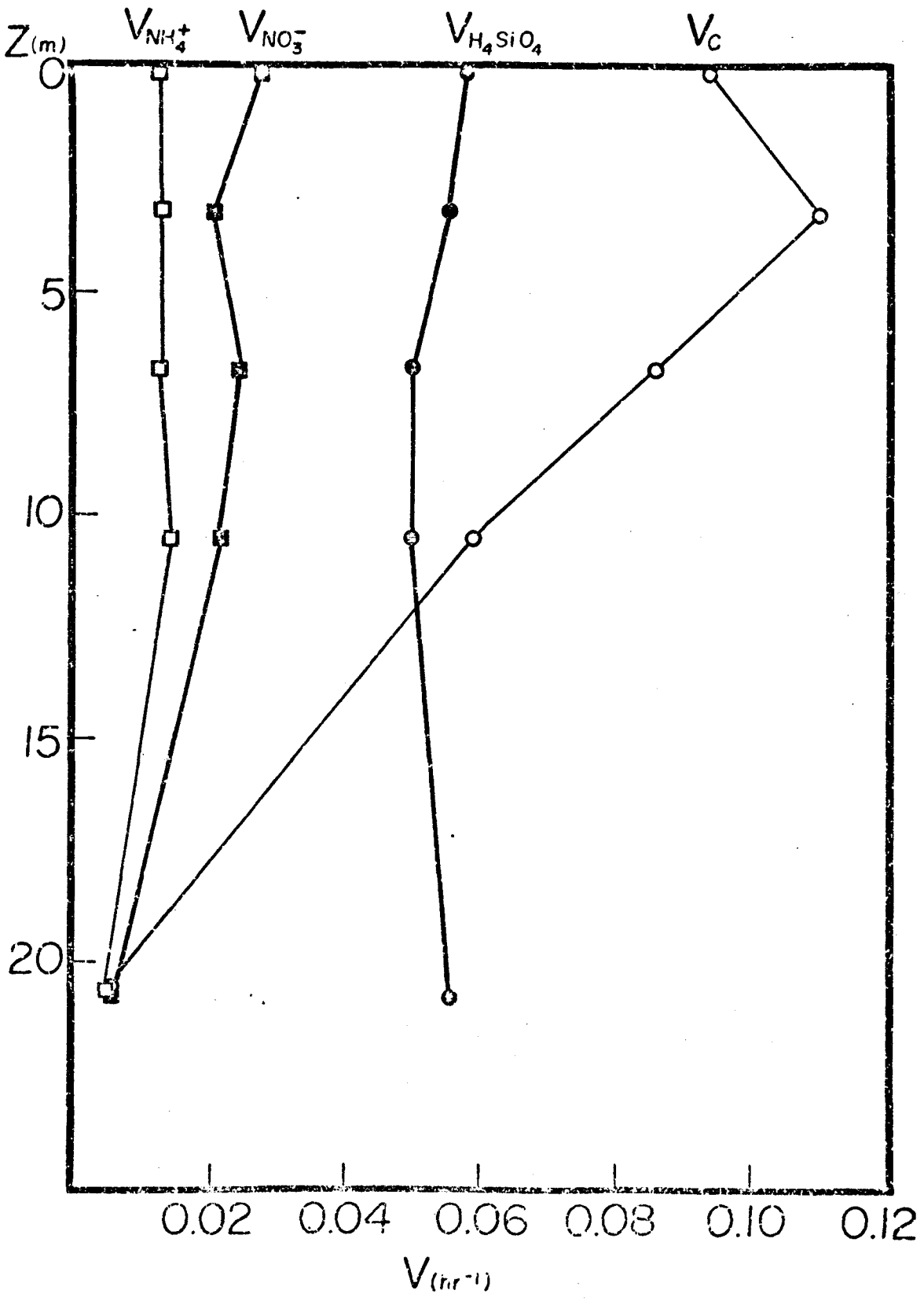
Z(m)
$V_{NH_4^+}$
$V_{NO_3^-}$
$V_{H_4SiO_4}$
V_C
0
5
10
15
20
0.02
0.04
0.06
0.08
0.10
0.12
$V_{(hr^{-1})}$

still analytically detectable at the calculated depth of 0.01% light penetration, which is twice the 1% light depth. Since tracer experiments have never shown abiotic uptake of silicic acid to proceed at a measurable rate in near-surface seawater (Goering, Nelson and Carter, 1973; Nelson and Goering, unpublished; see also section on northwest Africa results in this chapter.) and radiolarians were not observed off Baja California during MESCAL II (Blasco, unpublished) this deep uptake is probably attributable to living diatoms.

Light dependence of uptake rate

The degree of light dependence of silicic acid uptake by phytoplankton populations collected from the 50% light depth was found to be highly variable during MESCAL II. A series of 26 comparisons of the silicic acid uptake rate of populations collected from the 50% light depth and incubated at 50% surface light and in the dark yielded ratios of dark to light uptake which ranged from 1.102 (no light dependence) to 0.000 (absolute light dependence) with a mean of 0.636 and a standard deviation of 0.384.

In general, the light dependence of uptake was substantially stronger during stratified periods than during upwelling periods. Samples collected during periods of upwelling (stations 3-30, 48-58 and 67-82) demonstrated a mean ratio of dark to light uptake of 0.797 with a standard deviation of 0.303 while samples collected during stratified periods (stations 35-47 and 59-65) had a significantly lower

mean ratio of 0.296 with a standard deviation of 0.354.* Exclusion of data from stations 9, 30 and 44, where light dependence did not fit the general pattern, would result in a mean ratio of dark to light uptake during upwelling periods of 0.881 with a standard deviation of 0.215 and during stratified periods of 0.131 with a standard deviation of 0.163. These mean ratios are significantly different at the 99.9% confidence level, but there is no obvious reason, other than anomalous results in this experiment, for eliminating any of these three stations.

Plots of the silicic acid uptake rate versus percent surface light intensity for near-surface populations at stations 9, 35, 71 and 82, where water from the 50% light depth was incubated at 100, 50, 25, 10, 1 and 0% of the surface light intensity, are presented in Figure 12. These more detailed light dependence experiments reflect the variability in the dark to light uptake ratio observed during the cruise as a whole, but give no indication that uptake is inhibited until light is decreased to 10% or less of the surface intensity. These stations were all occupied during periods of upwelling, and no comparable experiment was performed during a stratified period.

There is no strong evidence in data from stations 9 and 82, where the same light dependence experiment was performed on populations from greater depths, that populations collected from the deeper part of the euphotic zone respond differently to light than do near-surface populations with respect to silicic acid uptake.

---

* A t test shows the mean ratios of dark to light uptake under the two circulation regimes to be significantly different at the 99% confidence level.

FIGURE 12

Plots of the specific uptake rate of silicic acid, V, versus percent surface light intensity for populations collected from the 50% light depth at four stations on MESCAL II.

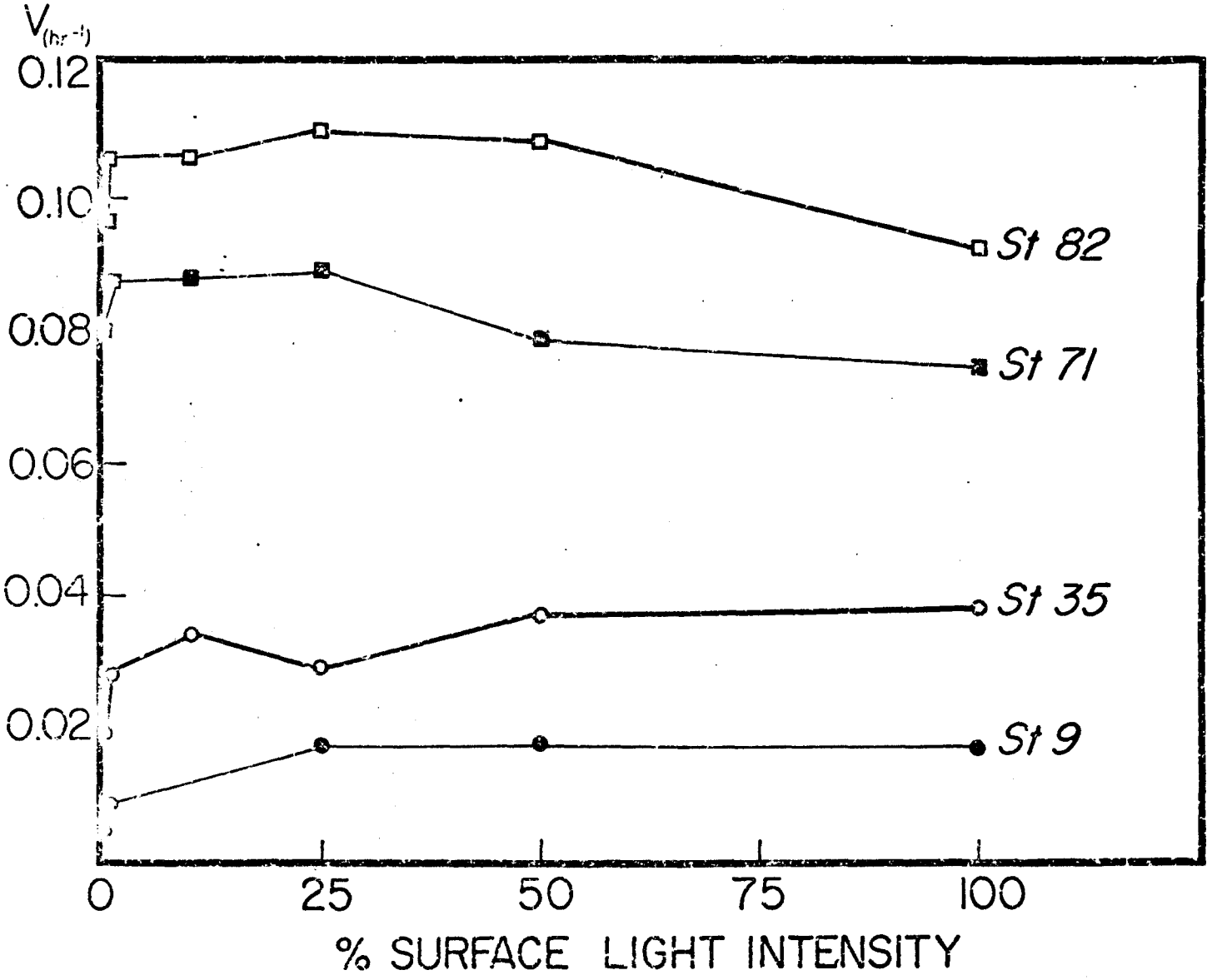
$V_{(hr^{-1})}$
0.12
0.10
0.08
0.06
0.04
0.02
St 82
St 71
St 35
St 9
0
25
50
75
100
% SURFACE LIGHT INTENSITY

Data from nocturnal incubations at stations 18, 19, 22 and 23, taken during the drogue study, indicate that silicic acid uptake was substantial at night, when nitrate and ammonium uptake were greatly reduced (Conway, Harmon and Dugdale, unpublished) and carbon uptake did not occur (Huntsman, Jones and Barber, unpublished). A similar relationship was observed in the upwelling region off Peru (Goering, Nelson and Carter, 1973).

Concentration dependence of uptake rate

Uptake kinetic experiments performed on populations collected from the 50% light depth at stations 25 and 67 fail to show enhancement of silicic acid uptake by additions of silicic acid ranging from 0.085 to 13.0 μg atoms Si · ℓ^{-1}. These experiments, performed at stations selected for their low ambient surface concentrations, provide strong evidence that silicic acid uptake was never substrate limited during MESCAL II.

Northwest Africa Results

Results of all silicic acid uptake and silica dissolution rate measurements performed on JOINT I are given in Appendix B. The following features of the silicon cycle off northwest Africa are apparent based on these data.

Vertical profile of silicic acid uptake

The specific uptake rate of silicic acid was observed to decrease with depth between the surface and the depth of 1% light penetration at most stations on JOINT I, and to be nearly constant, and at times

substantial, between the 1% and 0.01% light depths. Mean specific uptake rates of silicic acid, nitrate, ammonium and carbon* from all stations where vertical profiles of silicic acid uptake were obtained are plotted versus depth in Figure 13. These time-averaged data show that specific uptake rates of carbon, silicon and nitrogen ($NH_4^+ + NO_3^-$), integrated from the surface to the greatest depth where uptake was observed, were quite similar during JOINT I if data from 24-hour ^{14}C incubations are considered. The maintenance of approximately constant elemental composition of the phytoplankton requires that specific uptake rates of all elements, integrated over depth and time, be approximately equal. Thus the excess of $V_C(6)$ over $V_C(24)$ indicates that carbon assimilation was discontinuous in time, occurring almost entirely during daylight hours. Similarity between specific uptake rates of silicon and nitrogen, based upon six-hour incubations and carbon based upon 24-hour incubations indicates that uptake of silicon and nitrogen fluctuated much less from day to night than did carbon uptake, as was also observed in the upwelling regions off Peru (Goering, Nelson and Carter, 1973) and Baja California. Silicic acid uptake proceeded at a higher rate than that of nitrate and ammonium at the 1% light depth and was not observed to decrease sharply with depth in the region of 1% to 0.01% surface light penetration, thus probably exceeding nitrate, ammonium and carbon uptake throughout this depth region. Living diatoms were observed at all depths within the wind-mixed surface layer (Blasco, unpublished).

---

* As with MESCAL II data, the specific uptake rate of carbon was calculated from the ^{14}C assimilation and particulate carbon data of Huntsman, Jones and Barber (unpublished). Specific carbon uptake rates based upon both six-hour and 24-hour incubations are presented.

FIGURE 13

Time-averaged vertical profiles of specific uptake rates of silicic acid ($V_{H_4SiO_4}$), ammonium ($V_{NH_4}+$), nitrate ($V_{NO_3}-$) and carbon (V_C) during JOINT I. Depths of 100, 50, 30, 15, 5, 1, 0.1 and 0.01% surface light penetration are also time-averaged.

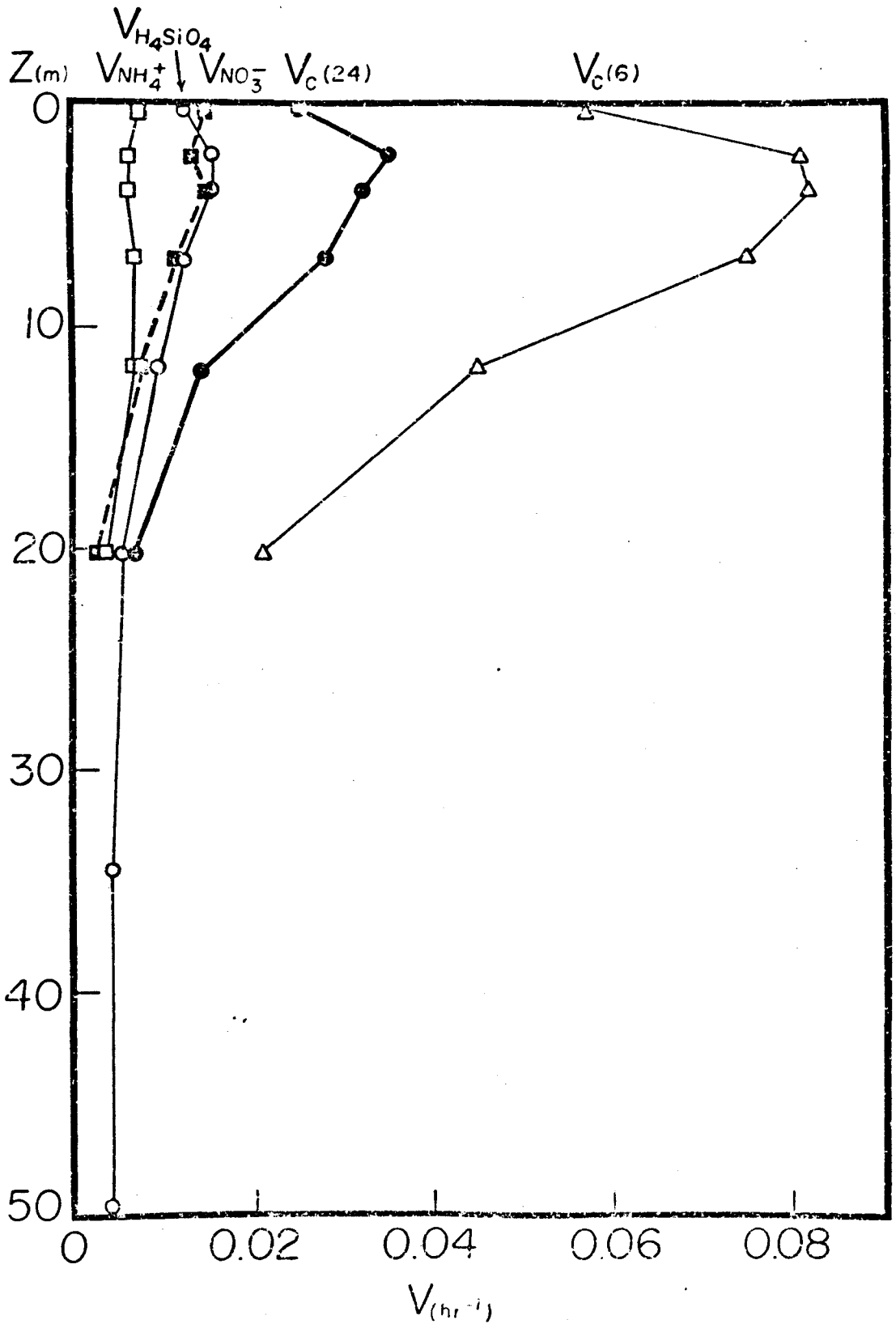
$V_{H_4SiO_4}$
$Z_{(m)}$ $V_{NH_4^+}$ $V_{NO_3^-}$ $V_c(24)$
$V_c(6)$
0
10
20
30
40
50
0
0.02
0.04
0.06
0.08
$V_{(hr^{-1})}$

The mean specific uptake rate of all four substrates was substantially lower at all depths on JOINT I than on MESCAL II.

Light dependence of uptake rate

The light dependence of silicic acid uptake by populations collected from the 50% light depth was found to be stronger and somewhat less variable on JOINT I than on MESCAL II. A series of 21 comparisons of the silicic acid uptake rate of populations collected from the 50% light depth and incubated at 50% surface light and in the dark yielded ratios of dark to light uptake which ranged from 1.000 (no light dependence) to 0.000 (absolute light dependence). However, the mean ratio of 0.311 with a standard deviation of 0.271 was significantly lower than the mean ratio for MESCAL II data at the 99% confidence level. Variability in the light dependence of silicic acid uptake during JOINT I was not clearly associated with variability in any measured hydrographic or biological parameter.

Plots of the silicic acid uptake rate versus percent surface light intensity for populations collected from the 50% light depth at stations 6, 31, 38, 62, 69 and 135 are presented in Figure 14. Light dependence of silicic acid uptake is much more apparent in northwest Africa phytoplankton (Figure 14) than in Baja California phytoplankton (Figure 12) or laboratory cultures of *Thalassiosira pseudonana* (Figure 6). Uptake appears to have been much more strongly light dependent between 0 and 15% of surface light than at higher intensities.

Data from stations 62 and 69 indicate that silicic acid uptake by populations collected from the 0.1% light depth was light dependent, but

FIGURE 14

Plots of the specific uptake rate of silicic acid, V, versus percent surface light intensity for populations collected from the 50% light depth at six stations on JOINT I.

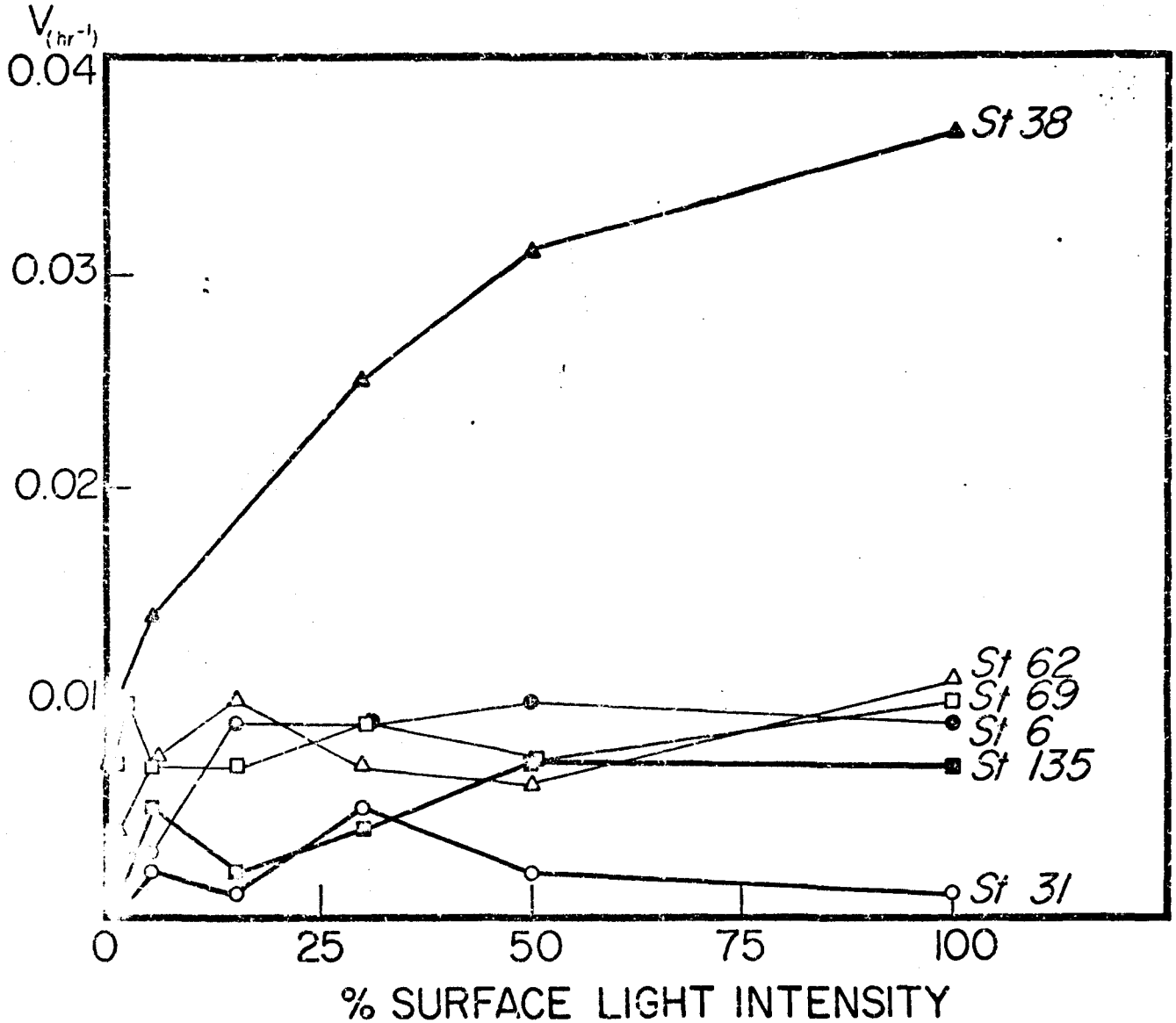
V(hr⁻¹)
0.04
0.03
0.02
0.01
St 38
St 62
St 69
St 6
St 135
St 31
0
25
50
75
100
% SURFACE LIGHT INTENSITY

do not show conclusively whether the light dependence was stronger, weaker, or unchanged compared to light dependence in near-surface populations.

Concentration dependence of uptake rate

Of the four uptake kinetic experiments performed on populations collected from the 50% light depth, one (station 31) shows substantial enhancement of the uptake rate by additions of silicic acid and the other three show none. Kinetic data from stations 31, 37 and 38 are plotted in Figure 15. These experiments, conducted at stations selected for their low ambient silicic acid concentrations, indicate that silicic acid uptake in the northwest Africa upwelling region may at times be substrate limited, but suggest that such limitation is not common. The experiment performed at station 119 to determine whether uptake at high ambient concentration is enhanced by large additions of silicic acid indicates that it is not.

Inorganic uptake of silicic acid

Uptake of silicic acid by suspended Sahara sand was undetectable in all five tracer experiments performed on sand collected from air near the coast. This indicates strongly that all conversion of silicic acid to particulate matter measured in seawater samples was a result of biological uptake. The lack of uptake in samples collected from the 50% light depth at stations 135 and 164 and injected with mercuric chloride prior to inoculation with labeled silicic acid provides further evidence that inorganic uptake of silicic acid in the northwest Africa upwelling region does not occur.

FIGURE 15

Plot of the specific uptake rate of silicic acid, V, versus silicic acid concentration, S_2, for populations collected from the 50% light depth at three stations on JOINT I.

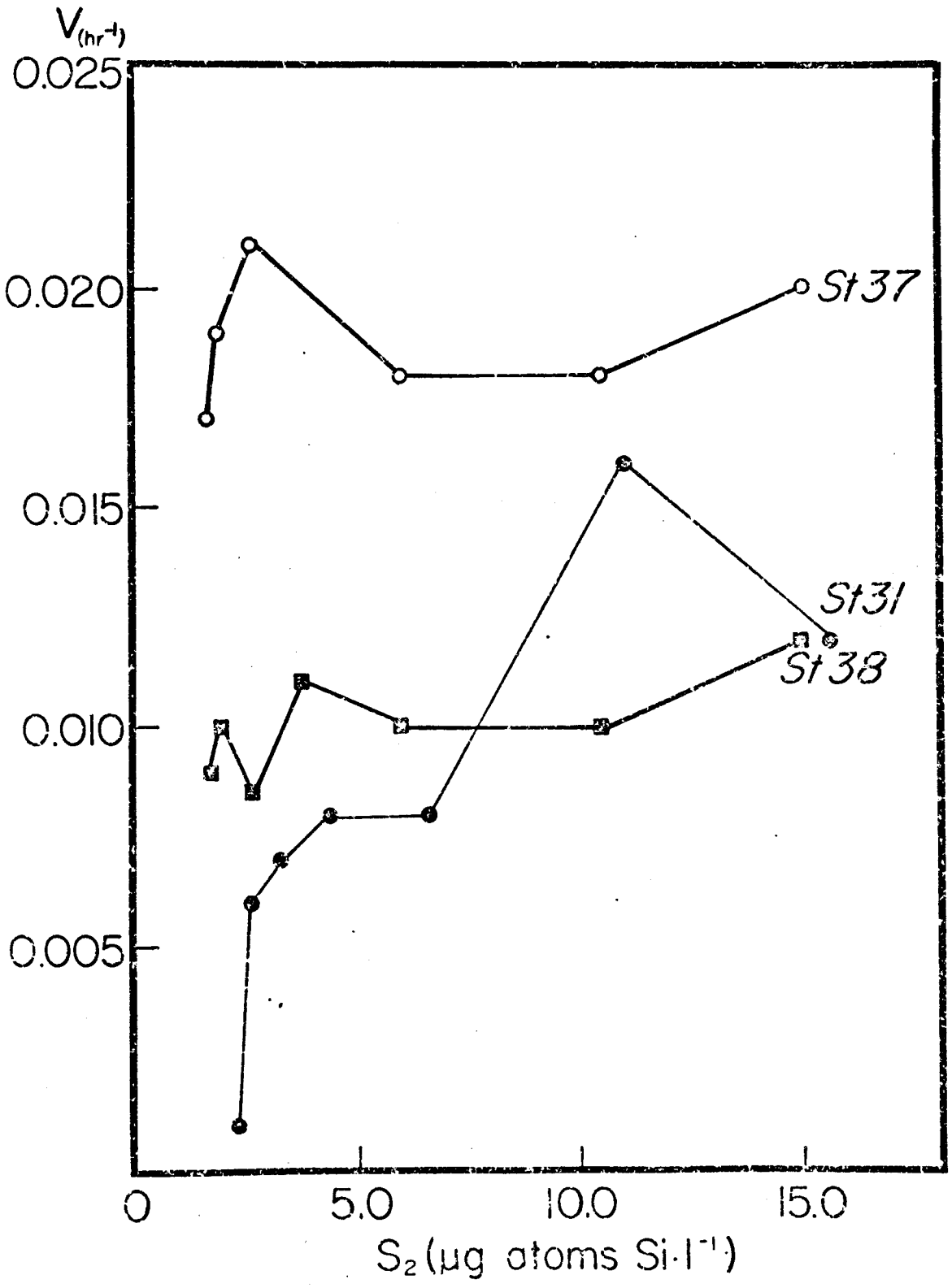
V(hr⁻¹)
0.025
0.020
0.015
0.010
0.005
St 37
St 31
St 38
0
5.0
10.0
15.0
S₂ (µg atoms Si·l⁻¹)

Silica dissolution

Vertical profiles of the absolute silica dissolution rate, ρ_{dis} and particulate silicon concentration at the seven stations where dissolution rates were determined are presented in Figure 16. Generally the absolute rate of silica dissolution tended to be low in the upper 10 m and to increase with depth below 10 m. This trend was apparent at all stations except the two (23 and 112) which were sampled to only 25 m. There was no clear increase or decrease in the rate of silica dissolution with distance from the coast.

The specific uptake rate of silicic acid, V, and the specific silica dissolution rate, V_{dis}, are plotted versus depth in Figure 17. V_{dis} had the same pattern of increase with depth as ρ_{dis}, indicating that the higher dissolution rates at 20-60 m resulted from the presence of silica which dissolved more readily than that at the surface, rather than from an increased particle density at depth. The particulate silicon concentration did not vary greatly with depth at any of these seven stations. Comparison of the vertical profiles of V and V_{dis} indicates that while uptake proceeded at a higher rate than dissolution in the upper few meters at all stations, dissolution predominated at depths below 30 m, and appears to have become predominant at depths of 5 to 10 m over the inner continental shelf. In general there was sufficient silica dissolution in the upper 50 m over the continental shelf to supply all silicic acid consumed by the phytoplankton.

FIGURE 16

Vertical profiles of the absolute dissolution rate of silica, ρ_{dis}, and particulate silicon concentration at seven stations on JOINT I. Positions of the station curves reflect station locations.

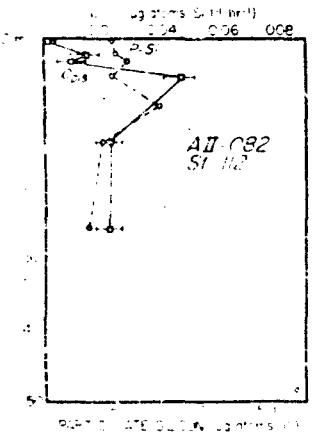
P-Si
AII-082
St 112

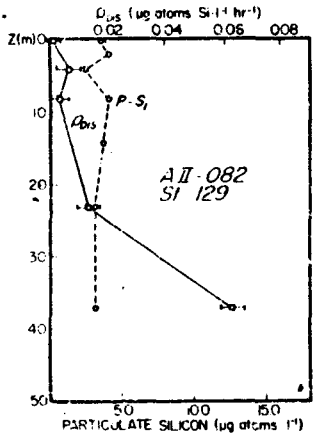
ρ_{bs} (ug atoms Si·l⁻¹ hr⁻¹)
0.02 0.04 0.06 0.08
Z(m)
0
10
20
30
40
50
$P\text{-}S_i$
ρ_{bs}
AII-082
St 129
50 100 150
PARTICULATE SILICON (ug atoms l⁻¹)

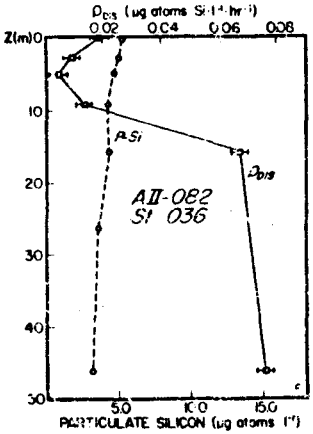
ρ_{bs} (ug atoms Si·l⁻¹ hr⁻¹)
0.02 0.04 0.06 0.08
Z(m)
0
10
20
30
40
P-Si
ρ_{bs}
AII-082
St 036
50 100 150
PARTICULATE SILICON (ug atoms l⁻¹)

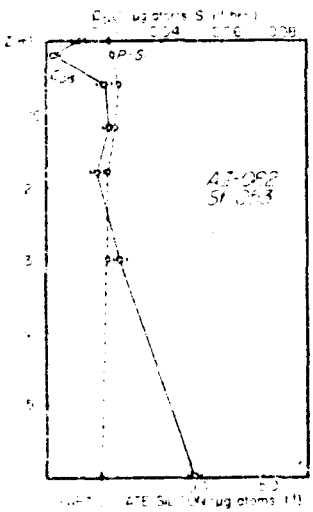
P-Si
AII-082
St 083

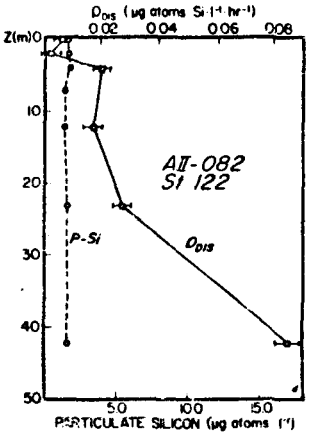
Z(m)
0.02
0.04
0.06
0.08
10
20
30
40
50
AII-082
SI 122
P-Si
D_{dis}
5.0
10.0
15.0
PARTICULATE SILICON (µg atoms l⁻¹)

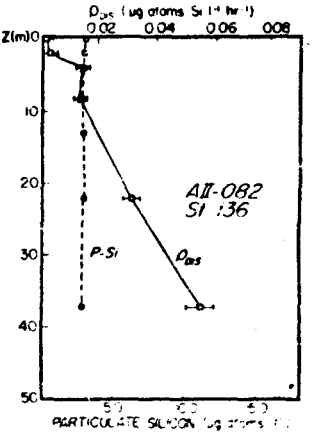
Z(m)
0.02
0.04
0.06
0.08
10
20
30
40
50
AII-082
SI 136
P-Si
D_{dis}
PARTICULATE SILICON

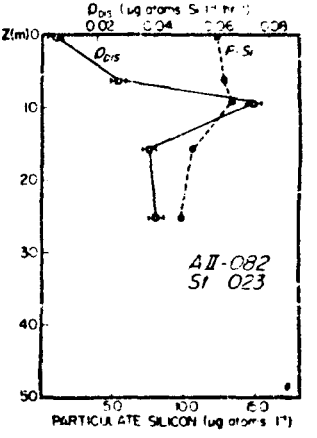
Z(m)
0.02
0.04
0.06
0.08
10
20
30
40
50
D_{dis}
P-Si
AII-082
SI 023
5.0
10.0
PARTICULATE SILICON (µg atoms l⁻¹)

FIGURE 17

Vertical profiles of the specific uptake rate of silicic acid, V, and the specific dissolution rate of silica, V_{dis}, at seven stations on JOINT I. Positions of the station curves reflect station locations.

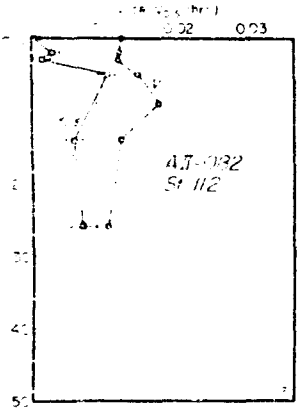
0.02
0.03
AII-082
St 112

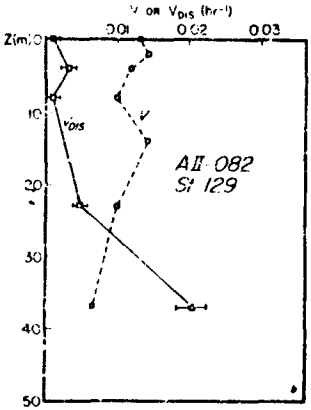
V OR V_{DIS} (hr^{-1})
0.01
0.02
0.03
Z(m)
10
20
30
40
50
V_{DIS}
V
AII-082
St 129

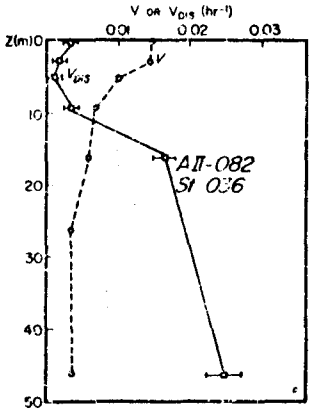
V OR V_{DIS} (hr^{-1})
0.01
0.02
0.03
Z(m)
10
20
30
40
50
V_{DIS}
V
AII-082
St 036

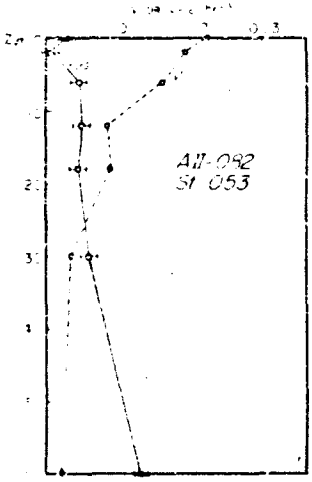
0.3
AII-082
St 053

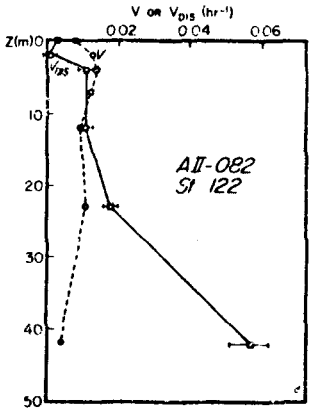
V or V_{DIS} (hr^{-1})
0.02
0.04
0.06
Z(m)
0
10
20
30
40
50
V_{DIS}
V
AII-082
St 122

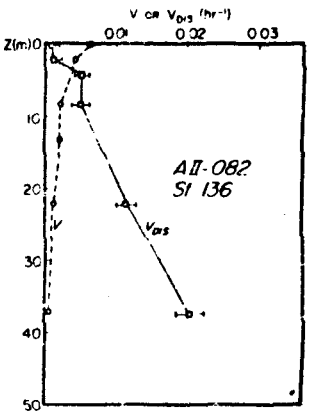
V or V_{DIS} (hr^{-1})
0.01
0.02
0.03
Z(m)
0
10
20
30
40
50
V
V_{DIS}
AII-082
St 136

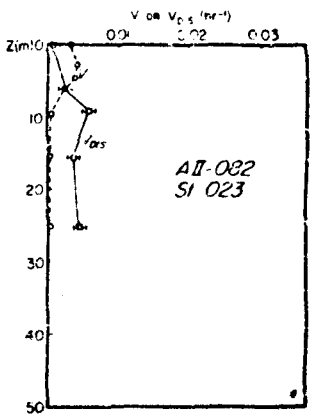
V or V_{DIS} (hr^{-1})
0.01
0.02
0.03
Z(m)
0
10
20
30
40
50
V
V_{DIS}
AII-082
St 023

Discussion

Data reported in this chapter result from preliminary experiments designed to describe gross features of the silicon cycle in two coastal upwelling regions. The results are readily interpretable as descriptions of phenomena, but almost uninterpretable at present in determining cause and effect relationships within the two ecosystems. On a purely descriptive level, the following features of silicon dynamics in the Baja California and northwest Africa upwelling systems are apparent:

Vertical extent and light dependence of silicic acid uptake by natural phytoplankton populations

Silicic acid uptake extended well beyond the depth of 1% light penetration in both the Baja California and northwest Africa upwelling regions, while photosynthesis did not. In addition data from MESCAL II stations 18, 19, 22 and 23 where seawater was collected and incubated at night during the drogue study, and JOINT I stations 70 and 78 where vertical profiles of both light and dark uptake were obtained indicate that silicic acid uptake at all light depths could proceed at a substantial rate in the absence of photosynthesis. Living diatoms appear to have accounted for all silicic acid uptake in both regions, and unquestionably have an absolute requirement for light, so photosynthesis and silicic acid uptake cannot be entirely independent of one another. However, coupling between the two processes is clearly indirect and it is possible that the only interaction is the energetic dependence of silicic acid uptake upon aerobic respiration and ATP production

(Lewin, 1955), which proceed at the expense of energy fixed photosynthetically by the cell.

The degree of light dependence of silicic acid uptake observed in natural photoplankton populations off Baja California and northwest Africa was intermediate between the very weak dependence in *Thalassiosira pseudonana* grown under optimal light conditions, reported in Chapter III, and the strong dependence in *Skeletonema costatum* when sub-optimal light conditions were allowed to persist for several days (Davis, 1973). This implies that if the interaction between light and silicic acid uptake is purely energetic, then natural phytoplankton may generally be in an energetic state intermediate between those of the populations in the two laboratory experiments. Extension of this reasoning suggests both that Baja California phytoplankton were in better energetic condition than northwest Africa phytoplankton and that Baja California phytoplankton had greater energetic reserves during upwelling periods than during stratified periods.

Whatever mechanism imposes light dependence on silicic acid uptake in natural phytoplankton populations, fluctuations of both the Baja California and northwest Africa populations between no light dependence and absolute light dependence indicates that coupling between silicic acid uptake and photosynthesis can develop and disappear rapidly with time.

Near-surface silica dissolution off northwest Africa

The classical picture of nutrient dynamics in an upwelling region involves a net influx of dissolved inorganic nutrients which drive the

production of biogenic particulate matter. It appears that in the region bounded by the 21°00' and 21°40' N. parallels, the 17°30' W. meridian and the African coast (See Figure 10.) the exact opposite was true for silicon during JOINT I. That is, to maintain a net dissolution of silica in the upper 50 m there must have been a net flux of particulate silicon into the area and a net outward flux of silicic acid. The source of this required particle flux is uncertain, but at least three possibilities exist: a net influx of particulate silicon across the sea surface in the form of a finely divided airborne Sahara sand, resuspension of recently sedimented silica by vigorous wind mixing, which frequently extends to the bottom in the spring, and advective transport of suspended particulate matter from the north by the Canary current.

It is not possible on the basis of present data to identify any one of these processes conclusively as the source of the required particulate silicon. However, the fact that both the solubility and the dissolution rate constant of quartz are approximately an order of magnitude lower than those of biogenic silica (Stöber, 1967; Wollast, 1974) and that the two parameters affect the dissolution rate independently (See equation (8).), increases the probability that the imported silica which brought about net dissolution in this region was biogenic. The high particulate silicon concentration, low specific uptake rate and rapid light extinction at station 23, and its proximity to the coast all suggest that its particulate silicon was predominantly suspended desert sand. This station had the lowest specific dissolution

rates of any station where rates were determined, again suggesting that the high values of V_{dis} observed at other stations resulted from dissolution of biogenic silica. The source of this silica cannot be inferred from available data, but its existence is demanded by the excess of dissolution over uptake apparent in Figure 17.

It is likely that the silica dissolution rate measurements reported here represent an extreme case. Vigorous wind mixing over the continental shelf almost undoubtedly kept diatom debris suspended which would have been removed from the system by sinking under less turbulent conditions. Additionally the possibility remains that the observed high dissolution rates were a strictly local effect resulting from the presence of suspended desert sand. Nevertheless, these direct measurements tend to support the predictions of Wollast (1974) and Hurd (1972) and the inferences of Kozlova (1964) that dissolution of biogenic silica may proceed at a high rate in near-surface seawater, and to refute the assumption of Dugdale (1972) and Walsh (1975) that regeneration of silicic acid is negligible in upwelling regions.

CHAPTER V

HYPOTHESES

The previous four chapters have presented a synopsis of current knowledge of the chemical behavior and biological significance of silicon in the ocean, a set of tracer techniques which allow rates of some processes in the marine silicon cycle to be measured, some experimental data, and several fairly conservative interpretations of the data collected to date.

There are inferences to be drawn from data presented in this dissertation which are consistent with all available data, with current knowledge of the dynamics of silicon in marine production, and which may be true but which are beyond the scope of the experiments reported in Chapters III and IV, and thus not firmly supported experimentally at this time. These inferences will be presented as hypotheses, and should be distinguished clearly from interpretations presented in previous chapters, which are strongly supported by experimental data. It is possible that the only feature of the following hypotheses which makes them more attractive than others which could be proposed is that they are directly testable using available experimental procedures, and thus may not last long if incorrect. They are presented less as interpretations of present data than as possible areas of future investigation as study of the marine silicon cycle, and of nutrient dynamics in general, moves forward from description of phenomena to a determination of cause and effect.

Prevention of Silicon Limitation off Baja California

One feature of the Baja California upwelling ecosystem which seems absolutely clear is that silicon is never limiting to primary production. The silicic acid concentration of the near-surface water is seldom less than 3 μg atoms Si · ℓ^{-1}, and almost never less than the total combined nitrogen concentration (Whitledge and Bishop, 1974). Silicic acid uptake kinetic experiments conducted at two stations selected for their low ambient silicic acid concentration demonstate a lack of concentration dependence for uptake even at the lowest substrate concentrations encountered and strongly imply a lack of concentration dependence throughout the system.

The flux of silicic acid into the surface water via upwelling is approximately equal to that of nitrate (Walsh, 1973). During periods of upwelling the phytoplankton is dominated by a large and heavily silicified diatom of the genus *Coscinodiscus*, and comparison of MESCAL II ^{30}Si data (Appendix A) with ^{15}N data for the same cruise (Conway, Harmon and Dugdale, unpublished) indicates both that the concentration of particulate silicon exceeded that of particulate nitrogen and that absolute and specific rates of silicic acid uptake exceeded corresponding rates of nitrate plus ammonium uptake at almost every station sampled. With nitrogen and silicon supplied to the euphotic zone at nearly equal rates and silicon taken up by the phytoplankton at a consistently higher rate one would expect silicic acid to become more depleted than total combined nitrogen in the surface layer, yet the exact opposite was observed.

If proposed nutrient budgets for the Baja California upwelling system (Walsh, 1973; Walsh, Kelley, Whitledge, Huntsman and Pillsbury, 1975) are even approximately correct, then the net rate of removal of combined nitrogen from solution must exceed that of silicon, implying a regeneration rate of silicic acid which is high compared to that of combined nitrogen. Silica dissolution has been suggested by Paasche (1973 b) and shown by experiments reported in Chapter III to proceed at an appreciable rate even in healthy, growing diatom populations, and comparison of the dissolution data of Lewin (1961) and Hurd (1972) with uptake kinetic data reported here indicates that biogenic silica stripped of its organic coating may dissolve at a rate about equal to V_{max} for uptake. Dissolution rates approaching this maximum were observed in the 30-50 m depth layer off northwest Africa. It seems likely that dissolution of diatom silica, perhaps enhanced by the action of grazers, proceeds at a significant rate in the Baja California upwelling system and that the net result is to increase the total primary production of the region by preventing silicon limitation.

An analogous mechanism has been invoked to explain the absence of nitrogen limitation in the Peru upwelling system (Dugdale, 1972; Walsh, 1975). The dominant herbivore in that system, the Peruvian anchoveta *Engraulis ringens* has been shown to excrete reduced nitrogen compounds at a rate some twenty times greater than silicic acid (Whitledge and Packard, 1971). Reduced nitrogen compounds, chiefly ammonium (Conway, 1974) and possibly urea (Schell, 1971), are taken up preferentially to nitrate by phytoplankton with the result that nitrate is still present

at *ca.* 4 μg atoms N · ℓ^{-1} at a distance of 70-80 km downstream from the source of upwelling, where silicic acid is depleted to < 0.5 μg atom Si · ℓ^{-1}. It is likely that the main role of herbivores in silicic acid regeneration is the production of detrital particulate silica which dissolves at a higher rate than would ungrazed diatoms, rather than direct excretion of silicic acid, and that the main component of silicic acid regeneration may have been overlooked in the experiments of Whitledge and Packard (1971) and Walsh's (1975) model. Nevertheless, it is clear that the Peru system, grazed by fish, is silicon limited while the Baja California system, grazed by crabs, is nitrogen limited. Walsh, Kelley, Whitledge, Huntsman and Pillsbury (1975) have set forth hypotheses concerning the role of habitat variables, mainly constancy of the wind stress, in selecting the type of organism to occupy the dominant herbivore niche in an upwelling ecosystem. It appears quite possible that the factors which select the dominant herbivore may consequently select the limiting nutrient in such systems by providing a mechanism for potentially limiting nutrients to be regenerated at unequal rates.

Time-Dependent Light Stress off Northwest Africa

Experiments reported in Chapters III and IV have shown the light dependence of silicic acid uptake to be very weak in cultures of *Thalassiosira pseudonana* grown under optimal light conditions prior to the experiment, highly variable in natural diatom populations off Baja California, and stronger and less variable in natural diatom populations off northwest Africa. Comparison of light dependence data in

Chapter III with those of Davis (1973) indicates that a stress may develop with time in a diatom population under sub-optimal light conditions and depress the silicic acid uptake rate. If such a stress develops it may explain both the relatively strong light dependence of uptake and the relatively low uptake rates observed off northwest Africa.

Strong winds off Cap Blanc in the spring result in a wind-mixed surface layer which frequently extends to a depth of 60-100 m over the continental shelf (Codispoti, unpublished). Except for a zone near the coast where high turbidity resulting from suspended Sahara sand reduces the depth of the euphotic zone to *ca.* 10 m and occasionally less, the depth of 1% light penetration is generally *ca.* 20-25 m, with the result that under normally strong winds the depth of the mixed surface layer is three to four times that of 1% light penetration and six to eight times that of 10% surface light intensity. A cell circulating randomly within the wind-mixed layer would thus spend six to eight hours of any 24-hour period at depths of 1% or greater light penetration and only two to three hours at or above the 10% light depth. Since half of each 24-hour period is night, a randomly circulating cell would experience only two to three hours of illumination equal to or greater than 1% of that at the surface in daylight, including only one to one and a half hours of light strong enough that photosynthesis is not inhibited.* Photosynthetically fixed energy is expended by the cell in

* ^{14}C uptake generally declined sharply between the 15% and 5% light depths on JOINT I (Huntsman, Jones, Smith and Barber, unpublished), so the depth of 10% light penetration is an approximation of the lower limit of the region of light saturation.

taking up silicic acid (Lewin, 1955). If the cells' energetic reserves are depleted due to sub-optimal light conditions, uptake may well become light dependent as the availability of energy to drive the uptake mechanism becomes dependent upon the rate of photosynthetic fixation of new energy.

If cell growth is dependent upon intracellular rather than extracellular nutrient concentrations (Caperon and Meyer, 1972 b; Droop, 1974) and if impairment of energy-requiring nutrient uptake pathways because of insufficient photosynthetic energy fixation actually occurs in natural phytoplankton populations, then cell growth and subsequently primary production in such populations may be nutrient limited even at high external nutrient concentrations.

^{30}Si Uptake as an Estimate of Primary Production

Five different types of rate measurement were applied to the phytoplankton off Baja California during MESCAL II, all of which can be used as estimates of primary production if certain assumptions are accepted. Three of these estimates involved isotopic tracers: the traditional ^{14}C estimate (Steeman-Nielsen, 1952), the more recent ^{15}N estimate (Dugdale and Goering, 1967) and the ^{30}Si estimate described here. In addition, direct observations of phytoplankton growth rates (Smayda, unpublished) and nutrient budgets for the upwelling region (Walsh, Kelley, Whitledge, Huntsman and Pillsbury, 1975) were obtained.

The three tracer methods should provide comparable estimates of primary production assuming that the elemental composition of the

phytoplankton is not changing with time, and that all utilized pools of each element are labeled. Adding the additional assumption that the cell quota for each element remains constant with time the observed growth rate, in divisions · day^{-1} can be related to the specific uptake rate of any element by the equation:

$$V(hr^{-1}) = \frac{\ln 2}{24} \cdot \mu \text{ (divisions} \cdot day^{-1}) \qquad (32)$$

Nutrient budget data are incapable of providing estimates of instantaneous uptake rates at any specified point in the system, but do provide an estimate of overall net uptake integrated over depth and time. This net uptake estimate is converted to a carbon assimilation estimate by assuming that the C:N:P ratio of phytoplankton is constant and known (Redfield, Ketchum and Richards, 1963).

During the longest observed upwelling period on MESCAL II the measured ^{14}C primary production averaged somewhat less than 2.0 g C · m^{-2} · day^{-1} which would correspond to a phytoplankton growth rate of 0.5-1.0 divisions · day^{-1} (Walsh, Kelley, Whitledge, Huntsman and Pillsbury, 1975). ^{15}N estimates for this period (Conway, Harmon and Dugdale, unpublished) correspond to equal or lower production rates, as is apparent in Figure 11. However, ^{30}Si estimates indicate a mean specific growth rate of *ca.* 2.0 divisions · day^{-1} during this period with estimates at some stations ranging as high as 5 divisions · day^{-1}. A nitrogen budget for this period suggests a carbon production of *ca.* 7 g C · m^{-2} · day^{-1}, or nearly four times that measured by ^{14}C (Walsh, Kelley, Whitledge, Huntsman and Pillsbury, 1975). Direct observations of phytoplankton growth rates (Smayda, unpublished), which

range as high as 5-6 divisions • day^{-1} during this period, are consistent with the higher production estimates based on ^{30}Si uptake and the nitrogen budget, and lend support to the argument that primary production was underestimated by at least 50% and more likely by about 75% using both ^{14}C and ^{15}N.

The operational definition of "uptake" in any tracer experiment is conversion of the labeled element from its chemical form at the time of inoculation to some other form which will not pass through a filter of chosen pore size. Assimilation from pools not labeled in the experiment, and uptake followed by rapid conversion to a filter-passing form are not measured. Besides nitrate and ammonium, the substrates normally labeled in ^{15}N experiments at sea, marine phytoplankton from various environments have been shown to utilize nitrite (Hattori and Wada, 1972), molecular nitrogen (Goering, Dugdale and Menzel, 1966) and a number of organic substrates (Schell, 1971) as nitrogen sources, raising the question of whether total nitrogen assimilation is often measured in the type of ^{15}N experiments performed on natural phytoplankton populations at sea. In addition the fact that a large number of organic compounds produced by the cell contain nitrogen, and all contain carbon, indicates that the intracellular biochemistry of these elements is extremely complex, and may at times lead to rapid resolubilization, and at other times not, in response to factors not presently known.

The biochemistry of silicon is not well understood, but it appears that at least most and perhaps all silicon taken up by diatoms is deposited as hydrated amorphous silica in the cell wall within minutes

(Mehard, Sullivan, Azam and Volcani, 1973; Azam, Hemmingsen and Volcani, 1974). Dissolution of cellular silica would not result in appreciable resolubilization of labeled substrate until labeled material comprised an appreciable proportion of the cellular silica, a condition which must be avoided in tracer experiments using any element (Sheppard, 1962). The relative biochemical simplicity of silicification increases the probability that ^{30}Si taken up during an incubation will be present in particulate form at the time of filtration and that the uptake rate will be measured accurately.

Obviously ^{30}Si uptake estimates only the diatom component of primary production, and can be used as an estimate of overall primary production only in phytoplankton populations dominated by diatoms. Additionally, estimation of the rate of production of new plant material from the assimilation rate of any one element assumes the cell quota for that element to be constant with time. However, the close agreement among estimates of primary production based on ^{30}Si uptake, the nitrogen budget and direct observations of phytoplankton growth rates off Baja California where the above conditions appear to have been met (Walsh, Kelley, Whitledge, Huntsman and Pillsbury, 1975), and where both ^{14}C and ^{15}N may have substantially underestimated production, indicates that in nearly steady-state, diatom-dominated phytoplankton populations ^{30}Si may provide an exceedingly reliable estimate of primary production.

CHAPTER VI

SUMMARY

Research reported in this dissertation has established the following facts concerning the dynamics of silicon in laboratory cultures of *Thalassiosira pseudonana* and natural phytoplankton populations in the Baja California and northwest Africa upwelling regions:

1. Rates of silicic acid uptake and silica dissolution in both laboratory and natural diatom populations are measurable using silicon stable isotope tracer techniques.
2. Silicic acid uptake by *T. pseudonana* in batch culture is describable by the Michaelis-Menten equation for enzyme kinetics, and proceeds at substrate concentrations down to 0.25 μg atom Si · ℓ^{-1}. There appears to be no threshold concentration below which uptake does not take place.
3. Clone 3H of *T. pseudonana*, isolated from a high silicon environment demonstrates a higher maximum silicic acid uptake rate than does clone 13-1 of the same species, isolated from a low silicon environment. Half saturation constants for uptake by the two clones are similar.
4. Light dependence of silicic acid uptake by *T. pseudonana* grown under optimal light conditions prior to the experiment is weak or nonexistent.
5. Exponentially growing populations of *T. pseudonana* release silicon to the medium by dissolution at rates ranging from *ca.* 6 to 15% of

the maximum uptake rate.

6. Silicic acid uptake by natural phytoplankton populations in two upwelling regions extends to approximately twice the depth to which carbon and nitrogen uptake were observed.
7. There is no evidence in Baja California data, and very little in northwest Africa data, that silicic acid uptake is ever substrate limited in these regions.
8. The degree of light dependence of silicic acid uptake is highly variable in natural phytoplankton populations.
9. The silica dissolution rate increases with depth between 10 and 60 m in the upwelling region off northwest Africa, and is sufficient in the upper 50 m in the Cap Blanc region to supply all silicic acid consumed by the phytoplankton.

Consideration of these experimental results in the context of present knowledge of the marine silicon cycle and of nutrient dynamics in general has led to the following hypotheses concerning mechanisms regulating primary production and the use of ^{30}Si uptake as a primary production estimate:

1. Silica dissolution may proceed at a high rate off Baja California, as it does off northwest Africa, and if it does the net effect is to increase overall primary production in the region by preventing silicon limitation. A substantial ecological role of herbivores in upwelling regions is indicated, both in preventing nutrient limitation by regenerating nutrients, and in determining the eventual limiting nutrient by providing a mechanism whereby

potentially limiting nutrients may be regenerated at unequal rates.

2. An energetic stress may develop with time in diatom populations growing at sub-optimal light intensities and impair the cells' ability to take up silicic acid. The degree of development of this light stress may be highly variable in natural planktonic diatom populations and may in certain regions be a major factor in limiting primary production.

3. In a diatom-dominated phytoplankton population whose elemental composition is not changing with time, ^{30}Si uptake may provide a more reliable estimate of primary production than either ^{14}C or ^{15}N uptake because of the relative simplicity of intracellular biochemical processes involving silicon and the resulting high probability that silicon taken up by the cell is deposited as silica in the cell wall, rather than being converted rapidly to some soluble or filter-passing chemical form.

LITERATURE CITED

Antia, N. J., C. D. McAllister, R. R. Parsons, K. Stebens and J. D. H. Strickland (1963) Further measurements of primary production using a large-volume sphere. *Limnol. Oceanogr.* 8:166-173.

Azam, F., B. B. Hemmingsen and B. E. Volcani (1974) Role of silicon in diatom metabolism. V. Silicic acid transport in the heterotrophic diatom *Nitzschia alba*. *Arch. Mikrobiol.* 97:103-114.

Armstrong, F. A. J. (1965) Silicon. In: J. P. Riley and G. Skirrow (eds.), *Chemical Oceanography*, Vol. 1, Academic Press, New York, pp. 409-432.

Berger, W. H. (1968) Radiolarian skeletons: solution at depth. *Science* 159:1237-1238.

Berger, W. H. (1970) Biogenous deep sea sediments: fractionation by deep-sea circulation. *Geol. Soc. Amer. Bull.* 81(5):1385-1401.

Blackburn, M. (1975) Summary of existing information on nekton of Spanish Sahara and adjacent regions, northwest Africa. *Coastal Upwelling Ecosystems Analysis Technical Report 8*, University of Washington, Seattle, 49 pp.

Busby, W. F. and J. C. Lewin (1967) Silicate uptake and silica shell formation by synchronously dividing cells of the diatom *Navicula pelliculosa* (Bréb.) Hilse. *J. Phycol.* 3:127-131.

Calvert, S. E. (1968) Silica balance in the ocean and diagenesis. *Nature* 219:919-920.

Caperon, J. (1968) Population growth response of *Isochrysis galbana* to nitrate variation at limiting concentration. *Ecology* 49:866-872.

Caperon, J. and J. Meyer (1972 a) Nitrogen-limited growth of marine phytoplankton. Part I: Changes in population characteristics with steady state growth rate. *Deep-Sea Res.* 19:601-618.

Caperon, J. and J. Meyer (1972 b) Nitrogen-limited growth of marine phytoplankton. Part II: Uptake kinetics and their role in nutrient limited growth of phytoplankton. *Deep-Sea Res.* 19:619-632.

Conway, H. L. (1974) The uptake and assimilation of inorganic nitrogen by *Skeletonema costatum* (Grev.) Cleve. Ph.D. Dissertation, University of Washington, Seattle, 125 pp.

Coombs, J., W. M. Darley, O. Holm-Hansen and B. E. Volcani (1967) Studies on the biochemistry and fine structure of silica shell formation in diatoms. Chemical composition of *Navicula pelliculosa* during silicon-starvation synchrony. *Plant Physiol.* 42:1601-1606.

Cooper, L. H. N. (1933) Chemical constituents of biological importance in the English Channel. Pt I. phosphate, silicate, nitrate, nitrite, ammonia. *J. Mar. Biol. Ass. U. K.* 18:677-728.

Cooper, L. H. N. (1952) Factors affecting the distribution of silicate in the North Atlantic Ocean and the formation of North Atlantic Deep Water. *J. Mar. Biol. Ass. U. K.* 30:511-526.

Cushing, D. H. (1971) Upwelling and the production of fish. *Adv. Mar. Biol.* 9:255-334.

Darley, W. M. (1970) Silicon and the division cycle of the diatoms *Navicula pelliculosa* and *Cylindrotheca fusiformis*. *Proc. North American Paleontological Convention, September, 1969,* Part 6: 994-1009.

Davis, C. O. (1973) Effects of changes in light intensity and photoperiod on the silicate-limited continuous culture of the marine diatom *Skeletonema costatum* (Grev.) Cleve. Ph.D. Dissertation, University of Washington, Seattle, 122 pp.

Delury, G. E. (ed.) (1973) *The World Alamanac and Book of Facts*, Newspaper Enterprise Association, Incorporated, New York, 1040 pp.

Droop, M. R. (1968) Vitamin B-12 and marine ecology. IV. The kinetics of uptake, growth and inhibition in *Monochrysis lutheri*. *J. Mar. Biol. Ass. U. K.* 48:689-733.

Droop, M. R. (1973) Some thoughts on nutrient limitation in algae. *J. Phycol.* 9:264-272.

Droop, M. R. (1974) The nutrient status of algal cells in continuous culture. *J. Mar. Biol. Ass. U. K.* 54:825-855.

Dugdale, R. C. (1967) Nutrient limitation in the sea: Dynamics, identification and significance. *Limnol. Oceanogr.* 12:285-295.

Dugdale, R. C. (1972) Chemical oceanography and primary productivity in upwelling regions. *Geoforum* 11:47-61.

Dugdale, R. C. and J. J. Goering (1967) Uptake of new and regenerated forms of nitrogen in primary productivity. *Liminol. Oceanogr.* 12(2):196-206.

Dugdale, R. C. and J. J. Goering (1970) Nutrient limitation and the path of nitrogen in Peru Current production. *Anton Bruun Rep. No. 4*, Texas A. & M. Press, 5.3-5.8.

Ekman, W. V. (1905) On the influence of the earth's rotation on ocean currents. *Ark. f. Mät. Astron. och Fysik* 2(11):1-53.

Eppley, R. W., J. N. Rogers and J. L. McCarthy (1969) Half-saturation constants for uptake of nitrate and ammonium by marine phytoplankton. *Limnol. Oceanogr.* 14:912-920.

Eppley, R. W. and W. H. Thomas (1969) Comparison of half-saturation constants for growth and nitrate uptake of marine phytoplankton. *J. Phycol.* 5:375-379.

Fanning, K. A. and M. E. Q. Pilson (1974) Diffusion of silica out of deep-sea sediments. *J. Geophys. Res.* 79:1293-1297.

Fuhs, G. W. (1969) Phosphorus content and rate of growth in the diatoms *Cyclotella nana* and *Thalassiosira fluviatilis*. *J. Phycol.* 5:312-321.

Goering, J. J., R. C. Dugdale and D. W. Menzel (1966) Estimates of *in situ* rates of nitrogen uptake by *Trichodesmium* sp. in the tropical Atlantic Ocean. *Limnol. Oceanogr.* 11(4):614-620.

Goering, J. J., D. M. Nelson and J. A. Carter (1973) Silicic acid uptake by natural populations of marine phytoplankton. *Deep-Sea Res.* 20:777-789.

Grill, E. V. (1970) A mathematical model for the marine dissolved silicate cycle. *Deep-Sea Res.* 17:245-266.

Grill, E. V. and F. A. Richards (1964) Nutrient regeneration from phytoplankton decomposing in seawater. *J. Mar. Res.* 22:51-69.

Guillard, R. R. L., P. Kilham and T. A. Jackson (1973) Kinetics of silicon limited growth in the marine diatom *Thalassiosira pseudonana* Hasle and Heimdal (=*Cyclotella nana* Hustedt). *J. Phycol.* 9:233-237.

Guillard, R. R. L. and J. Ryther (1962) Studies of marine planktonic diatoms. I. *Cyclotella nana* Hustedt and *Detonula confervacea* (Cleve) Gran. *Can. J. Microbiol.* 8:229-239.

Hager, S. W., L. I. Gordon and P. K. Park (1968) A practical manual for use of the Technicon AutoAnalyzer in seawater nutrient analysis. A final report to BCF, Contract 14-17-0001-1759, Oregon State University. October, 1968. Ref. 68-33 (Unpublished manuscript).

Harrison, P. J. (1974) Continuous culture of the marine diatom *Skeletonema costatum* (Grev.) Cleve under silicate-limitation. Ph.D. Dissertation, University of Washington, Seattle, 140 pp.

Harriss, R. C. (1966) Biological buffering of oceanic silica. *Nature* 212:275-276.

Hattori, A. and E. Wada (1972) Biogeochemical cycle of inorganic nitrogen in marine environments with special reference to nitrite metabolism. In: E. Ingerson (ed.) *Proceedings of symposium on hydrogeochemistry and biogeochemistry*, Vol. II, The Clarke Company, Washington, D. C., pp. 28-39.

Heath, G. R. (1973) Dissolved silica and deep-sea sediments. In: W. W. Hay (ed.) *Soc. Econ. Paleont. Min. Special Publ. No. 18*, 57 pp.

Herbert, D. (1961) The chemical composition of micro-organisms as a function of their environment. *Symp. Soc. Gen. Microbiol.* 11: 391-416.

Herbert, D., R. Elsworth and R. C. Telling (1956) The continuous culture of bacteria: a theoretical and experimental study. *J. Gen. Microbiol.* 14:601-622.

Hurd, D. C. (1972) Factors affecting solution rate of biogenic opal in seawater. *Earth and Planet. Sci. Letters* 15:411-417.

Hurd, D. C. (1973) Interactions of biogenic opal sediment and seawater in the Central Equatorial Pacific. *Geochim. Cosmochim. Acta* 37: 2257-2282.

Jannasch, H. W. (1974) Steady state and the chemostat in ecology. *Limnol. Oceanogr.* 19(4):716-720.

Jones, M. M. and R. M. Pytkowicz (1973) Solubility of silica in seawater at high pressures. *Bull. de la Soc. Roy des Sci. de Liege* 42:118-120.

Jorgensen, E. G. (1955) Solubility of the silica in diatoms. *Physiol. Plant.* 8:846-851.

Jorgensen, E. G. (1957) Diatom periodicity and silicon assimilation. *Dansk Botan. Arkiv.* 18:6-54.

Kamatani, A. (1969) Regeneration of inorganic nutrients from diatom decomposition. *J. Oceanogr. Soc. Japan* 25(2):63-74.

Kilham, P. (1971) A hypothesis concerning silica and the freshwater planktonic diatoms. *Limnol. Oceanogr.* 16:10-18.

Kozlova, O. G. (1964) Diatoms of the Indian and Pacific sectors of the Antarctic. *Moscow Publ. House Akad. Nauk. U. S. S. R.*

Lewin, J. C. (1954) Silicon metabolism in diatoms. I. Evidence for reduced sulfur compounds in Si utilization. *J. Gen. Physiol.* 37:589-599.

Lewin, J. C. (1955) Silicon metabolism in diatoms. III. Respiration and silicon uptake in *Navicula pelliculosa*. *J. Gen Physiol.* 39: 1-10.

Lewin, J. C. (1957) Silicon metabolism in diatoms. IV. Growth and frustule formation in *Navicula pelliculosa*. *Can. J. Microbiol.* 3:427-433.

Lewin, J. C. (1961) The dissolution of silica from diatom walls. *Geochim. Cosmochim. Acta* 21:182-195.

Lewin, J. C. (1962) Silicification. In: R. E. Lewin (ed.) *Physiology and Biochemistry of Algae*, Academic Press, New York, pp. 445-455.

Lewin, J. C., B. E. Reimann, W. F. Busby and B. E. Volcani (1966) Silica shell formation in synchronously dividing diatoms. In: I. L. Cameron and G. M. Padilla (eds.) *Cells Synchrony*, Academic Press, New York, pp. 169-188.

Lindner, M. (1953) New nuclides produced in chlorine spallation. *Phys. Rev.* 91:642-644.

Lisitzin, A. P. (1972) Sedimentation in the world ocean. *Soc. Econ. Paleont. Min. Special Publ. No. 17.*

Longhurst, A. R., C. J. Lorenzen, W. H. Thomas (1967) The role of pelagic crabs in the grazing of phytoplankton off Baja California. *Ecology* 48(2):192-200.

MacIsaac, J. J. and R. C. Dugdale (1969) The kinetics of nitrate and ammonia uptake by natural populations of marine phytoplankton. *Deep-Sea Res.* 16:45-57.

MacIsaac, J. J. and R. C. Dugdale (1972) Interactions of light and inorganic nitrogen in controlling nitrogen uptake in the sea. *Deep-Sea Res.* 19:209-232.

Mackenzie, F. T., R. M. Garrells, O. P. Bricker and F. Bickley (1967) Silica in seawater: control by silicate minerals. *Science* 155:1404-1406.

Mehard, C. W., C. W. Sullivan, F. Azam and B. E. Volcani (1973) Role of silicon in diatom metabolism. IV. Subcellular localization of silicon and germanium in *Nitzschia alba* and *Cylindrotheca fusisformis*. *Physol. Plant.* 30:265-272.

Mittelstaedt, E. and K. P. Koltermann (1973) On the currents over the shelf off Cap Blanc in the northwest African upwelling area. *Deutsche Hydrographische Zeitschrift* 5:193-215.

Monod, J. (1942) *Recherches sur la Croissance des Cultures Bactériennes*. Hermann et Cie., Paris, 210 pp.

Neese, J. C., R. C. Dugdale, V. A. Dugdale and J. J. Goering (1962) Nitrogen metabolism in lakes. I. Measurement of nitrogen fixation with ^{15}N. *Limnol. Oceanogr.* 7:163-169.

Neumann, G. and W. J. Pierson, Jr. (1966) *Principles of Physical Oceanography*, Prentice-Hall, Englewood Cliffs, New Jersey, 545 pp.

Odum, E. P. (1959) *Fundamentals of Ecology*, 2nd edition. W. B. Saunders, Philadelphia, 546 pp.

Paasche, E. (1973 a) Silicon and the ecology of marine plankton diatoms. I. *Thalassiosira pseudonana* (*Cyclotela nana*) grown in a chemostat with silicate as the limiting nutrient. *Mar. Biol.* 19: 117-126.

Paasche, E. (1973 b) Silicon and the ecology of marine plankton diatoms. II. Silicate-uptake kinetics in five diatom species. *Mar. Biol.* 19:262-269.

Park, P. K. (1967) Nutrient regeneration and preformed nutrients off Oregon. *Limnol. Oceanogr.* 12(2):353-357.

Redfield, A. C., B. H. Ketchum and F. A. Richards (1963) The influence of organisms on the composition of sea-water. In: M. N. Hill (ed.) *The Sea*, Vol. II, Interscience Publishers, New York, pp. 26-77.

Ryther, J. H. (1969) Photosynthesis and fish production in the sea. *Science* 166:72-76.

Schell, D. M. (1971) Uptake and Regeneration of Dissolved Organic Nitrogen in Southeastern Alaskan Marine Waters. Ph.D. Dissertation, University of Alaska, Fairbanks, 142 pp.

Schink, D. R. (1965) Determination of silica in sea water using solvent extration. *Anal. Chem.* 37:764-765.

Sheppard, C. W. (1962) *Basic principles of the tracer method.* Wiley, New York, 282 pp.

Siever, R. (1962) Silica solubility at 0° C-200° C and the diagenesis of siliceous sediments. *J. Geol.* 70:127-150.

Steeman-Nielsen, E. (1952) The use of radioactive carbon (^{14}C) for measuring organic production in the sea. *J. Cons. Perm. Int. Explor. Mer* 18:117-140.

Stöber, W. (1967) Formation of silicic acid in aqueous suspensions of different silica modification. In: W. Stumm (ed.) *Equilibrium Concepts in Natural Water Systems*, Am. Chem. Soc. Series 67, Washington, D.C., pp. 161-182.

Strickland, J. D. H. and T. R. Parsons (1968) A Practical handbook of seawater analysis. *Bull. Fish. Res. Bd. Can.* 167:311 pp.

Stumm, W. and J. J. Morgan (1970) *Aquatic Chemistry*. Wiley-Interscience, New York, 583 pp.

Sullivan, C. W. and B. E. Volcani (1973 a) Role of silicon in diatom metabolism. II. Endogenous nucleoside triphosphate pools during silicic acid starvation of synchronized *Cylindrotheca fusiformis*. *Biochim. Biophys. Acta* 308:205-211.

Sullivan, C. W. and B. E. Volcani (1973 b) Role of silicon in diatom metabolism. III. The effects of silicic acid on DNA polymerase, TMP kinase and DNA synthesis in *Cylindrotheca fusiformis*. *Biochim. Biophys. Acta* 308:219-229.

Sullivan, W. H. (1957) *Trilinear Chart of Nuclides*. U. S. Atomic Energy Commission Publication, Wiley and Sons, New York.

Sverdrup, H. U., M. W. Johnson and R. H. Fleming (1941) *The Oceans*. Prentice-Hall, Incorporated, New York, 1080 pp.

Thompson, T. G. and R. J. Robinson (1932) Chemistry of the Sea. *Bull. Nat. Res. Coun. Wash.* 85:95-203.

van Lier, J. A., P. L. De Bruyn and J. Th. G. Overbeek (1960) The solubility of quartz. *J. Phys. Chem.* 64:1675-1682.

Walsh, J. J. (1973) Modelled processes in the sea. In: D. H. Cushing and J. J. Walsh (eds.) *Ecology of the Sea*, Blackwells, Oxford, In press.

Walsh, J. J. (1975) A spatial simulation model of the Peru upwelling ecosystem. *Deep-Sea Res.*, In press.

Walsh, J. J., J. C. Kelley, T. E. Whitledge, S. A. Huntsman and R. D. Pillsbury (1975) Further transition states of the Baja California upwelling ecosystem. *Limnol. Oceanogr.*, In press.

Walsh, J. J., J. C. Kelley, T. E. Whitledge, J. J. MacIsaac and S. A. Huntsman (1974) Spin-up of the Baja California upwelling ecosystem. *Limnol. Oceanogr.* 19(4):553-572.

Weiler, R. R. and A. A. Mills (1965) Surface properties and pore structure of marine sediments. *Deep-Sea Res.* 12:511-529.

Whitledge, T. E. and D. Bishop (1974) Coastal Upwelling Ecosystems Analysis and Upwelling Biome Data Report II. R/V *T. G. Thompson* cruise 78 (MESCAL II), University of Washington, Seattle.

Whitledge, T. E. and T. T. Packard (1971) Nutrient excretion by anchovies and zooplankton in Pacific upwelling regions. *Invest. Pesq.* 35(1):243-250.

Williams, F. M. (1971) Dynamics of microbial populations. In: B. C. Patten (ed.) *Systems Analysis and Simulation in Ecology*, Vol. 1, Academic Press, New York, pp. 117-267.

Wollast, R. (1974) The silica problem. In: E. D. Goldberg (ed.) *The Sea*, Vol. 5, Wiley-Interscience, New York, pp. 359-392.

Wollast, R. and R. M. Garrells (1971) Diffusion coefficient of silica in seawater. *Nature Phys. Sci.* 229(3):94.

Wooster, W. S. and J. L. Reid, Jr. (1963) Eastern boundary currents. In: M. N. Hill (ed.) *The Sea*, Vol. 2, Wiley-Interscience, New York, pp. 97-122.

Zoller, W. H. (1966) Production and half-life of silicon-32. Nuclear Chemistry Proposition, Massachusetts Institute of Technology, Cambridge, 16 pp.

APPENDIX A

SILICIC ACID UPTAKE DATA FROM MESCAL II

Station 3

Lt. depth (% surface intensity)	Depth (m)	V (hr^{-1})	S_1 (μg atoms $Si \cdot \ell^{-1}$)	ρ (μg atoms $Si \cdot \ell^{-1} \cdot hr^{-1}$)
100	0.0	0.013	1.63	0.020
50	3.2	0.011	1.05	0.011
25	6.3	0.013	1.33	0.018
10	10.5	0.012	2.64	0.031
1	21.0	0.016	0.87	0.014
50 @ 0	3.2	0.010	1.21	0.012

Station 9

Lt. depth (% surface intensity)	Depth (m)	V (hr^{-1})	S_1 (μg atoms $Si \cdot \ell^{-1}$)	ρ (μg atoms $Si \cdot \ell^{-1} \cdot hr^{-1}$)
100	0.0	0.032	3.11	0.099
50	2.5	0.017	5.94	0.099
25	5.0	0.020	5.31	0.105
10	9.0	0.005	2.15	0.011
1	18.0	0.016	5.41	0.091
50 @ 0	2.5	0.004	3.35	0.017

Station 17

Lt. depth (% surface intensity)	Depth (m)	V (hr^{-1})	S_1 (μg atoms $Si \cdot \ell^{-1}$)	ρ (μg atoms $Si \cdot \ell^{-1} \cdot hr^{-1}$)
100	0.0	0.113	3.36	0.379
50	3.5	0.132	3.39	0.449
25	7.0	0.091	3.84	0.351
10	12.0	0.103	3.22	0.334
1	23.0	0.149	3.84	0.576
50 @ 0	3.5	0.135	2.78	0.376

Station 18

Lt. depth (% surface intensity)	Depth (m)	V (hr^{-1})	S_1 (μg atoms $Si \cdot \ell^{-1}$)	ρ (μg atoms $Si \cdot \ell^{-1} \cdot hr^{-1}$)
100	0.0	0.010	4.64	0.044
50	3.5	0.012	5.38	0.067
25	7.0	--	--	--
10	12.0	0.001	2.67	0.003
1	23.0	0.010	5.51	0.053
0.1	34.0	--	--	--
0.01	46.0	0.001	2.61	0.002

Station 19

Lt. depth (% surface intensity)	Depth (m)	V (hr^{-1})	S_1 (μg atoms $Si \cdot \ell^{-1}$)	ρ (μg atoms $Si \cdot \ell^{-1} \cdot hr^{-1}$)
100	0.0	0.020	7.17	0.144
50	3.5	0.027	5.91	0.159
25	7.0	0.029	7.13	0.207
10	12.0	0.027	6.38	0.169
1	23.0	0.028	6.07	0.169
50 @ 0	3.5	0.025	5.77	0.142

Station 20

Lt. depth (% surface intensity)	Depth (m)	V (hr^{-1})	S_1 (μg atoms $Si \cdot \ell^{-1}$)	ρ (μg atoms $Si \cdot \ell^{-1} \cdot hr^{-1}$)
100	0.0	0.029	5.75	0.164
50	3.5	0.027	4.53	0.122
25	7.0	0.018	2.71	0.048
10	12.0	0.019	3.22	0.060
1	23.0	0.017	3.89	0.067
50 @ 0	3.5	0.017	4.16	0.072

Station 21

Lt. depth (% surface intensity)	Depth (m)	V (hr^{-1})	S_1 (μg atoms $Si \cdot \ell^{-1}$)	ρ (μg atoms $Si \cdot \ell^{-1} \cdot hr^{-1}$)
100	0.0	0.020	3.31	0.068
50	3.0	0.018	3.43	0.060
25	7.0	0.014	4.63	0.064
10	10.5	0.064	4.01	0.277
1	21.0	0.006	2.29	0.015
50 @ 0	3.0	0.009	2.53	0.023

Station 22 (22-hour incubation)

Lt. depth (% surface intensity)	Depth (m)	V (hr^{-1})	S_1 (μg atoms $Si \cdot \ell^{-1}$)	ρ (μg atoms $Si \cdot \ell^{-1} \cdot hr^{-1}$)
100	0.0	0.007	3.34	0.023
50	3.0	0.024	3.27	0.077
25	7.0	0.012	4.57	0.054
10	10.5	0.008	3.91	0.032
1	21.0	0.005	3.39	0.018
0.1	31.0	0.006	4.78	0.031
0.01	42.0	0.003	6.47	0.017

Station 23

Lt. depth (% surface intensity)	Depth (m)	V (hr^{-1})	S_1 (μg atoms $Si \cdot \ell^{-1}$)	ρ (μg atoms $Si \cdot \ell^{-1} \cdot hr^{-1}$)
100	0.0	0.135	3.34	0.450
50	3.0	0.134	3.36	0.451
25	7.0	0.127	3.33	0.424
10	10.5	0.138	4.07	0.560
1	21.0	0.152	3.61	0.550
50 @ 0	3.0	0.124	3.54	0.430

Station 24

Lt. depth (% surface intensity)	Depth (m)	V (hr^{-1})	S_1 (μg atoms $Si \cdot \ell^{-1}$)	ρ (μg atoms $Si \cdot \ell^{-1} \cdot hr^{-1}$)
100	0.0	0.130	3.03	0.392
50	3.0	--	--	--
25	7.0	0.111	2.94	0.326
10	10.5	0.114	2.98	0.340
1	21.0	0.143	3.61	0.516
50 @ 0	3.0	0.131	3.78	0.494

Station 27

Lt. depth (% surface intensity)	Depth (m)	V (hr^{-1})	S_1 (μg atoms $Si \cdot \ell^{-1}$)	ρ (μg atoms $Si \cdot \ell^{-1} \cdot hr^{-1}$)
100	0.0	0.023	7.19	0.162
50	2.5	0.018	9.19	0.164
25	6.0	0.012	5.15	0.064
10	8.0	0.018	8.95	0.158
1	15.5	0.014	5.07	0.072
50 @ 0	2.5	0.007	6.79	0.047

Station 30

Lt. depth (% surface intensity)	Depth (m)	V (hr^{-1})	S_1 (μg atoms $Si \cdot \ell^{-1}$)	ρ (μg atoms $Si \cdot \ell^{-1} \cdot hr^{-1}$)
100	0.0	0.043	5.29	0.225
50	3.0	0.130	7.25	0.945
25	6.5	0.039	4.31	0.168
10	10.5	0.036	5.68	0.204
1	21.0	0.033	6.22	0.204
50 @ 0	3.0	0.025	4.46	0.112

Station 38

Lt. depth (% surface intensity)	Depth (m)	V (hr^{-1})	S_1 (μg atoms $Si \cdot \ell^{-1}$)	ρ (μg atoms $Si \cdot \ell^{-1} \cdot hr^{-1}$)
100	0.0	0.054	3.10	0.167
50	3.0	0.035	2.66	0.093
25	5.5	0.001	4.67	0.006
10	9.0	0.000	4.25	0.000
1	18.0	0.004	4.52	0.018
50 @ 0	3.0	0.000	4.29	0.000

Station 40

Lt. depth (% surface intensity)	Depth (m)	V (hr^{-1})	S_1 (μg atoms $Si \cdot \ell^{-1}$)	ρ (μg atoms $Si \cdot \ell^{-1} \cdot hr^{-1}$)
100	0.0	0.005	3.28	0.018
50	3.0	0.004	4.50	0.020
25	6.0	0.003	4.68	0.016
10	10.5	0.003	6.44	0.018
1	21.0	--	--	--
50 @ 0	3.0	--	--	--

Station 43

Lt. depth (% surface intensity)	Depth (m)	V (hr^{-1})	S_1 (μg atoms $Si \cdot \ell^{-1}$)	ρ (μg atoms $Si \cdot \ell^{-1} \cdot hr^{-1}$)
100	0.0	0.002	3.45	0.008
50	3.0	0.034	3.54	0.120
25	6.0	0.005	3.50	0.017
10	10.5	0.001	3.31	0.003
1	21.0	0.003	3.35	0.010
50 @ 0	3.0	0.004	2.78	0.012

Station 44

Lt. depth (% surface intensity)	Depth (m)	V (hr^{-1})	S_1 (μg atoms $Si \cdot \ell^{-1}$)	ρ (μg atoms $Si \cdot \ell^{-1} \cdot hr^{-1}$)
100	0.0	0.004	4.08	0.015
50	3.0	0.005	3.23	0.015
25	5.5	0.019	2.99	0.058
10	9.0	0.003	2.91	0.009
1	18.0	0.003	2.91	0.009
50 @ 0	3.0	0.005	2.79	0.015

Station 45

Lt. depth (% surface intensity)	Depth (M)	V (hr^{-1})	S_1 (μg atoms $Si \cdot \ell^{-1}$)	ρ (μg atoms $Si \cdot \ell^{-1} \cdot hr^{-1}$)
100	0.0	0.006	3.10	0.018
50	3.0	0.009	2.96	0.027
25	5.5	0.004	3.04	0.012
10	9.0	0.003	2.60	0.009
1	18.0	0.002	2.79	0.004
50 @ 0	3.0	0.003	3.17	0.010

Station 46

Lt. depth (% surface intensity)	Depth (m)	V (hr^{-1})	S_1 (μg atoms $Si \cdot \ell^{-1}$)	ρ (μg atoms $Si \cdot \ell^{-1} \cdot hr^{-1}$)
100	0.0	0.008	2.87	0.022
50	3.0	0.003	2.99	0.011
25	5.5	0.027	3.43	0.095
10	9.0	0.005	2.35	0.012
1	18.0	0.003	2.88	0.008
50 @ 0	3.0	0.001	2.35	0.003

Station 47

Lt. depth (% surface intensity)	Depth (m)	V (hr^{-1})	S_1 (μg atoms $Si \cdot \ell^{-1}$)	ρ (μg atoms $Si \cdot \ell^{-1} \cdot hr^{-1}$)
100	0.0	0.009	3.51	0.033
50	3.0	0.012	2.97	0.035
25	5.5	0.009	3.12	0.028
10	9.0	0.008	3.19	0.026
1	18.0	0.013	3.36	0.044
50 @ 0	3.0	0.007	3.01	0.023

Station 48

Lt. depth (% surface intensity)	Depth (m)	V (hr^{-1})	S_1 (μg atoms $Si \cdot \ell^{-1}$)	ρ (μg atoms $Si \cdot \ell^{-1} \cdot hr^{-1}$)
100	0.0	--	--	--
50	3.0	0.090	3.51	0.314
25	6.0	0.024	3.42	0.082
10	10.5	0.028	3.15	0.087
1	21.0	0.043	3.02	0.129
50 @ 0	3.0	0.088	3.08	0.270

Station 49

Lt. depth (% surface intensity)	Depth (m)	V (hr^{-1})	S_1 (μg atoms $Si \cdot \ell^{-1}$)	ρ (μg atoms $Si \cdot \ell^{-1} \cdot hr^{-1}$)
100	0.0	0.033	3.72	0.122
50	4.0	0.049	2.95	0.145
25	7.0	0.047	2.99	0.140
10	12.0	0.052	2.86	0.148
1	23.0	0.042	4.99	0.212
50 @ 0	4.0	0.054	2.74	0.149

Station 53

Lt. depth (% surface intensity)	Depth (m)	V (hr^{-1})	S_1 (μg atoms $Si \cdot \ell^{-1}$)	ρ (μg atoms $Si \cdot \ell^{-1} \cdot hr^{-1}$)
100	0.0	0.115	3.45	0.396
50	3.0	0.125	3.06	0.381
25	6.0	--	--	--
10	10.5	0.138	3.45	0.476
1	21.0	0.154	3.45	0.534
50 @ 0	3.0	0.115	3.70	0.424

Station 58

Lt. depth (% surface intensity)	Depth (m)	V (hr^{-1})	S_1 (μg atoms $Si \cdot \ell^{-1}$)	ρ (μg atoms $Si \cdot \ell^{-1} \cdot hr^{-1}$)
100	0.0	--	--	--
50	3.0	--	--	--
25	6.0	0.121	3.71	0.450
10	10.5	0.321	6.48	2.079
1	21.0	0.156	4.12	0.644
50 @ 0	3.0	0.155	3.83	0.595

Station 59

Lt. depth (% surface intensity)	Depth (m)	V (hr^{-1})	S_1 (μg atoms $Si \cdot \ell^{-1}$)	ρ (μg atoms $Si \cdot \ell^{-1} \cdot hr^{-1}$)
100	0.0	0.001	1.91	0.002
50	3.0	0.020	2.45	0.048
25	6.0	--	--	--
10	10.5	0.005	2.69	0.013
1	21.0	0.001	2.39	0.003
50 @ 0	3.0	0.000	2.22	0.000

Station 65

Lt. depth (% surface intensity)	Depth (m)	V (hr^{-1})	S_1 (μg atoms $Si \cdot \ell^{-1}$)	ρ (μg atoms $Si \cdot \ell^{-1} \cdot hr^{-1}$)
100	0.0	0.018	0.45	0.008
50	3.0	0.020	0.39	0.008
25	6.0	0.010	0.51	0.005
10	10.5	0.011	0.41	0.004
1	21.0	0.007	0.26	0.002
50 @ 0	3.0	0.000	0.39	0.000

Station 67

Lt. depth (% surface intensity)	Depth (m)	V (hr^{-1})	S_1 (μg atoms $Si \cdot \ell^{-1}$)	ρ (μg atoms $Si \cdot \ell^{-1} \cdot hr^{-1}$)
100	0.0	0.082	4.74	0.388
50	5.0	0.087	3.58	0.310
25	10.0	0.083	3.45	0.286
10	17.0	0.092	3.69	0.339
1	34.0	0.119	3.70	0.438
50 @ 0	5.0	0.091	3.40	0.309

Station 78

Lt. depth (% surface intensity)	Depth (m)	V (hr^{-1})	S_1 (μg atoms $Si \cdot \ell^{-1}$)	ρ (μg atoms $Si \cdot \ell^{-1} \cdot hr^{-1}$)
100	0.0	0.088	2.18	0.193
50	7.5	0.089	2.58	0.231
25	15.0	0.092	2.21	0.204
10	25.0	0.091	1.94	0.177
1	49.0	0.172	2.69	0.462
50 @ 0	7.5	0.088	2.43	0.212

Station 79 (Glass bottles)

Lt. depth (% surface intensity)	Depth (m)	V (hr^{-1})	S_1 (μg atoms $Si \cdot \ell^{-1}$)	ρ (μg atoms $Si \cdot \ell^{-1} \cdot hr^{-1}$)
100	0.0	0.165	1.67	0.276
50	3.0	0.174	1.77	0.307
25	6.0	0.166	1.53	0.254
10	9.0	0.159	1.57	0.249
1	18.0	--	--	--
50 @ 0	3.0	0.173	2.03	0.354

Station 79 (Plexiglas bottles)

Lt. depth (% surface intensity)	Depth (m)	V (hr^{-1})	S_1 (μg atoms $Si \cdot \ell^{-1}$)	ρ (μg atoms $Si \cdot \ell^{-1} \cdot hr^{-1}$)
100	0.0	0.179	1.84	0.329
50	3.0	0.178	1.87	0.333
25	6.0	0.173	2.20	0.381
10	9.0	0.170	2.38	0.405
1	18.0	--	--	--
50 @ 0	3.0	--	--	--

Station 9 (Light experiment)

Experimental light conditions (% surface intensity)	Depth (m)	V (hr^{-1})	S_1 (μg atoms $Si \cdot \ell^{-1}$)	ρ (μg atoms $Si \cdot \ell^{-1} \cdot hr^{-1}$)
100 @ 100	0	0.032	3.11	0.99
100 @ 50	0	0.009	2.60	0.23
100 @ 25	0	0.010	3.02	0.29
100 @ 10	0	0.015	2.64	0.39
100 @ 1	0	0.011	3.39	0.38
100 @ 0	0	0.011	2.78	0.40

Station 9 (Light experiment)

Experimental light conditions (% surface intensity)	Depth (m)	V (hr^{-1})	S_1 (μg atoms $Si \cdot \ell^{-1}$)	ρ (μg atoms $Si \cdot \ell^{-1} \cdot hr^{-1}$)
50 @ 100	2.5	0.017	5.39	0.094
50 @ 50	2.5	0.017	5.94	0.099
50 @ 25	2.5	0.017	6.76	0.113
50 @ 10	2.5	--	--	--
50 @ 1	2.5	0.008	5.85	0.046
50 @ 0	2.5	0.004	3.35	0.017

Station 9 (Light experiment)

Experimental light conditions (% surface intensity)	Depth (m)	V (hr^{-1})	S_1 (μg atoms $Si \cdot \ell^{-1}$)	ρ (μg atoms $Si \cdot \ell^{-1} \cdot hr^{-1}$)
25 @ 100	7	0.026	3.90	0.100
25 @ 50	7	0.019	4.54	0.087
25 @ 25	7	0.020	5.31	0.105
25 @ 10	7	0.011	2.53	0.027
25 @ 1	7	--	--	--
25 @ 0	7	0.003	2.82	0.006

Station 9 (Light experiment)

Experimental light conditions (% surface intensity)	Depth (m)	V (hr^{-1})	S_1 (μg atoms $Si \cdot \ell^{-1}$)	ρ (μg atoms $Si \cdot \ell^{-1} \cdot hr^{-1}$)
10 @ 100	12	0.015	2.22	0.034
10 @ 50	12	--	--	--
10 @ 25	12	0.007	2.31	0.016
10 @ 10	12	0.004	2.15	0.011
10 @ 1	12	0.011	2.61	0.029
10 @ 0	12	--	--	--

Station 9 (Light experiment)

Experimental light conditions (% surface intensity)	Depth (m)	V (hr^{-1})	S_1 (μg atoms $Si \cdot \ell^{-1}$)	ρ (μg atoms $Si \cdot \ell^{-1} \cdot hr^{-1}$)
1 @ 100	23	--	--	--
1 @ 50	23	0.017	5.41	0.091
1 @ 25	23	0.016	5.60	0.089
1 @ 10	23	--	--	--
1 @ 1	23	0.019	5.58	0.106
1 @ 0	23	--	--	--

Station 35 (Light experiment)

Experimental light conditions (% surface intensity)	Depth (m)	V (hr^{-1})	S_1 (μg atoms $Si \cdot \ell^{-1}$)	ρ (μg atoms $Si \cdot \ell^{-1} \cdot hr^{-1}$)
50 @ 100	3	0.038	8.14	0.308
50 @ 50	3	0.037	7.41	0.276
50 @ 25	3	0.029	3.11	0.091
50 @ 10	3	0.033	3.60	0.118
50 @ 1	3	0.024	4.96	0.119
50 @ 0	3	0.019	4.48	0.084

Station 71 (Light experiment)

Experimental light conditions (% surface intensity)	Depth (m)	V (hr^{-1})	S_1 (μg atoms $Si \cdot \ell^{-1}$)	ρ (μg atoms $Si \cdot \ell^{-1} \cdot hr^{-1}$)
50 @ 100	3	0.077	1.76	0.135
50 @ 50	3	0.079	1.53	0.121
50 @ 25	3	0.089	1.59	0.141
50 @ 10	3	0.088	1.34	0.118
50 @ 1	3	0.087	2.29	0.199
50 @ 0	3	0.079	1.74	0.137

Station 82 (Light experiment)

Experimental light conditions (% surface intensity)	Depth (m)	V (hr^{-1})	S_1 (μg atoms $Si \cdot \ell^{-1}$)	ρ (μg atoms $Si \cdot \ell^{-1} \cdot hr^{-1}$)
50 @ 100	5	0.090	1.78	0.161
50 @ 50	5	0.108	1.72	0.186
50 @ 25	5	0.110	1.70	0.188
50 @ 10	5	0.106	1.78	0.189
50 @ 1	5	0.106	1.85	0.196
50 @ 0	5	0.096	1.78	0.172

Station 82 (Light experiment)

Experimental light conditions (% surface intensity)	Depth (m)	V (hr^{-1})	S_1 (μg atoms $Si \cdot \ell^{-1}$)	ρ (μg atoms $Si \cdot \ell^{-1} \cdot hr^{-1}$)
10 @ 100	16	0.100	2.10	0.210
10 @ 50	16	0.077	1.64	0.125
10 @ 25	16	0.086	2.31	0.199
10 @ 10	16	0.076	1.72	0.130
10 @ 1	16	0.092	1.83	0.168
10 @ 0	16	0.057	2.80	0.158

Station 25 (Kinetic experiment)

Addition (μg atoms $Si \cdot \ell^{-1}$)	Depth (m)	V (hr^{-1})	S_1 (μg atoms $Si \cdot \ell^{-1}$)	ρ (μg atoms $Si \cdot \ell^{-1} \cdot hr^{-1}$)
0.085	3	0.029	3.68	0.108
0.435	3	0.020	3.98	0.079
0.875	3	0.033	3.01	0.196
1.75	3	0.034	2.59	0.175
6.50	3	0.049	2.87	0.141
13.0	3	0.032	3.95	0.130

Station 67 (Kinetic experiment)

Addition (μg atoms $Si \cdot \ell^{-1}$)	Depth (m)	V (hr^{-1})	S_1 (μg atoms $Si \cdot \ell^{-1}$)	ρ (μg atoms $Si \cdot \ell^{-1} \cdot hr^{-1}$)
0.085	3	0.056	2.33	0.131
0.435	3	--	--	--
0.875	3	0.062	2.38	0.148
1.75	3	0.066	1.96	0.132
6.50	3	0.055	1.83	0.100
13.0	3	0.067	1.92	1.121

APPENDIX B

SILICIC ACID UPTAKE AND SILICA DISSOLUTION DATA FROM JOINT I

Station 13

Lt. depth (% surface intensity)	Depth (m)	V (hr^{-1})	S_1 (μg atoms $Si \cdot \ell^{-1}$)	ρ (μg atoms $Si \cdot \ell^{-1} \cdot hr^{-1}$)
100	0.0	0.007	2.23	0.016
50	2.0	0.006	4.95	0.031
30	4.0	0.006	3.79	0.023
15	8.0	0.016	2.11	0.035
5	13.0	0.006	2.24	0.014
1	22.0	0.002	5.55	0.013
0.1	33.0	0.000	4.73	0.000
50 @ 0	2.0	0.006	4.37	0.029

Station 14

Lt. depth (% surface intensity)	Depth (m)	V (hr^{-1})	S_1 (μg atoms $Si \cdot \ell^{-1}$)	ρ (μg atoms $Si \cdot \ell^{-1} \cdot hr^{-1}$)
100	0.0	0.000	16.89	0.000
50	1.0	0.006	16.22	0.089
30	1.7	0.001	18.47	0.026
15	2.7	0.000	18.97	0.000
5	3.6	0.000	19.16	0.000
1	4.7	0.000	19.43	0.000
0.1	7.0	0.000	19.07	0.000
50 @ 0	1.0	0.000	18.55	0.000

Station 18

Lt. depth (% surface intensity)	Depth (m)	V (hr^{-1})	S_1 (μg atoms $Si \cdot \ell^{-1}$)	ρ (μg atoms $Si \cdot \ell^{-1} \cdot hr^{-1}$)
100	0.0	0.003	4.91	0.012
50	2.0	--	--	--
30	3.6	0.003	4.23	0.013
15	6.4	0.003	4.50	0.013
5	11.2	0.003	4.02	0.011
1	20.0	0.002	4.36	0.009
0.1	50.0	0.001	4.18	0.004
50 @ 0	2.0	0.002	4.51	0.009

Station 23 (24-hour incubation)

Lt. depth (% surface intensity)	Depth (m)	V (hr^{-1})	S_1 (μg atoms $Si \cdot \ell^{-1}$)	ρ (μg atoms $Si \cdot \ell^{-1} \cdot hr^{-1}$)
100	0.0	0.003	12.26	0.037
50	2.6	0.004	12.48	0.051
30	4.4	0.004	12.66	0.053
15	6.0	0.002	12.71	0.025
5	9.5	0.000	13.28	0.000
1	15.5	0.000	10.44	0.000
0.1	25.0	0.000	9.76	0.000

Station 30

Lt. depth (% surface intensity)	Depth (m)	V (hr^{-1})	S_1 (μg atoms $Si \cdot \ell^{-1}$)	ρ (μg atoms $Si \cdot \ell^{-1} \cdot hr^{-1}$)
100	0.0	0.003	5.52	0.015
50	2.2	0.001	5.63	0.006
30	4.2	0.001	5.81	0.006
15	7.0	--	--	--
5	12.0	0.001	5.91	0.006
1	20.4	0.000	6.72	0.000
0.1	33.0	0.000	5.76	0.000
0.01	50.0	0.000	6.71	0.000

Station 36 (24-hour incubation)

Lt. depth (% surface intensity)	Depth (m)	V (hr^{-1})	S_1 (μg atoms $Si \cdot \ell^{-1}$)	ρ (μg atoms $Si \cdot \ell^{-1} \cdot hr^{-1}$)
100	0.0	0.014	5.07	0.071
50	2.8	0.014	4.93	0.069
30	5.0	0.010	4.65	0.047
15	9.0	0.007	4.17	0.029
5	16.0	0.006	4.28	0.026
1	26.0	0.003	3.46	0.010
0.1	46.0	0.003	3.08	0.009
50 @ 0	2.8	0.004	4.85	0.019

Station 38

Lt. depth (% surface intensity)	Depth (m)	V (hr^{-1})	S_1 (μg atoms $Si \cdot \ell^{-1}$)	ρ (μg atoms $Si \cdot \ell^{-1} \cdot hr^{-1}$)
100	0.0	0.033	4.16	0.137
50	2.0	0.038	4.22	0.160
30	3.8	0.039	3.50	0.138
15	6.7	0.043	3.13	0.135
5	12.6	0.029	2.67	0.078
1	23.0	--	--	--
0.1	50.0	0.009	2.49	0.023
50 @ 0	2.0	0.007	3.57	0.024

Station 52

Lt. depth (% surface intensity)	Depth (m)	V (hr^{-1})	S_1 (μg atoms $Si \cdot \ell^{-1}$)	ρ (μg atoms $Si \cdot \ell^{-1} \cdot hr^{-1}$)
100	0.0	0.010	3.23	0.031
50	2.6	0.016	3.22	0.052
30	4.4	--	--	--
15	5.5	0.012	3.32	0.040
5	10.6	0.010	3.25	0.032
1	22.4	0.006	3.23	0.018
0.1	38.0	0.006	4.18	0.026
0.01	80.0	0.000	2.22	0.000
50 @ 0	2.6	0.007	3.06	0.022

Station 53 (24-hour incubation)

Lt. depth (% surface intensity)	Depth (m)	V (hr^{-1})	S_1 (μg atoms $Si \cdot \ell^{-1}$)	ρ (μg atoms $Si \cdot \ell^{-1} \cdot hr^{-1}$)
100	0.0	0.022	4.21	0.093
50	2.0	0.019	4.46	0.085
30	6.0	0.016	4.93	0.079
15	12.0	0.008	4.64	0.037
5	18.0	0.009	4.18	0.038
1	30.0	0.003	4.10	0.012
0.1	60.0	0.002	3.76	0.008

Station 70

Lt. depth (% surface intensity)	Depth (m)	V (hr^{-1})	S_1 (μg atoms $Si \cdot \ell^{-1}$)	ρ (μg atoms $Si \cdot \ell^{-1} \cdot hr^{-1}$)
100	0.0	0.012	1.93	0.022
50	2.0	0.011	1.88	0.020
30	4.0	0.011	1.76	0.019
15	7.0	0.009	2.17	0.019
5	12.0	0.007	2.25	0.016
1	21.0	0.004	2.84	0.011
0.1	35.0	0.002	2.70	0.004
50 @ 0	2.0	0.002	1.70	0.004

Station 70 (Dark profile)

Lt. depth (% surface intensity)	Depth (m)	V (hr^{-1})	S_1 (μg atoms $Si \cdot \ell^{-1}$)	ρ (μg atoms $Si \cdot \ell^{-1} \cdot hr^{-1}$)
100 @ 0	0.0	0.005	2.02	0.009
50 @ 0	2.0	0.002	1.70	0.004
30 @ 0	4.0	0.002	1.59	0.003
15 @ 0	7.0	0.003	1.93	0.006
5 @ 0	12.0	0.004	1.97	0.008
1 @ 0	21.0	--	--	--
0.1 @ 0	35.0	0.002	1.78	0.003

Station 78

Lt. depth (% surface intensity)	Depth (m)	V (hr^{-1})	S_1 (μg atoms $Si \cdot \ell^{-1}$)	ρ (μg atoms $Si \cdot \ell^{-1} \cdot hr^{-1}$)
100	0.0	0.023	2.04	0.046
50	2.0	0.028	1.70	0.048
30	3.0	0.024	2.06	0.049
15	5.0	--	--	--
5	9.0	0.017	1.95	0.033
1	15.0	0.002	1.90	0.004
0.1	27.0	0.007	1.93	0.013
50 @ 0	2.0	0.009	1.62	0.014

Station 78 (Dark profile)

Lt. depth (% surface intensity)	Depth (m)	V (hr^{-1})	S_1 (μg atoms $Si \cdot \ell^{-1}$)	ρ (μg atoms $Si \cdot \ell^{-1} \cdot hr^{-1}$)
100 @ 0	0.0	--	--	--
50 @ 0	2.0	0.009	1.62	0.014
30 @ 0	3.0	0.011	2.18	0.020
15 @ 0	5.0	0.010	3.10	0.030
5 @ 0	9.0	--	--	--
1 @ 0	15.0	0.002	1.89	0.004
0.1 @ 0	27.0	0.007	1.93	0.013

Station 85

Lt. depth (% surface intensity)	Depth (m)	V (hr^{-1})	S_1 (μg atoms $Si \cdot \ell^{-1}$)	ρ (μg atoms $Si \cdot \ell^{-1} \cdot hr^{-1}$)
100	0.0	0.022	3.40	0.074
50	2.0	0.028	3.03	0.086
30	3.0	0.031	2.95	0.090
15	6.0	0.029	3.21	0.094
5	11.0	0.015	3.46	0.053
1	20.0	0.010	3.55	0.037
0.1	33.0	0.009	3.77	0.034
50 @ 0	2.0	0.007	3.15	0.022

Station 89

Lt. depth (% surface intensity)	Depth (m)	V (hr^{-1})	S_1 (μg atoms $Si \cdot \ell^{-1}$)	ρ (μg atoms $Si \cdot \ell^{-1} \cdot hr^{-1}$)
100	0.0	0.008	2.24	0.018
50	2.0	0.026	1.03	0.027
30	4.0	--	--	--
15	6.0	--	--	--
5	10.0	0.005	1.89	0.009
1	18.0	0.006	0.91	0.005
0.1	29.0	0.002	1.40	0.002
0.01	41.0	0.007	0.67	0.005
50 @ 0	2.0	0.006	1.21	0.007

Station 97

Lt. depth (% surface intensity)	Depth (m)	V (hr^{-1})	S_1 (μg atoms $Si \cdot \ell^{-1}$)	ρ (μg atoms $Si \cdot \ell^{-1} \cdot hr^{-1}$)
100	0.0	0.016	2.15	0.034
50	2.0	0.016	2.04	0.032
30	3.0	0.015	2.87	0.044
15	6.0	0.018	2.39	0.042
5	10.0	0.008	3.49	0.026
1	20.0	0.005	3.42	0.017
0.1	40.0	0.002	2.42	0.006
0.01	58.0	0.001	3.15	0.002

Station 99

Lt. depth (% surface intensity)	Depth (m)	V (hr^{-1})	S_1 (μg atoms $Si \cdot \ell^{-1}$)	ρ (μg atoms $Si \cdot \ell^{-1} \cdot hr^{-1}$)
100	0.0	0.005	2.11	0.012
50	2.0	0.012	2.30	0.027
30	5.0	0.007	2.38	0.016
15	9.0	0.001	2.53	0.020
5	14.0	0.000	4.13	0.000
1	26.0	0.000	2.15	0.000
0.1	41.0	0.000	2.60	0.000
0.01	55.0	0.000	2.76	0.000
50 @ 0	2.0	0.000	2.57	0.000

Station 112 (24-hour incubation)

Lt. depth (% surface intensity)	Depth (m)	V (hr^{-1})	S_1 (μg atoms $Si \cdot \ell^{-1}$)	ρ (μg atoms $Si \cdot \ell^{-1} \cdot hr^{-1}$)
100	0.0	0.012	4.72	0.057
50	2.0	0.012	4.78	0.057
30	3.0	0.012	5.15	0.062
15	5.0	0.015	4.50	0.068
5	9.0	0.017	7.83	0.133
1	14.0	0.012	3.92	0.047
0.1	26.0	0.010	2.88	0.029

Station 122 (24-hour incubation)

Lt. depth (% surface intensity)	Depth (m)	V (hr^{-1})	S_1 (μg atoms $Si \cdot \ell^{-1}$)	ρ (μg atoms $Si \cdot \ell^{-1} \cdot hr^{-1}$)
100	0.0	0.008	1.61	0.013
50	2.0	0.013	1.66	0.022
30	4.0	0.014	1.78	0.025
15	7.0	0.012	1.47	0.018
5	12.0	0.010	1.33	0.013
1	23.0	0.010	1.62	0.016
0.1	42.0	0.004	1.48	0.006

Station 127

Lt. depth (% surface intensity)	Depth (m)	V (hr^{-1})	S_1 (μg atoms $Si \cdot \ell^{-1}$)	ρ (μg atoms $Si \cdot \ell^{-1} \cdot hr^{-1}$)
100	0.0	0.018	2.50	0.046
50	2.0	0.019	2.52	0.048
30	4.0	0.020	2.64	0.053
15	6.0	0.003	2.53	0.009
5	10.0	0.002	3.30	0.005
1	17.0	0.003	4.14	0.012
0.1	28.0	0.000	3.39	0.000
0.01	39.0	0.000	2.74	0.000
0.001	95.0	0.000	1.27	0.000

Station 129 (24-hour incubation)

Lt. depth (% surface intensity)	Depth (m)	V (hr^{-1})	S_1 (μg atoms $Si \cdot \ell^{-1}$)	ρ (μg atoms $Si \cdot \ell^{-1} \cdot hr^{-1}$)
100	0.0	0.013	3.45	0.045
50	2.0	0.014	4.02	0.056
30	4.0	0.012	2.30	0.028
15	8.0	0.010	4.04	0.040
5	14.0	0.014	3.61	0.050
1	23.0	0.010	2.97	0.030
0.1	37.0	0.006	2.91	0.017

Station 136 (24-hour incubation)

Lt. depth (% surface intensity)	Depth (m)	V (hr^{-1})	S_1 (μg atoms $Si \cdot \ell^{-1}$)	ρ (μg atoms $Si \cdot \ell^{-1} \cdot hr^{-1}$)
100	0.0	0.006	2.96	0.018
50	2.0	0.004	2.87	0.011
30	4.0	--	--	--
15	8.0	0.002	2.77	0.006
5	13.0	0.002	2.83	0.006
1	22.0	0.001	2.64	0.003
0.1	37.0	0.000	2.71	0.000

Station 138

Lt. depth (% surface intensity)	Depth (m)	V (hr^{-1})	S_1 (μg atoms $Si \cdot \ell^{-1}$)	ρ (μg atoms $Si \cdot \ell^{-1} \cdot hr^{-1}$)
100	0.0	0.006	1.26	0.007
50	2.0	0.003	1.01	0.003
30	4.0	--	--	--
15	8.0	0.004	1.94	0.008
5	15.0	--	--	--
1	27.0	0.000	1.18	0.000
0.1	45.0	0.000	1.26	0.000
50 @ 0	2.0	0.001	0.98	0.001

Station 153

Lt. depth (% surface intensity)	Depth (m)	V (hr^{-1})	S_1 (μg atoms $Si \cdot \ell^{-1}$)	ρ (μg atoms $Si \cdot \ell^{-1} \cdot hr^{-1}$)
100	0.0	0.018	3.72	0.065
50	2.0	0.010	4.03	0.041
30	3.0	0.016	3.89	0.062
15	5.0	0.009	3.42	0.029
5	10.0	0.007	4.23	0.031
1	18.0	--	--	--
0.1	28.0	0.001	4.85	0.005
50 @ 0	2.0	0.001	3.81	0.004

Station 164

Lt. depth (% surface intensity)	Depth (m)	V (hr^{-1})	S_1 (μg atoms $Si \cdot \ell^{-1}$)	ρ (μg atoms $Si \cdot \ell^{-1} \cdot hr^{-1}$)
100	0.0	0.020	4.20	0.084
50	2.0	0.039	4.01	0.158
30	5.5	0.030	4.42	0.131
15	9.0	0.038	4.02	0.153
5	14.0	0.028	4.67	0.132
1	22.0	0.028	4.39	0.123
0.1	32.0	0.027	3.87	0.104
0.01	44.0	0.022	2.35	0.052
50 @ 0	2.0	0.021	4.51	0.098
50 ($HgCl_2$)	2.0	0.000	4.33	0.000

Station 175

Lt. depth (% surface intensity)	Depth (m)	V (hr^{-1})	S_1 (μg atoms $Si \cdot \ell^{-1}$)	ρ (μg atoms $Si \cdot \ell^{-1} \cdot hr^{-1}$)
100	0.0	0.002	6.82	0.017
50	2.0	0.003	6.34	0.017
30	5.0	--	--	--
15	9.0	0.002	6.64	0.016
5	15.0	0.003	6.56	0.017
1	25.0	0.001	4.62	0.002
0.1	37.0	0.002	5.74	0.010
0.01	50.0	0.003	5.05	0.014
50 @ 0	2.0	0.002	5.74	0.014

Station 6 (Light experiment)

Experimental light conditions (% surface intensity)	Depth (m)	V (hr^{-1})	S_1 (μg atoms $Si \cdot \ell^{-1}$)	ρ (μg atoms $Si \cdot \ell^{-1} \cdot hr^{-1}$)
50 @ 100	3.0	0.009	4.88	0.043
50 @ 50	3.0	0.010	4.21	0.042
50 @ 30	3.0	0.009	4.36	0.038
50 @ 15	3.0	0.009	4.58	0.040
50 @ 5	3.0	0.003	5.04	0.014
50 @ 1	3.0	0.003	4.53	0.018
50 @ 0	3.0	0.000	4.91	0.000

Station 31 (Light experiment)

Experimental light conditions (% surface intensity)	Depth (m)	V (hr^{-1})	S_1 (μg atoms $Si \cdot \ell^{-1}$)	ρ (μg atoms $Si \cdot \ell^{-1} \cdot hr^{-1}$)
50 @ 100	2.2	0.001	4.49	0.006
50 @ 50	2.2	0.002	4.76	0.013
50 @ 30	2.2	0.005	4.91	0.025
50 @ 15	2.2	0.001	4.79	0.007
50 @ 5	2.2	0.002	5.02	0.008
50 @ 1	2.2	0.000	4.98	0.000
50 @ 0	2.2	0.000	5.02	0.000

Station 38 (Light experiment)

Experimental light conditions (% surface intensity)	Depth (m)	V (hr^{-1})	S_1 (μg atoms $Si \cdot \ell^{-1}$)	ρ (μg atoms $Si \cdot \ell^{-1} \cdot hr^{-1}$)
50 @ 100	2.0	0.037	3.25	0.121
50 @ 50	2.0	0.031	3.38	0.101
50 @ 30	2.0	0.025	2.60	0.066
50 @ 15	2.0	--	--	--
50 @ 5	2.0	0.014	3.05	0.043
50 @ 1	2.0	0.010	3.67	0.037
50 @ 0	2.0	0.007	3.56	0.024

Station 62 (Light experiment)

Experimental light conditions (% surface intensity)	Depth (m)	V (hr^{-1})	S_1 (μg atoms $Si \cdot \ell^{-1}$)	ρ (μg atoms $Si \cdot \ell^{-1} \cdot hr^{-1}$)
50 @ 100	3.0	0.011	4.39	0.046
50 @ 50	3.0	0.006	2.75	0.017
50 @ 30	3.0	0.007	4.83	0.032
50 @ 15	3.0	0.010	3.16	0.033
50 @ 5	3.0	0.007	3.13	0.023
50 @ 1	3.0	0.004	2.86	0.014
50 @ 0	3.0	0.001	3.95	0.005

Station 62 (Light experiment)

Experimental light conditions (% surface intensity)	Depth (m)	V (hr^{-1})	S_1 (μg atoms $Si \cdot \ell^{-1}$)	ρ (μg atoms $Si \cdot \ell^{-1} \cdot hr^{-1}$)
0.1 @ 100	60.0	0.003	2.71	0.009
0.1 @ 50	60.0	0.003	2.41	0.008
0.1 @ 30	60.0	0.005	2.58	0.013
0.1 @ 15	60.0	0.001	3.33	0.003
0.1 @ 5	60.0	--	--	--
0.1 @ 1	60.0	0.002	3.48	0.007
0.1 @ 0	60.0	0.001	2.73	0.003

Station 69 (Light experiment)

Experimental light conditions (% surface intensity)	Depth (m)	V (hr^{-1})	S_1 (μg atoms $Si \cdot \ell^{-1}$)	ρ (μg atoms $Si \cdot \ell^{-1} \cdot hr^{-1}$)
50 @ 100	2.0	0.010	2.89	0.030
50 @ 50	2.0	0.007	3.23	0.022
50 @ 30	2.0	0.009	3.17	0.029
50 @ 15	2.0	0.007	3.05	0.021
50 @ 5	2.0	0.007	2.62	0.018
50 @ 1	2.0	0.010	3.24	0.031
50 @ 0	2.0	0.007	3.09	0.021

Station 69 (Light experiment)

Experimental light conditions (% surface intensity)	Depth (m)	V (hr^{-1})	S_1 (μg atoms $Si \cdot \ell^{-1}$)	ρ (μg atoms $Si \cdot \ell^{-1} \cdot hr^{-1}$)
0.1 @ 100	55.0	0.005	4.89	0.025
0.1 @ 50	55.0	0.007	4.44	0.032
0.1 @ 30	55.0	0.006	3.81	0.023
0.1 @ 15	55.0	0.004	3.98	0.016
0.1 @ 5	55.0	0.002	3.77	0.008
0.1 @ 1	55.0	0.002	3.46	0.007
0.1 @ 0	55.0	0.000	3.67	0.000

Station 135 (Light experiment)

Experimental light conditions (% surface intensity)	Depth (m)	V (hr^{-1})	S_1 (μg atoms $Si \cdot \ell^{-1}$)	ρ (μg atoms $Si \cdot \ell^{-1} \cdot hr^{-1}$)
50 @ 100	2.0	0.007	7.78	0.050
50 @ 50	2.0	0.007	5.99	0.041
50 @ 30	2.0	0.004	7.30	0.026
50 @ 15	2.0	0.002	5.11	0.007
50 @ 5	2.0	0.005	6.29	0.031
50 @ 1	2.0	0.001	6.53	0.006
50 @ 0	2.0	0.000	6.87	0.000
50 ($HgCl_2$)	2.0	0.000	6.92	0.000

Station 44 (Light-dark comparison)

Experimental light conditions (% surface intensity)	Depth (m)	V (hr^{-1})	S_1 (μg atoms $Si \cdot \ell^{-1}$)	ρ (μg atoms $Si \cdot \ell^{-1} \cdot hr^{-1}$)
50 @ 50	2.0	0.019	6.19	0.118
50 @ 50	2.0	0.021	6.41	0.134
50 @ 0	2.0	0.000	6.71	0.000
50 @ 0	2.0	0.000	6.58	0.000

Station 45 (Light-dark comparison)

Experimental light conditions (% surface intensity)	Depth (m)	V (hr^{-1})	S_1 (μg atoms $Si \cdot \ell^{-1}$)	ρ (μg atoms $Si \cdot \ell^{-1} \cdot hr^{-1}$)
50 @ 50	2.0	0.004	2.57	0.010
50 @ 50	2.0	0.003	2.49	0.008
50 @ 0	2.0	0.000	2.71	0.000
50 @ 0	2.0	0.001	2.62	0.003

Station 31 (Kinetic experiment)

Addition (μg atoms $Si \cdot \ell^{-1}$)	Depth (m)	V (hr^{-1})	S_1 (μg atoms $Si \cdot \ell^{-1}$)	ρ (μg atoms $Si \cdot \ell^{-1} \cdot hr^{-1}$)
0.20	2.2	0.001	4.66	0.005
0.40	2.2	0.006	6.04	0.024
1.10	2.2	0.007	4.44	0.033
2.20	2.2	0.008	6.06	0.049
4.50	2.2	0.008	5.76	0.046
9.00	2.2	0.016	4.53	0.073
13.50	2.2	0.012	5.53	0.065

Station 37 (Kinetic experiment)

Addition (μg atoms $Si \cdot \ell^{-1}$)	Depth (m)	V (hr^{-1})	S_1 (μg atoms $Si \cdot \ell^{-1}$)	ρ (μg atoms $Si \cdot \ell^{-1} \cdot hr^{-1}$)
0.20	1.4	0.017	2.43	0.041
0.40	1.4	0.019	2.75	0.052
1.10	1.4	0.023	2.83	0.066
2.20	1.4	--	--	--
4.50	1.4	0.018	3.06	0.053
9.00	1.4	0.018	2.93	0.052
13.50	1.4	0.020	3.12	0.062

Station 38 (Kinetic experiment)

Addition (μg atoms $Si \cdot \ell^{-1}$)	Depth (m)	V (hr^{-1})	S_1 (μg atoms $Si \cdot \ell^{-1}$)	ρ (μg atoms $Si \cdot \ell^{-1} \cdot hr^{-1}$)
0.20	3.0	0.009	1.76	0.016
0.40	3.0	0.010	1.86	0.019
1.10	3.0	0.008	1.69	0.013
2.20	3.0	0.011	1.98	0.022
4.50	3.0	0.010	2.07	0.021
9.00	3.0	0.010	1.84	0.018
13.50	3.0	0.012	2.11	0.026

Station 119 (Kinetic experiment)

Addition (μg atoms $Si \cdot \ell^{-1}$)	Depth (m)	V (hr^{-1})	S_1 (μg atoms $Si \cdot \ell^{-1}$)	ρ (μg atoms $Si \cdot \ell^{-1} \cdot hr^{-1}$)
8.3	2.0	0.006	3.72	0.022
16.7	2.0	0.008	3.61	0.025
25.0	2.0	0.004	4.43	0.017
33.3	2.0	--	--	--
41.7	2.0	0.004	4.60	0.020
83.3	2.0	0.008	4.03	0.034

Station 23 (Dissolution profile)

Lt. depth (% surface intensity)	Depth (m)	V_{dis} (hr^{-1})	±	ρ_{dis} (μg atoms $Si \cdot \ell^{-1} \cdot hr^{-1}$)	±
100	0.0	0.0004	0.0004	0.0046	0.0045
50	2.6	--	--	--	--
30	4.4	--	--	--	--
15	6.0	0.0021	0.0004	0.0260	0.0045
5	9.5	0.0057	0.0004	0.0716	0.0045
1	15.5	0.0032	0.0004	0.0385	0.0045
0.1	25.0	0.0042	0.0005	0.0396	0.0047

Station 36 (Dissolution profile)

Lt. depth (% surface intensity)	Depth (m)	V_{dis} (hr^{-1})	±	ρ_{dis} (μg atoms $Si \cdot \ell^{-1} \cdot hr^{-1}$)	±
100	0.0	0.0034	0.0012	0.0177	0.0052
50	2.8	0.0016	0.0012	0.0081	0.0052
30	5.0	0.0007	0.0012	0.0036	0.0052
15	9.0	0.0032	0.0013	0.0128	0.0054
5	16.0	0.0162	0.0016	0.0168	0.0055
1	26.0	--	--	--	--
0.1	46.0	0.0246	0.0025	0.0753	0.0056

Station 53 (Dissolution profile)

Lt. depth (% surface intensity)	Depth (m)	V_{dis} (hr^{-1})	±	ρ_{dis} (μg atoms $Si \cdot \ell^{-1} \cdot hr^{-1}$)	±
100	0.0	0.0023	0.0012	0.0110	0.0060
50	2.0	0.0006	0.0012	0.0026	0.0060
30	6.0	0.0043	0.0012	0.0198	0.0060
15	12.0	0.0049	0.0012	0.0213	0.0060
5	18.0	0.0042	0.0012	0.0172	0.0060
1	30.0	0.0057	0.0012	0.0250	0.0060
0.1	60.0	0.0125	0.0013	0.0510	0.0062

Station 112 (Dissolution profile)

Lt. depth (% surface intensity)	Depth (m)	V_{dis} (hr^{-1})	±	ρ_{dis} (μg atoms $Si \cdot \ell^{-1} \cdot hr^{-1}$)	±
100	0.0	0.0003	0.0011	0.0014	0.0053
50	2.0	0.0029	0.0011	0.0136	0.0053
30	3.0	0.0014	0.0011	0.0085	0.0053
15	5.0	0.0103	0.0011	0.0468	0.0054
5	9.0	--	--	--	--
1	14.0	0.0058	0.0016	0.0221	0.0057
0.1	26.0	0.0067	0.0016	0.0215	0.0057

Station 122 (Dissolution profile)

Lt. depth (% surface intensity)	Depth (m)	V_{dis} (hr^{-1})	±	ρ_{dis} (μg atoms $Si \cdot \ell^{-1} \cdot hr^{-1}$)	±
100	0.0	0.0033	0.0016	0.0060	0.0030
50	2.0	0.0009	0.0016	0.0017	0.0030
30	4.0	0.0112	0.0016	0.0199	0.0030
15	7.0	--	--	--	--
5	12.0	0.0114	0.0016	0.0163	0.0031
1	23.0	0.0157	0.0016	0.0265	0.0031
0.1	42.0	0.0564	0.0056	0.0843	0.0034

Station 129 (Dissolution profile)

Lt. depth (% surface intensity)	Depth (m)	V_{dis} (hr^{-1})	±	ρ_{dis} (μg atoms $Si \cdot \ell^{-1} \cdot hr^{-1}$)	±
100	0.0	0.0007	0.0012	0.0024	0.0045
50	2.0	--	--	--	--
30	4.0	0.0031	0.0012	0.0068	0.0045
15	8.0	0.0012	0.0012	0.0042	0.0045
5	14.0	--	--	--	--
1	23.0	0.0046	0.0012	0.0128	0.0045
0.1	37.0	0.0203	0.0020	0.0620	0.0048

Station 136 (Dissolution profile)

Lt. depth (% surface intensity)	Depth (m)	V_{dis} (hr^{-1})	±	ρ_{dis} (μg atoms $Si \cdot \ell^{-1} \cdot hr^{-1}$)	±
100	0.0	0.0009	0.0011	0.0026	0.0032
50	2.0	0.0010	0.0011	0.0030	0.0032
30	4.0	0.0048	0.0011	0.0141	0.0032
15	8.0	0.0047	0.0012	0.0136	0.0032
5	13.0	--	--	--	--
1	22.0	0.0113	0.0013	0.0287	0.0034
0.1	37.0	0.0201	0.0020	0.0550	0.0035